ADVANCED GUN FIRE CONTROL SYSTEM

(AGFCS)

DESIGN STUDY (PHASE II)

AFAL-TR-74-198 VOLUME I

MCDONNELL AIRCRAFT COMPANY

MCDONNELL DOUGLAS CORPORATION
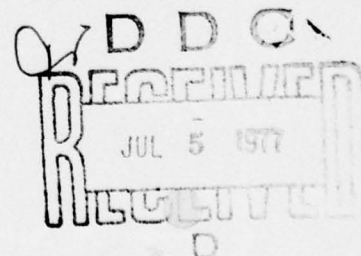
BOX 516. ST. LOUIS. MO. 63166

APRIL 1977

TECHNICAL REPORT AFAL-TR-74-198

FINAL REPORT FOR PERIOD JUNE 1973 - APRIL 1974

DDC
RECEIVED
JUL 5 1977

AD No.
DDC FILE COPY.

ADA041240

REPORT DOCUMENTATION PAGE	READ INSTRUCTIONS BEFORE COMPLETING FORM

1. REPORT NUMBER	2. GOVT ACCESSION NO.	3. RECIPIENT'S CATALOG NUMBER
AFAL-TR-74-198 VOLUME I		

4. TITLE (and Subtitle)	5. TYPE OF REPORT & PERIOD COVERED
ADVANCED GUN FIRE CONTROL SYSTEM (AGFCS) DESIGN STUDY (PHASE II). Volume I.	Final Report. June 1973 — April 1974.
	6. PERFORMING ORG. REPORT NUMBER N/A

7. AUTHOR(s)	8. CONTRACT OR GRANT NUMBER(s)
Robert L. Berg, William J. Murphy Dennis E. Simmons	F33615-73-C-1319

9. PERFORMING ORGANIZATION NAME AND ADDRESS	10. PROGRAM ELEMENT, PROJECT, TASK AREA & WORK UNIT NUMBERS
McDonnell Aircraft Company St. Louis, Missouri 63166	Project 7629 Task 762903 Work Unit 76290315

11. CONTROLLING OFFICE NAME AND ADDRESS	12. REPORT DATE
Air Force Avionics Laboratory (RWT) Wright-Patterson Air Force Base, Ohio	April 1977
	13. NUMBER OF PAGES 119

14. MONITORING AGENCY NAME & ADDRESS(if different from Controlling Office)	15. SECURITY CLASS. (of this report)
	Unclassified
	15a. DECLASSIFICATION/DOWNGRADING SCHEDULE

16. DISTRIBUTION STATEMENT (of this Report)

Approved for public release; distribution unlimited.

17. DISTRIBUTION STATEMENT (of the abstract entered in Block 20, if different from Report)

18. SUPPLEMENTARY NOTES

VOLUME II – ATS Angle Sensor Design Description
VOLUME III – ATS Range Sensor Design Description
VOLUME IV – ATS Software Design Description

19. KEY WORDS (Continue on reverse side if necessary and identify by block number)

Gun Fire Control System
Gunsights
Tracking System
EO Sensor
Radar Sensor

20. ABSTRACT (Continue on reverse side if necessary and identify by block number)

The Advanced Gun Fire Control System (AGFCS) program is a multi-phase
program to investigate technical approaches exhibiting potentially
significant improvement in present gun fire control systems effectiveness.
Phase I, the AGFCS Definition Study, considered the overall design, effective-
ness, complexity and mission requirements of a post-1976 air superiority
aircraft. The purpose of Phase II, the AGFCS Design Study, was to design

Continued - Block 20 (Abstract)

an Augmented Tracking System (ATS) for possible fabrication and flight test evaluation in a later AGFCS Program Phase. The ATS includes the range and angle tracking sensors, the computer, and the software used to process the tracking signals. It provides the target-dependent variables required to solve the lead angle equation in a director AGFCS mechanization. The ATS will ultimately serve as the core of an advanced gun fire control system.

The selected configuration serves as the basic element of a modular advanced gun fire control system. Its salient feature is the use of strapdown sensors in both the angle tracking and range tracking systems. The angle sensor is the Bendix Corporation Adaptive Scan Optical Tracker (ASCOT); the range sensor is the General Electric Solid State Radar (SSR-1). Both sensors satisfy the requirements of the ATS application and have adequate technical maturity for timely fabrication and flight test. The principal ATS subsystem and software features are:

o Principal Subsystems
   o Bendix Adaptive Scan Optical Tracker
   o GE Solid-State Radar
   o ATS Digital Computer
   o Strapdown Gyro/Accelerometer Package

o Software Features
   o Kalman Angle Tracking Filter
   o Kalman Range Tracking Filter
   o Director Gun Fire Control Equations

PREFACE

This report was prepared by the McDonnell Douglas Corporation, St. Louis, Missouri, McDonnell Aircraft Company, Avionics Systems Technology Department under U.S. Air Force Contract F33615-73-C-1319. The program was administered by the Air Force Avionics Laboratory Systems Avionics Division, Wright-Patterson Air Force Base, Ohio. The Air Force project engineer directing the technical aspects of the study was Captain Richard H. Hackford Jr., AFAL/NVA.

This report summarizes the principal program activity of the Advanced Air-to-Air Gun Fire Control System Design Study, Project 7629, Task 762903, from June, 1973 to April, 1974.

The authors were R. L. Berg, who also served as Principal Investigator, Dr. W. J. Murphy, and D. E. Simmons. Contributions to this report from Messrs. J. S. Arnold, R. D. Schoeffel and G. W. Zirkle of McDonnell Aircraft Company are gratefully acknowledged. The authors also wish to acknowledge the technical guidance of Mr. E. A. Rosenkoetter, Manager, Electronics Systems Technology, McDonnell Aircraft.

The authors wish to thank Messrs. R. J. Daugherty and W. C. Feuchter, and Dr. R. R. Olson of Bendix Corporation Aerospace Systems Division; and Messrs. L. W. Burdette and J. J. O'Leary of General Electric Company Aerospace Electronics for their cooperation throughout the study.

Three report VOLUMES are published under separate cover due to their volume and, in the case of VOLUME II, to protect subcontractor proprietary rights. VOLUME II is subtitled ATS Angle Sensor Design Description, VOLUME III is subtitled ATS Range Sensor Design Description, and VOLUME IV is subtitled ATS Software Design Description.

This report was submitted by the authors in April, 1974.

1

TABLE OF CONTENTS

TABLE OF CONTENTS (Continued)

TABLE OF CONTENTS (Concluded)

LIST OF ILLUSTRATIONS

LIST OF TABLES

SECTION 1   INTRODUCTION AND SUMMARY

1.1   OBJECTIVES AND SCOPE OF THE AGFCS DESIGN STUDY

The Advanced Gun Fire Control System (AGFCS) program is a multi-phase program to investigate, through analysis, manned simulation and flight test evaluation, technical approaches which exhibit the potential of providing significant improvement in the effectiveness of present gun fire control systems employed in the aerial attack phase of the air superiority mission. Phase I, the AGFCS Definition Study, was a three-way, competitive gun fire control system definition study considering the overall general design, effectiveness, complexity, and mission requirements of a post-1976 time period air superiority aircraft.   Several systems and their performance parameters, requirements, risks and error budgets were defined.   Systems, from a simple baseline system to more complex systems, were defined in sufficient detail to allow subsequent detailed specification.

The purpose of Phase II, the AGFCS Design Study, was to design an Augmented Tracking System (ATS) for possible fabrication and flight test evaluation in a later phase of the AGFCS Program.   The ATS is defined to be the tracking sensors, the computer and the software used to process the tracking signals.   The task of the ATS is to determine the target-dependent variables which are required to solve the lead angle equation in a director mechanization of the AGFCS.   The ATS will ultimately serve as the core of an advanced gun fire control system.

This report describes the results of the AGFCS Design Study.   In the remainder of this section, the principal results are summarized in a discussion of the rationale and selection process used in the determination of the ATS configuration, subsystems and subcontractors.   Subsequent sections coincide with the task definitions in the contracted statement of work and describe the individual study items in detail.

Section 2 presents the general features of the ATS including a description of pilot utilization in a complete AGFCS configuration, a discussion of its automatic search/acquisition capability, a description of the ATS Kalman tracking filters and director gun fire control equations, and a summary of the ATS error budget.

Section 3 summarizes the principal ATS subsystem design features and interface requirements.   Detailed design descriptions are presented in appendices.

Section 4 presents the ATS performance analysis.   Included are detailed discussions on the ATS sensor math modeling, Kalman filter design, error sources and system performance considerations.

Section 5 summarizes the program planning activity which was undertaken throughout the study.   It includes options regarding follow-on procurement, fabrication and testing of ATS hardware.

11

VOLUME II presents a functional description of the ATS angle sensor, the Bendix ASCOT (Adaptive Scan Optical Tracker). Also presented in VOLUME II are detailed discussions of ASCOT design considerations. Since many of the design features incorporated in the ASCOT are proprietary to the Bendix Corporation, VOLUME II is submitted under limited rights provision.

VOLUME III presents a detailed description of the ATS range sensor, the General Electric Solid State Radar (SSR-1).

VOLUME IV presents documentation of the ATS software design. Computer flow charts and their descriptions are given in sufficient detail to allow assembly language programming in subsequent AGFCS program phases.

1.2 ATS CONFIGURATION

The ATS was configured as the basic element of a modular advanced gun fire control system similar to that described in the AGFCS Phase I final report. The general configuration of the overall AGFCS is depicted in Figure 1, identifying the ATS configuration as a modular subsystem, and including various augmenting and modifying system elements for growth potential. The salient features of the selected ATS configuration are the use of a strapdown, non-imaging electro-optical (EO) sensor in the angle tracking system and a strapdown, range-only radar in the range tracking
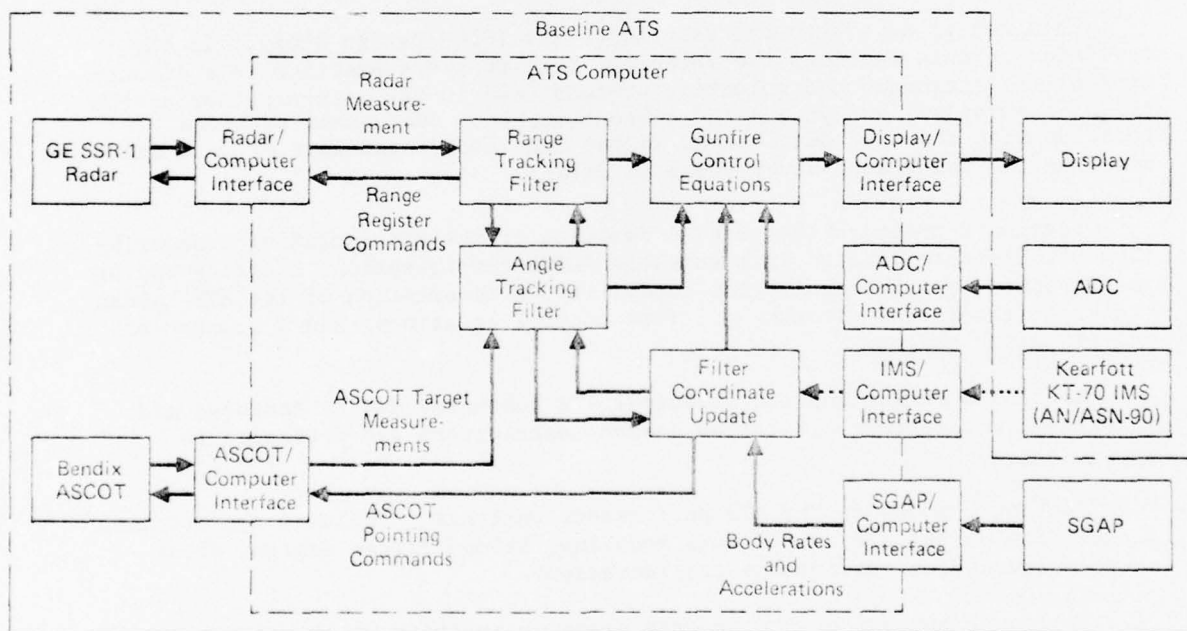
FIGURE 1
ATS CONFIGURATION

GP74-0122-41

12

system. Specifically, Figure 1 identifies the baseline ATS and its principal subsystem and software features as:

- o Principal Subsystems

  - o Bendix ASCOT (Adaptive Scan Optical Tracker)

  - o GE Solid-State, Range-Only Radar (SSR-1)

  - o ATS Digital Computer

  - o Strapdown Gyro/Accelerometer Package (SGAP)

- o Software Features

  - o Angle Tracking Filter

  - o Range Tracking Filter

  - o Director Gun Fire Control Equations

It is noted that, while the strapdown gyro/accelerometer package (SGAP) is the selected baseline approach to the measurement of ownship body rates and accelerations, provision is made in the ATS software to accept measurements from a gimballed inertial measurement set as an alternate mechanization. Each of the hardware and software elements selected for the ATS configuration is described in detail in Sections 2 and 3, together with their interface. In this subsection some of the principal considerations leading to their selection are summarized.

1.2.1 ATS Hardware Configuration Considerations

The selected ATS sensors can be characterized by the following features: 1) a strapdown design approach is used throughout; 2) the angle sensor is an electro-optical (EO), non-imaging device; and 3) the range sensor is a range-only radar. Each of these features and their principal alternatives is discussed below.

1.2.1.1 Selection of Strapdown Rather Than Gimballed Sensors - Some of the principal reasons that strapdown sensors rather than gimballed sensors were selected for the ATS are:

- o Strapdown sensors are inherently less complex than gimballed sensors. A strapdown ATS will, therefore, be less expensive, more easily maintained, more reliable, weigh less and take up less space than its gimballed counterpart.

- o Strapdown angle sensors and range sensors with sufficiently wide fields-of-view for air-to-air gunnery were available for ATS development.

13

o Stabilization of the strapdown angle sensor is conveniently and accurately accomplished through the use of a medium quality strapdown gyro/accelerometer package (SGAP). The SGAP provides high data rate measurements of ownship body rates for sensor stabilization without the need to derive rates from inertial platform data.

o Growth potential exists for employing flight control system quality gyros and accelerometers for the SGAP as their requirements increase for fly-by-wire and control configured vehicle (CCV) applications. This would provide a hardware base for integrated fire/flight control systems.

o The strapdown AGFCS approach is consistent with a low-cost, light-weight approach to air superiority aircraft.

1.2.1.2 Selection of EO Rather Than IR Angle Sensor - Some of the principal reasons that an EO rather than IR type sensor was selected for the ATS are:

o EO devices require smaller entrance apertures (optical windows) which increases their installation flexibility and reduces the aerodynamic drag penalty.

o The EO centroid of a target (particularly for the case of a non-imaging sensor) more nearly matches the target center-of-gravity than does its IR centroid.

o The EO target centroid (particularly for the case of a non-imaging sensor) is more stable. This is particularly evidenced during angle-off changes. These changes generally cause the IR centroid to drift across the target yielding erroneous line-of-sight rates which are difficult to discriminate in the tracking filter.

o EO sensors require no special environmental control as opposed to the cooling requirements of an IR sensor. The fast reaction time required during air-to-air gunnery poses particularly demanding problems with IR sensors unless they are maintained at operating temperature throughout a major portion of the mission. This, in turn, poses weight problems depending somewhat on the approach to the cooling task.

o Since the EO target signature is more closely correlated with target projected area, it can be made less sensitive to range changes. For this reason it is also more amenable to stadiametric ranging techniques.

o Most of the advantageous features of IR (e.g., visibility through clouds, at night, and during other poor visibility conditions) are not applicable to the requirements established for the AGFCS, particularly the initial austere version.

1.2.1.3 Selection of Non-Imaging Rather Than Imaging Angle Sensor - A non-imaging rather than an imaging EO sensor configuration was selected for the following reasons:

o The non-imaging approach requires no storage of data prior to error processing, whereas all imaging approaches require the storage of data to generate an image prior to producing an error signal. Elimination of the data storage requirements permits higher tracking loop data rates for non-imaging sensors resulting in reduced lock-on times, increased maintain-lock capability under very dynamic conditions, and decreased system complexity.

o Non-imaging sensors are basically less sensitive to sun glint and other preferential optical targets within the overall target shape. As a consequence, their noise characteristic tends to be more continuous without the step changes (discontinuities) which appear to be characteristic of most imaging sensors, both EO and IR.

o The combination of high data rates and continuous wide-band noise permits a significant system improvement by employing a high-frequency analog tracking loop closure in conjunction with a rudimentary digital prefilter and low-frequency Kalman filter processing.

o Because of its relative simplicity, a non-imaging approach is less expensive, more reliable, and more easily maintained than an imaging approach.

o If an image is desired for the purpose of aiding in target identification and attitude cueing (which are desirable features in conjunction with a Helmet Sight/Display), or if an image is desired to enhance system evaluation during flight test, one can be provided by a parallel optical path and an associated imaging system for display purposes without disturbing the basic advantages of the non-imaging tracking systems.

1.2.1.4 <u>Selection of Radar Rather Than Laser Range Sensor</u> - A radar rather than a laser type sensor has been selected for the initial austere ATS for the following reasons:

o Radar is a well-established technology with demonstrated performance capability in air-to-air ranging with little or no aid from external sources.

o While laser technology is becoming well established in air-to-ground applications, the narrow beams involved require highly accurate pointing from an external source to achieve air-to-air ranging. Alternately, the beam can be spoiled to relieve the pointing accuracy requirement but this results in decreased range capability or increased power requirements and associated increased size, weight, and system complexity.

o A directly applicable low-weight, low-cost Radar system existed in a hardware state which permitted the direction of maximum effort in the AGFCS Phase II study to the design and development of the more critical angle sensor.

o While a variety of generally applicable Laser Rangers exist in a hardware state, they all require a significant degree of development for application to air-to-air ranging which would detract from the current emphasis being placed on the angle sensor development.

o Radar ranging provides either a conventional Lead Computing Optical Sight (LCOS) mode or a range-designator Tracer Sight mode in the event of failure of the angle sensor and prior to lock-on of the angle sensor.

o Since a Laser Ranger would depend on the angle sensor and the angle tracking filter, the only back-up to a full operating Director Mode would be a no-range tracer mode, or a fixed-range LCOS mode. A no-range tracer mode provides poor aid to the lock-on task. A fixed-range LCOS mode, while it provides suitable aid to the lock-on task, yields an ineffective gunnery solution prior to transition to the Director mode.

In addition to the considerations listed above, the following additional considerations become pertinent when growth potential is considered:

o In a growth potential version, Radar can provide a wider field-of-view than that required for the angle sensor, particularly with a gimballed or phased-array antenna. This provides range/range-rate signals during the acquisition phase of gunnery encounters which are useful for pilot displays and for automatic range control systems.

o A Laser Ranger is restricted to the field-of-view of the associated angle sensor. Therefore, a wide field-of-view range capability is achieved at the expense of a large optical window with its attendant installation problems and high aerodynamic drag penalties.

o Radar permits a more convenient modular approach, employing different antenna configurations and transmitter powers, to yield desired performance characteristics over a wide range of applications.

o Since Radar systems are already included on all of the existing aircraft of interest, AGFCS effort directed to radar ranging would provide a more effective means of updating these aircraft to an AGFCS capability.

o Radar ranging permits a growth capability to include radar angle tracking which can aid the primary EO angle tracking system in lock-on and can provide tracking augmentation during periods of weak signal of the primary system. It can also provide an independent Director mode prior to lock-on of the primary angle sensor or a back-up Director mode in the event of failure of the primary sensor.

o After having selected a strapdown angle sensor, the selection of a Laser Ranger is less desirable because its requirement for a gimbal system poses alignment problems between the two sensors. That is,

errors in both the computed line-of-sight angles of the strapdown
sensor and the gimbal angle readouts of the Laser Ranger *affect the*
correlation between the two line-of-sight orientations. This requires
an increase in laser beam width to ensure sufficient target radiation
for range measurements.

o The above situation can be alleviated by a common mounting of the
angle and laser sensors. However, this precludes the use of a strap-
down approach for the angle sensor and leads to a significant increase
in system complexity. While this configuration represents a viable
approach to a growth potential system, it does not appear to show
promise of a low-cost, low-risk system to the same degree that is
expected for the selected ATS configuration.

1.2.2 ATS Hardware Subcontractor Selection

As a result of the hardware considerations summarized in the previous
subsection, ATS hardware subcontractors were selected to provide: 1) a strap-
down, non-imaging EO angle sensor and 2) a strapdown range-only radar. The
angle sensor selected was the Bendix Corporation ASCOT (Adaptive Scan Optical
Tracker); while the range sensor selected was the General Electric Solid State
Radar (SSR-1). Both of these systems provided the basic sensor requirements
demanded of the ATS application, particularly the wide fields-of-view demanded
of strapdown sensors, and the technical maturity required for timely fabrica-
tion for flight test in later program phases.

Summaries of ASCOT and SSR-1 design features are presented in Subsections
3.2 and 3.3 respectively. Both can be fabricated within six months.

1.2.3 ATS Software Configuration Considerations

The selected ATS software configuration can be characterized by the
following features: 1) the ATS utilizes three Kalman tracking filters, two
independent Angle Tracking Filters and a Range Tracking Filter; 2) filtering
is accomplished in a set of roll-stabilized line-of-sight (LOS) coordinates;
3) filter coordinate updating utilizes a four-element quaternion representa-
tion in conjunction with Angle Tracking Filter and SGAP outputs; and 4) Kalman
tracking filter state variables are selected for convenient interface with
the ATS angle and range sensors.

The basic approach to the ATS Kalman tracking filter design was developed
during the AGFCS Phase 1 definition study, Reference 1. Modifications were
made to accommodate the strapdown angle and range sensors. The tracking filter
design approach is discussed in detail in Subsections 2.4 and 4.3.

The utilization of Kalman Range and Angle Tracking Filters in the ATS is
considered a highly important feature of the ATS design. First, through the
use of optimal filtering design techniques, estimates of the target's posi-
tion, velocity and acceleration are obtained during gun attack situations
with sufficient accuracy to significantly improve gunnery performance.
Second, because of the adaptive gain features of the Kalman filter gain com-
putations, the high Angle Tracking Filter gains at initial target acquisition,

coupled with the use of stabilized pointing commands, is expected to substantially improve the acquisition capability of the strapdown ATS angle sensor. Finally, a significant advantage in employing a Kalman tracking filter in the ATS is that the filter's increased memory and prediction capability permits effective operation for significant intervals without measurements by employing extrapolate tracking modes. During acquisition periods, when oscillatory steering characteristics cause the target to periodically leave the respective sensors' fields-of-view, no loss of tracking capability results with such extrapolate modes. While a momentary decrease in accuracy occurs during such periods of no measurements, the basic tracking system accuracy is quickly restored soon after measurements are restored, without the need for recycling through the original search/acquisition/ tracking sequence. Thus, full system accuracy can be anticipated in most cases prior to times of gunfire. In any case, the periodic loss of measurement inputs has little or no impact on system operation regarding pilot tasks or system transients.

The significance of the extrapolate tracking modes is that the basic requirements of coarse tracking and present position estimation over a wide field-of-view are satisfied without imposing physically large field-of-view requirements on the sensors themselves. Furthermore, the requirements of precision tracking, present position estimation, and future position prediction are satisfied by the selected strapdown ATS configuration over the smaller field-of-view associated with actual periods of gunfire.

1.3 ATS PERFORMANCE SUMMARY

ATS performance considerations are presented in Subsection 4.4. A principal consideration in the ATS design was its performance under dynamic conditions. Dynamic design and analysis was performed using a CDC 6600 digital computer simulation of the ATS Range and Angle Tracking Filters in conjunction with the MCAIR Terminal Aerial Gunnery Simulation (TAGS) program, Reference 1. TAGS provides realistic relative geometry and adjustable measurement noise conditions for filter testing.

1.3.1 Effect of SSR-1 Error Sources

The principal error contributions of the SSR-1 radar are: 1) a random error which varies as a function of radar signal-to-noise ratio and range glint effects, and 2) a systematic error which can be as large as 80 feet at short range (500 feet) if not compensated. For the relatively short ranges pertinent in air-to-air gunnery combat (less than 3000 feet), the range glint term predominates the random radar errors and results in approximately 12 feet (1σ) of error. This error source in combination with the ATS Kalman Range Tracking Filter results in target state estimation errors (1σ) along the line of sight of approximately: 1) 4 feet in range; 2) 10 feet/second in range rate; and 3) 20 feet/second^2 in range acceleration.

The short-range systematic error is compensated for in the Range Tracking filter insofar as it is predictable. Compensation reduces this error to 35 feet at 500 feet of range. At 1000 feet this error contribution is

18

negligible and the total range bias error is approximately 20 feet. The predominant effect of a range bias error is in the estimated range state of the Range Tracking Filter. The range measurement bias reflects directly into an error in estimated range; there is no effect on either the estimated range rate or range acceleration. A secondary effect of range bias error is an error in estimated target velocity normal to the line-of-sight as computed in the Angle Tracking Filter. This error is given by the product of the line-of-sight rate with the range bias error. For example, a range bias error of 20 feet will produce, approximately, a 3 feet/second error in estimated target velocity with a 10 degree/second line-of-sight rate.

1.3.2 Effect of ASCOT Error Sources

The error contributors of the ASCOT are not as well defined as those of the SSR-1. Analysis indicates that the effect of atmospheric and receiver noise are negligible in comparison with even small amounts (.5 feet) of glint error. Glint error denotes here the displacement of the contrast centroid as measured by the ASCOT from the geometric centroid of the target. While the ASCOT is designed to minimize the glint error, its magnitude is unknown and, hence, the ATS angle tracking accuracy is impossible to quantify accurately until experimental results are obtained in follow-on effort.

However, it is possible to provide some indication of ATS angle tracking performance. An error budget of 2.5 milliradians(1σ) has been established as an upper limit to the error in the measured angle sensor pointing direction at maximum firing range (3000 ft). This measurement error in combination with a matched ATS Angle Tracking Filter and 10-sample prefiltering will provide pointing errors (1σ) of less than 1.5 feet and errors in estimated velocity normal to the line-of-sight of slightly more than 10 feet/second for range conditions of 3000 feet and less.

1.3.3 Effect of SGAP Error Sources

The predominant errors of the strapdown gyro/acceleration package (SGAP) selected for the ATS design are deterministic errors which are sensitive to both ownship body rates and acceleration. For the nearly constant body rates and accelerations which exist during gunnery solutions, these errors result in an effective bias on each of the rate gyros' measurements. The primary effect of rate gyro bias is to bias the estimate of relative velocity normal to the line-of-sight. This error is given by the product of the gyro error and range. The maximum rate gyro error anticipated is 1.5 milli-radians/second resulting from command rate scale factor error. Thus at maximum range (3000 feet) the error in estimated velocity due to gyro bias will be about 4.5 feet/second.

SECTION 2   ATS CONFIGURATION DEFINITION

2.1   GENERAL

Detailed ATS subsystem design and interface considerations are discussed
in Section 3.   The following subsections describe the operational features of
the ATS, particularly its automatic search and acquisition capability, a
general description of the ATS Kalman tracking filters, the director sight
algorithms and ATS error budgets.

2.2   ASSUMED SCENARIO APPLICABLE TO ATS CONFIGURATION

The ATS configuration is postulated on gunnery situations in which the
attacking pilot successfully accomplishes the acquisition phase without
assistance from the AGFCS, and has the target in the general field-of-view
applicable to gunfire with a fixed gun.   Up to this time it is postulated
that his sight display will be a Damped Tracer Line with no measured-range
designator.   Upon achieving the above encounter geometry situation (which
is within the field-of-view of the range sensor), measured range is auto-
matically obtained and a corresponding reticle added to the Damped Tracer
Line.   Prior to range lock-on, the angle sensor search field is centered
on the gun cross.   After range lock-on, the angle sensor search field remains
centered on the gun cross if measured range exceeds the maximum effective
gun-firing range.   (This is done because gun-cross tracking is the convention-
al acquisition technique employed while outside of firing range.)

When the target moves into the search field of the angle sensor
(depending on the pilot's skill in flying the Damped Tracer sight), the
angle sensor will lock on, convert to its tracking mode, and supply data
necessary to perform a Director Line sight computation.   When the Director
Line becomes available, the Damped Tracer Line is blended with the Director
Line (including the blending of the respective reticles) such that the
display transitions to a Director Line Sight.   If angle lock-on is not achiev-
ed when the measured range is less than the maximum effective gun-firing
range, the angle sensor search field will be centered on the Damped Tracer
Line reticle.   This permits attack with the Damped Tracer Line sight, while
retaining the potential for subsequent angle lock-on and transition to a
Director Line sight.

During the transition from Damped Tracer to Director, the pilot will
also transition from a Damped Tracer steering technique (i.e., bringing
the target and reticle slowly through successive coincidences, attempting
to decrease the amplitude of the excursions with each tracking cycle) to a
Director steering technique (i.e., bringing the target and reticle into
coincidence and attempting to maintain a tracking situation).   During this
transition, the pilot's firing logic will be a blend of those applicable to
a Damped Tracer and to a Director sight.   After the transition, the pilot
will employ the sight as a Director, firing at the time of target/reticle
coincidence.

It is apparent from the above that, for the basic AGFCS configuration described, pilot skill remains an important ingredient in the problem, depending to some degree on the size of the angle sensor's search field. This will, of course, remain the case for any fixed-gun system in which the pilot retains the terminal steering or gun-pointing task.

The pilot steering task would be relieved somewhat if a Helmet Sight were added to the AGFCS, since the angle sensor's lock-on and the transition to a Director reticle would be possible without the prior requirement of Damped Tracer steering. The pilot steering task would be further relieved with the addition of a gimballed gun or the use of an aircraft employing independent fuselage control capability since, after director computation is achieved, the precision gun pointing would be accomplished automatically. The pilot steering task would be relieved almost completely if, after director computation is achieved, the attack aircraft were flown automatically through the flight control system.

To best establish the adequacy of the proposed AGFCS configuration, it is useful to consider the potential advantages of an increased total field-of-view. Relative to the angle sensor, it is clear that lock-on could be achieved sooner with a larger total field-of-view. However, this would occur only if the sensor's search field could be positioned in the vicinity of the target by some external method. Only through the use of a Helmet Sight, or some other similar cueing device, would this be possible. The time required to search a large field-of-view to locate a target with an EO sensor is prohibitive.

To further consider the adequacy of the limited field-of-view of the selected ATS hardware, let us assume that an angle lock-on at a larger target bearing is achieved as a result of a larger sensor field-of-view. It is of little value to effect a corresponding director computation at the large bearing angle, unless the system is to be used either: 1) to automatically steer the aircraft in an acquisition mode; or 2) to direct a gimballed gun having large degrees of freedom to a corresponding gun-pointing solution. In all other cases, the director information is available for a considerable time prior to one's ability to make effective use of it. Furthermore, even in the case of a fixed gun or a gimballed gun with a small amount of freedom, automatic steering would be equally or more effective if it were based on the line-of-sight data alone until the target is closer to a gun solution. Accordingly, for an AGFCS which includes a Helmet Sight (as it might for an ultimate AGFCS), it would be better to base such automatic steering commands on the Helmet Sight measurements rather than on an automatic tracking system.

From the above discussion it is clear that the only significant advantage of a target lock-on at high bearing angles is that the tracking function is initiated and the director computation already available when the target is brought into the gun firing field-of-view. However, if the time from search initiation to director computation is kept suitably small, this advantage can be of little value in view of the corresponding penalty

in system complexity. The critical requirement, therefore, of a system with limited field-of-view sensors (such as the ATS configuration), is that the search/acquisition/tracking sequence must be accomplished in a minimal time. Accordingly, this feature has been given primary attention in our design efforts.

2.3 ATS AUTOMATIC SEARCH/ACQUISITION CAPABILITY

As mentioned in the previous subsection, it is expected that under normal circumstances radar lock-on will occur prior to ASCOT lock-on. Design details concerning the ASCOT and SSR-1 search, detection and acquisition sequences are discussed in detail in VOLUMES II & III , respectively. In this subsection the principal features of the SSR-1 and ASCOT automatic search and detection capability, and the initialization of the ATS tracking filters are discussed.

2.3.1 Range Search, Acquisition and Tracking Filter Initialization

The search procedure of the SSR-1 is summarized in Figure 2. Basically, an 800 feet search interval is stepped out in range every 1/32 of a second in steps of 750 feet until the maximum search range is attained. The SRR-1 has manually selectable maximum search range options of 3000, 6000 and 24,000 feet. For the ATS application the 6000 feet option will normally be selected. Therefore, the ATS range search will require 0.25 second under normal circumstances and 1 second at most.
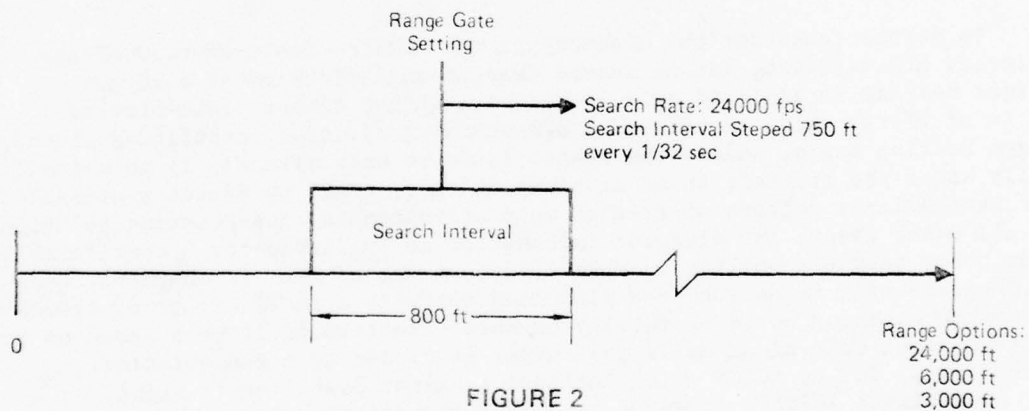
FIGURE 2
SSR-1 SEARCH PROCEDURE

GP74-0122-44

The search interval is stepped out by incrementing the SSR-1 digital range register by a fixed amount every 1/32 second until the maximum range is reached. It is then reset. Since the SSR-1 pulse repetition frequency (PRF) is 1024 Hz, this allows the integration of 32 potential return pulses in the search interval for threshold detection. If the integrated returns do not exceed a pre-established threshold, the range register is incremented by 750 feet. If the integrated returns exceed the threshold, a detection discrete is set and a 0.25 second acquisition period is entered. During the

22

acquisition period the range register is adjusted every 1/64 second so that the range tracking gates are centered about the average of the return signal (during acquisition and tracking 16-pulse integration is utilized). The total amount of the range-register adjustment during this 0.25 acquisition period provides a range-rate approximation to initialize the SSR-1 range-rate register. At the end of the acquisition period, providing the detection signal is maintained, the SSR-1 initiates its tracking mode by setting an acquisition (lock-on) discrete.

The acquisition discrete is monitored by the ATS computer at a 64 Hz rate. Upon noting that the SSR-1 has acquired, the ATS computer requests the contents of the SSR-1 range and range-rate registers. These values are then used to initialize the ATS Range Tracking Filter (see Subsection 2.4.3). After filter initialization, the ATS computer commands the SSR-1 to its Augmented Mode which opens the SSR-1's internal tracking loop and provides range-register settings to the SSR-1 every 1/64 second. In its Augmented Mode the SSR-1: 1) loads its range register with the range estimate provided by the ATS computer; 2) integrates the return signal over the next 16 return pulses to measure the error in the range register setting; and 3) adds the measured range-register correction to the range register contents to provide a 16-sample, smoothed range measurement to the ATS computer every 1/64 second.

Summarizing the normal time required for range search, acquisition and tracking filter initialization, assuming a target is within the SSR-1's field-of-view and 6000 feet search range:

o Maximum Search Duration - 0.250 second
o Acquisition Duration - 0.250 second
o Range Tracking Filter Initialization - 0.017 second

Thus, the ATS automatic range search/acquisition capability normally requires slightly over 1/2 second. If the maximum search range option is used, target acquisition could take as long as 1.25 seconds.

2.3.2 Angle Search, Acquisition and Tracking Filter Initialization

The search procedure of the ASCOT is summarized in Figure 3. Basically, a square search field is raster scanned and the ASCOT detection video is monitored by a threshold detector (see VOLUME II., Section 2). When the detection video exceeds a pre-established detection threshold, a detection discrete is generated. This detection discrete triggers the ASCOT acquisition sequence discussed in the following paragraphs. As indicated in Figure 3, alternate ASCOT search field sizes are provided in the ATS design. These alternate search field sizes are manually selectable and provide either a 2° x 2° or a 5° x 5° search field. The penalty paid for the larger field size is the correspondingly smaller search frame rate. Thus, the trade-off during automatic search is the requirement for increased pointing accuracy on the part of the pilot versus the amount of time required to completely scan the search field. This trade-off was considered of such importance that the two search field options were provided to allow evaluation during ATS flight testing.

5° x 5° Search Field

Pilot Selected Size
ATS Computer Selected Location

2° x 2° Search Field

Search Frame Rate: 4/sec

Search Frame Rate: 2/sec
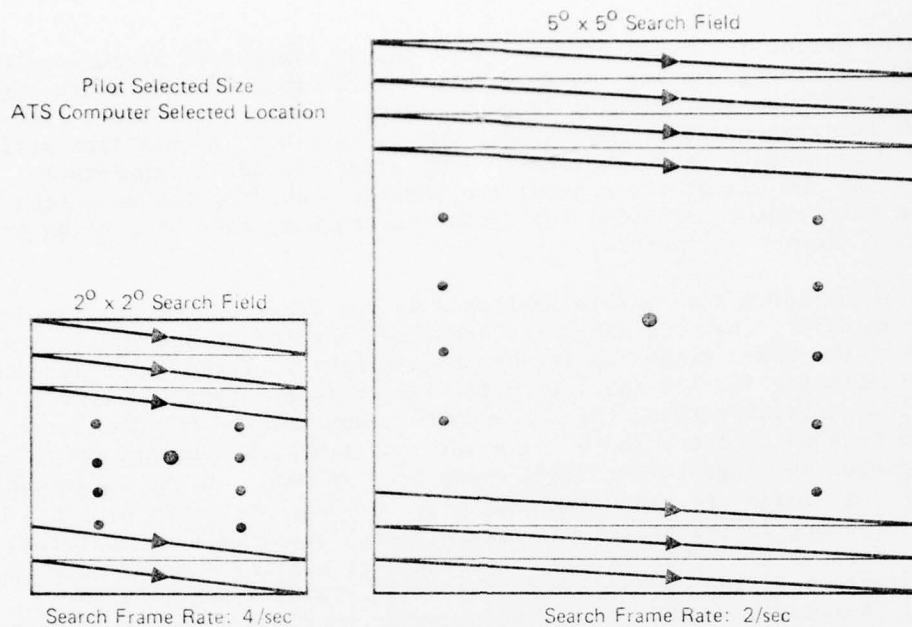
FIGURE 3
ASCOT SEARCH PROCEDURE

GP74-0122-43

As Figure 3 indicates the location of the ASCOT search field is established by the ATS computer. During initial search the ASCOT will be directed to point along a body-fixed, initial-acquisition axis for ATS flight tests. When incorporated into a complete AGFCS, the ASCOT search field will be directed to point at the gun cross if the radar has not locked on, or if measured range exceeds maximum effective firing range. If ASCOT is not yet locked on when measured range is below maximum effective firing range the search field will be directed to point at the Damped Tracer sight reticle.

After detection the ASCOT enters its acquisition sequence. This sequence consists of several coordinated actions by both the ASCOT and the ATS computer. Immediately upon the setting of the detection discrete the ASCOT stores the location of the detected target in the search field and transmits this location to the ATS computer on request. The ATS computer monitors the ASCOT detection discrete at a 160 Hz rate. Thus, the ATS computer is aware of detection almost immediately.

The period after detection is a trial period during which the ASCOT establishes whether or not the detection signal was based upon a valid target or a false alarm. Target authenticity is established on the basis of two criteria. First, the target must have a closed shape and, second, it must not exceed a computable maximum size. Therefore, before detection the maximum target angular size is computed (based on measured range and target wing span) and transmitted to the ASCOT. If range lock-on has not occurred a maximum allowable target size is used. The ASCOT then tests the region about the

24

point of detection in the search field to determine if a closed-shape of sufficient contrast with respect to the background is present. A total of 150 milliseconds are allowed for target verification. If a valid target is not identified in 150 milliseconds, the ASCOT reverts to its search mode after a 40 millisecond delay to allow for switching transients. If a valid target is detected an acquisition discrete is set.

At detection, i.e., after receipt of the ASCOT detection discrete, the ATS computer requests the location of the, as yet unvalidated, target. During the period in which the ASCOT passes judgement on the detection, the ATS computer initializes the Kalman Angle Tracking Filter (see Subsection 2.4.2) and provides a stabilized pointing command to the ASCOT. The Angle Tracking Filter is not completely energized, however, until the ASCOT acquisition discrete indicates that a valid target has been detected. The Angle Tracking Filter is initialized by establishing a coordinate transformation between the aircraft body axes and the line-of-sight (LOS) along the point of detection. The Angle Tracking Filter states utilized are elevation and traverse pointing error, relative target velocity orthogonal to the LOS and target acceleration orthogonal to the LOS. The filter states are initialized based upon measured target range, and ownship body rates and accelerations.

Until the acquisition discrete is set the Angle Tracking Filter's gains are zero, thereby causing the filter to extrapolate target motion based on its initial conditions and ownship motion only. The extrapolated target motion is used to update the body-to-LOS transformation from which a stabilized ASCOT pointing command is computed and transmitted to the ASCOT. In this way the ASCOT tests that region in space in which a detection was obtained (and its extrapolated position) rather than test a fixed region with respect to the aircraft body. This effectively isolates the acquisition process from ownship motion.

If the acquisition discrete is not set after 190 milliseconds, the detection is considered a false alarm and the system reverts to its search mode. That is, the ATS computer resets the body-to-LOS transformation to its fixed, initial-acquisition search position and commands the ASCOT to that search position. Simultaneously the ASCOT reverts to its search mode.

If the acquisition discrete is set before the 190 milliseconds transpire, the Angle Tracking Filter gains are computed from measured range, range rate and the extrapolated filter covariance matrix. The ASCOT tracking loop is automatically closed to provide a measure of pointing error. The measured pointing error is transmitted to the ATS computer where it is used to update the Kalman Angle Tracking Filter's state variable estimates. This completes the acquisition process.

Summarizing the maximum time required for angle search, acquisition and tracking filter initialization, assuming a target is within the ASCOT's search field and its detection range:

o Maximum Search Duration - 0.25 second for 2° x 2° search field, or
                                               0.5 second for 5° x 5° searc.. field

o   Acquisition Duration – 0.150 second

o   Angle Tracking Filter Initialization – 0.017 second

Thus, the automatic angle search/acquisition capability requires a maximum of slightly over 0.6 second for the large search field and slightly over 0.4 second for the small search field.

2.4   ATS KALMAN TRACKING FILTERS

The Kalman tracking filters are principal elements in the ATS. These filters have been briefly discussed in the preceding subsection in conjunction with the ATS automatic search/acquisition capability. A detailed discussion of the filter design procedure and its performance are presented in Section 4. However, because of the fundamental importance of the filter structure and its interface with the ASCOT and SSR-1, a general discussion of the ATS filter design and its relation to the principal sensors are presented here.

2.4.1   Selection of Sensor/Kalman Tracking Filter Configuration

Of primary importance in the design of the ATS configuration was the selection of the ASCOT and SSR-1 interface with the Kalman filter. Three of the principal sensor/Kalman filter configuration alternatives are shown in simplified, block diagram form in Figure 4. Because of the importance of selecting a configuration which best accomplished the goals of both the overall AGFCS program and the ATS design and flight test, the selection rationale is presented here in some detail.

2.4.1.1   Internal Feedback Structure – The first configuration shown in Figure 4(A) is by far the most common approach. It consists of an error detecting sensor used as an element in a tightly controlled feedback loop. By nulling the output of the error detecting sensor a measurement, M, of the physical variable, A, is provided. The control action usually takes the form of either a high-gain proportional control or an integral control, or their combination. This loop must be tightly closed since an accurate measurement is provided only when the detected error is small. The measurement is then used to improve the accuracy of the estimated state variables in the Kalman filter. Since the estimated system state variables are not used to control the sensor, this is an open-loop structure from the overall system standpoint; only internal feedback is used to direct the sensor. Hence, this configuration has been termed an "internal feedback structure".

The major weakness of this structure is its complete dependence upon the independent functioning of the measurement device. Many angle tracker designs making use of two-axis systems have exhibited poor tracking performance due to an inappropriate choice of coordinate reference frames. These systems have used non-roll-stabilized line-of-sight coordinates associated directly with the sensor as their computation frame (where roll applies to motion about the line-of-sight). This failure to perform filtering or smoothing operations in a suitable stable coordinate frame causes either of two tracking
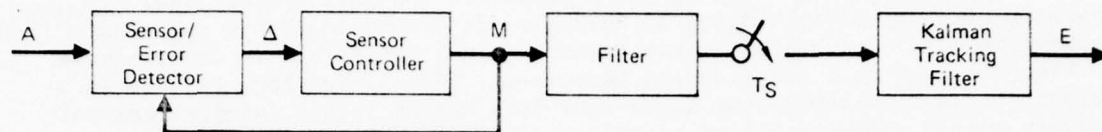
(A) Internal Feedback Structure
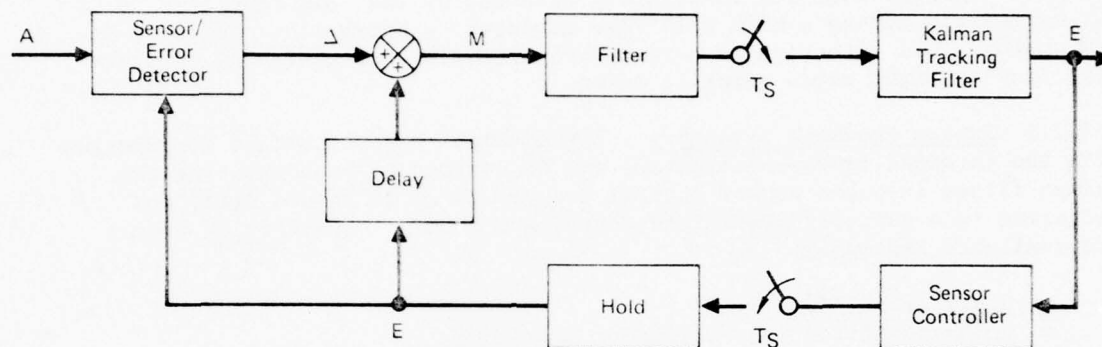
(B) System Feedback Structure
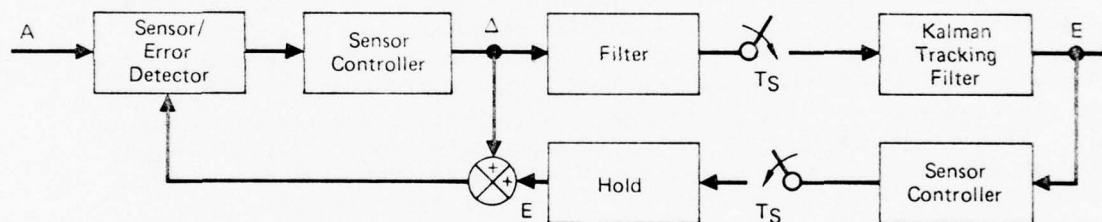
(C) Combined Internal/System Feedback Structure

A — Actual Target Variable (s)
M — Measured Target Variable (s)
E — Estimated Target Variable (s)
Δ — Error Signal

FIGURE 4
PRINCIPAL SENSOR/KALMAN FILTER CONFIGURATION ALTERNATIVES

GP74-0122-42

difficulties. If high-gain proportional channels are used to maintain tracking loop lock under highly dynamic conditions, there is a marked tendency to break lock in the presence of background clutter or target fading. This is due to the absence of angle-rate memory signals in the tracking channels that are strong enough to carry the tracker through periods of signal degradation.

27

On the other hand, tracking loops which use low-gain proportional channels with appropriate integral channels (to provide suitable angle-rate memory signals to minimize tracker dynamic error) break lock in the presence of high attacker roll rates during maneuvers. This is due to a failure to properly transform the vector angle-rate data stored in the integral channel signals into a roll-stabilized coordinate frame. As a result, the space orientation of the resultant vector angle rate of the tracker is not maintained independent of roll motion. The vector angle rate should be momentarily maintained because neither the magnitude nor the direction of the line-of-sight rate are immediately affected by the roll rate. If it is not maintained during a high roll rate maneuver, a break-lock condition is commanded. This situation is particularly prevalent at short ranges where high line-of-sight rates normally exist.

2.4.1.2 System Feedback Structure - The difficulty described in conjunction with the internal feedback structure can be avoided by incorporating the Kalman filter into the sensor control loop as shown in Figure 4(B), and filtering in a suitably stabilized coordinate frame. A variety of frames are available including:

o Earth coordinates
o Roll-stabilized line-of-sight coordinates
o Roll-stabilized attacker wind-axis coordinates, and others.

From this set of available coordinate frames, a roll-stabilized line-of-sight coordinate system was selected. In addition to avoiding the difficulties cited above, the selection of this coordinate system for tracking loop computations yields a more systematic variation of the corresponding target states, thereby contributing to improved target estimation and prediction. This can easily be seen in the case of a steady-state turning encounter in which the attacker turn rate, the target turn rate, and the line-of-sight rate are all equal. In this case the line-of-sight rate and the target acceleration are both constant in the roll-stabilized line-of-sight coordinate system. On the other hand, if an earth coordinate system were employed, both the corresponding target velocity and acceleration would be time-varying and hence more difficult to estimate in the filter computations.

In progressing from the internal feedback structure of Figure 4(A) to the system feedback structure of Figure 4(B), the following key changes take place in addition to the use of stabilized coordinates for control purposes:

o In the internal feedback structure the measured variable, M, is
   directly available. In the system feedback structure, the error
   (pointing error or ranging error) is measured directly and the
   total measured variable (angle or range) is determined by adding
   the measured error to the estimated variable.

o The measurement noise in the internal feedback structure is colored,
   with its spectral content being a function of the closed-loop
   response of the measurement device (usually of low bandwidth and
   changing with signal-to-noise level). In the system feedback

structure, the measurement noise is essentially that of the sensor itself, colored only by the prefiltering deemed desirable.

o The system feedback structure has the potential of using state variable feedback in the sensor/tracker control loop.

o The control signal in the system feedback structure has a much lower data rate than that of the internal feedback structure, caused both by the filtering action of the Kalman filter and the sampling interval used in the digital computer.

This system feedback structure was selected for the ATS SSR-1/Range Tracking Filter interface. It was ideally suited for this purpose due to the digital SSR-1 design philosophy. The estimated target range is transmitted directly to the SSR-1 where it is loaded into the range register, thereby positioning the range gates. The radar returns are integrated over 16 returns to generate a range correction every 1/64 second. The measured range correction is added to the range register contents to provide the total range measurement. After updating the Range Tracking Filter, the range register is reloaded with the current range estimate. The 64 Hz interface rate was selected to assure that the target will remain within the 100 feet tracking gates even during high closing rate conditions.

2.4.1.3 Combined Internal/System Feedback Structure - The system feedback structure provides the principal advantage that the sensor control law is based upon the full set of system state variables in roll-stabilized coordinates. However, it does not permit as timely and tight a control as that inherent in the internal feedback structure. Accordingly, it is sometimes desirable to achieve the advantages of both structures through the combined internal/system feedback structure shown in Figure 4(C). In this structure, the basic sensor control is obtained from the Kalman filter. However, it is blended with a vernier control obtained by internal feedback. The purpose of the basic control is to provide a reference pointing command which utilizes the estimated state variables of the system and is refreshed at a sufficiently fast rate to isolate the sensor from ownship motion. The purpose of the vernier control is to maintain a tight, fast-responding control loop through the use of integral action. Since the vernier control need only provide minor corrections to the reference pointing command, the break-lock problems associated with the internal feedback structure are avoided.

It was found that this interface structure was best suited for the ATS ASCOT/Angle Tracking Filter interface. Minimal modifications were required and the advantages of tight internal loop closure coupled with the ability to isolate the ASCOT from ownship motion through the ATS computer were primary considerations. The requirement to isolate the ASCOT from ownship motion dictated the use of a relatively high interface rate (160 Hz).

A significant advantage of both the system feedback structure and the combined internal/system feedback structure, particularly when used in conjunction with limited field-of-view sensors, is that the use of

extrapolate modes in the ATS configuration is facilitated. As the target moves out of either sensor's total field-of-view, the extrapolate mode of the corresponding Kalman filter is enabled. In this mode, the target motion is projected into the future based on estimated target state variables at the start of the extrapolate mode. During the extrapolation period, the reference control signal places the sensor's search field (ASCOT or SSR-1, as appropriate) at that location in its total field-of-view where the target is expected to reappear. During an extrapolation period, target state information would continually be supplied to the fire control equations in an AGFCS but at reduced accuracy. The extrapolation accuracy depends upon the duration of extrapolation, the quality of the target state estimates at the start of extrapolation, and the target's maneuvering during extrapolation.

2.4.2 ATS Angle Tracking Filter

The ATS tracking filter equations are composed of three separate but interconnected filters: two independent Angle Tracking Filters in LOS elevation and traverse coordinates; and a Range Tracking Filter. A detailed presentation of the ATS tracking filter design procedure is given in Section 4. In this subsection the basic structure of the ATS Angle Tracking Filter is presented and the Range Tracking Filter structure is given in the following subsection.

The equations of both the elevation and traverse ATS Angle Tracking Filters are similar and are presented in Figure 5. As shown in the figure, both angle filters utilize range and range-rate estimates. The state variables of each Angle Tracking Filter are the respective components orthogonal to the line-of-sight of: pointing error, target velocity relative to the attacker, and target acceleration. All variables are estimated in roll-stabilized, line-of-sight coordinates. Symmetry between the elevation and traverse filters is obtained by appropriate selection of the state variables. The symmetry results in equal Kalman gains, K_a, for both filters and minimizes computational requirements. The Kalman gains are computed in real time at a 16 Hz rate to account for changing target range and range rate. External signals to each Angle Tracking Filter consist in the respective components of: filter coordinate rates, ω; estimated range, $\hat{R}$; ownship accelerations, a_A, transformed into sensor coordinates; and measured pointing errors.

The measured pointing error used in each Kalman angle tracking filter is the respective component of the pointing error as measured in the roll-stabilized, line-of-sight coordinate system. The pointing error components are computed primarily from the ASCOT pointing error measurements, which are voltages related to the location of the center of the tracking scan in the focal plane of the ASCOT optical system. The pointing error computation also involves a coordinate transformation which requires a knowledge of the orientation of the aircraft body (sensor) axes with respect to the roll-stabilized LOS (filter) axes. Measurements from the ASCOT are taken at a 160 Hz data rate and are used to compute pointing errors in the LOS coordinates every 1/160 second. Ten samples of these transformed pointing errors are averaged to provide smoothed measurements to the Kalman filter every 1/16 second.

Measurement Model H_a

Delay

$\bar{P}$ Predicted Pointing Error

Estimated $\begin{bmatrix} \widehat{p} \\ \widehat{v} \\ \widehat{a}_T \end{bmatrix}$

Angle State Variables

Predicted $\begin{bmatrix} \bar{p} \\ \bar{v} \\ \bar{a}_T \end{bmatrix}$

P_M Measured Pointing Error

Kalman Gain K_a

Φ_a

W_i Aiding Inputs

Γ_a

Dynamic Model

Traverse Aiding Inputs $\begin{bmatrix} \omega(3)\widehat{R} \\ -a_A(2) \\ 0 \end{bmatrix}$; Elevation Aiding Inputs $\begin{bmatrix} -\omega(2)\widehat{R} \\ -a_A(3) \\ 0 \end{bmatrix}$

$$\Gamma_a = \begin{bmatrix} \Delta T & 1/2\Delta T^2 & 0 \\ 0 & [1-1/2\,(\widehat{\dot{R}}/\widehat{R})\,\Delta T]\,\Delta T & 1/2\Delta T^2 \\ 0 & 0 & [1-1/2\Delta T/\tau]\,\Delta T \end{bmatrix} ; H_a = \begin{bmatrix} \dfrac{K_{SF}}{\widehat{R}\,\text{GCFS}(1,1)} & 0 & 0 \end{bmatrix} ; K_a = \begin{bmatrix} K_p \\ K_v \\ K_a \end{bmatrix}$$

$$\Phi_a = \begin{bmatrix} 1 & [1-1/2(\widehat{\dot{R}}/\widehat{R})\,\Delta T]\,\Delta T & 1/2\Delta T^2 \\ 0 & 1-(\widehat{\dot{R}}/\widehat{R})\Delta T + 1/2\,(\widehat{\dot{R}}/\widehat{R})^2\,\Delta T^2 & \left\{1-1/2\,[(\widehat{\dot{R}}/\widehat{R})+1/\tau]\,\Delta T\right\}\,\Delta T \\ 0 & 0 & 1-\Delta T/\tau + 1/2\,(\Delta T/\tau)^2 \end{bmatrix}$$

FIGURE 5

KALMAN ANGLE TRACKING FILTER

GP74-0122-17

The sensor-to-filter coordinate transformation is updated at the 160 Hz rate through the use of the Strapdown Gyro/Accelerometer Package (SGAP). Incremental body attitude changes sampled every 1/160 second are compared to incremental LOS angle changes over the same interval to account for body rotation with respect to the LOS. The use of a SGAP in lieu of a gimballed

31

platform was prompted by the inherently smooth body-rate measurements obtained from the SGAP compared to the intrinsically noisy, derived rate information obtained from an Inertial Measurement Set (IMS).

For example, the AN/ASN-90 IMS employs a four-gimbal system in which the inner-roll gimbal angle is not provided as an output signal. As a result of the four-gimbal platform dynamics, in addition to the pick-off error characteristics and the analog-to-digital converter errors, the short-term attitude information is noisy. Moreover, while the IMS has "all-attitude" capability, accuracy is compromised during "over the top" conditions such as occur in dog fights.

Based upon the above considerations, it was decided that either a SGAP should be used in the ATS configuration or an Attitude/Attitude-Rate Filter should be configured to provide smoothed, derived body rates from IMS attitude measurements. The former approach was selected, based upon its superior anticipated performance and upon the availability of a suitable SGAP for ATS flight test on a no-cost consignment basis as required in the contracted Statement of Work. However, the capability of using an IMS in lieu of the SGAP is provided in the ATS software as a secondary design approach.

Several approaches to the sensor-to-filter coordinate transformation update were evaluated including an Euler angle representation, a direction cosine representation and a quaternion representation. The quaternion representation was selected because it provided an all-attitude capability consistent with the air-to-air gunnery environment without undue complexity. The coordinate transformation is completely specified by four quaternion elements. These four elements are constrained by a simple equation which, when satisfied, ensures orthogonality.

2.4.3 ATS Range Tracking Filter

Figure 6 summarizes the Range Tracking Filter equations. The range state variables are: range, range rate, and target acceleration along the line-of-sight. External signals to the filter are measured range and attacker acceleration transformed along the line-of-sight. The Range Tracking Filter utilizes the filter coordinate rates in elevation and traverse in its dynamic model. The Kalman gains, K_R, are computed in real time, taking into account the changing rates.

Measured range is provided by smoothed samples of range data from the SSR-1 range register. Each range measurement to the Kalman filter is the average of four radar range measurements taken at 1/64 second intervals. The residual is computed by differencing the range measurement and the estimated range measurement. The updated range filter state vector is obtained by summing the predicted state, the aiding signals and the residual multiplied by the 3 X 1 Kalman gain vector. This process is repeated every 1/16 second taking into account any change in the estimated target LOS rates and measured radar signal-to-noise ratio.
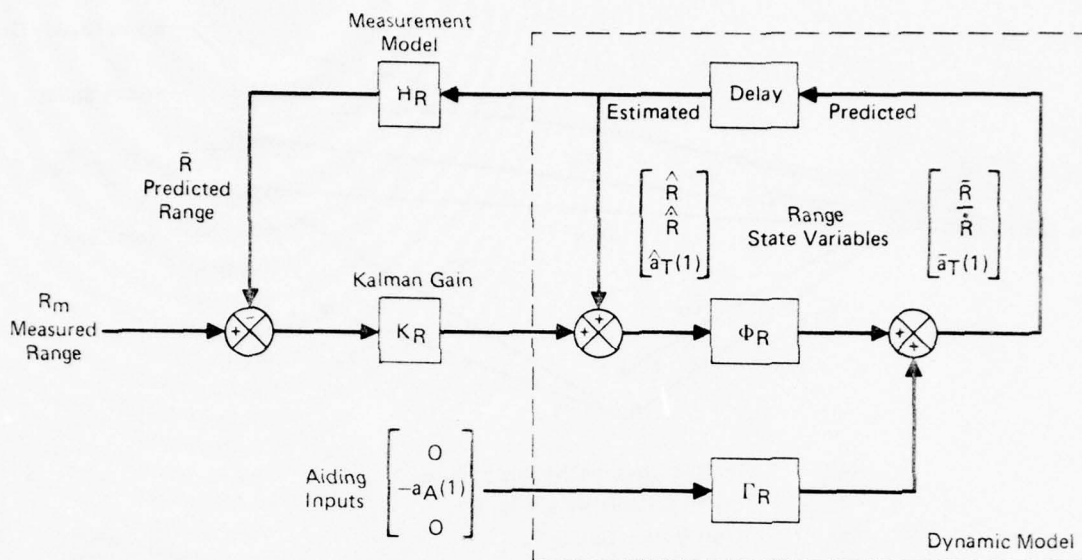
FIGURE 6
KALMAN RANGE TRACKING FILTER

$$\Gamma_R \triangleq \begin{bmatrix} \Delta T & \Delta T^2/2 & 0 \\ (\omega(2)^2 + \omega(3)^2)\,\Delta T/2 & \Delta T & \Delta T^2/2 \\ 0 & 0 & (1-\Delta T/2\tau)\Delta T \end{bmatrix} ; H_R \triangleq [\,1\ 0\ 0\,]$$

$$\Phi_R \triangleq \begin{bmatrix} 1 + (\omega(2)^2 + \omega(3)^2)\,\Delta T^2/2 & \Delta T & \Delta T^2/2 \\ (\omega(2)^2 + \omega(3)^2)\,\Delta T & 1 + (\omega(2)^2 + \omega(3)^2)\,\Delta T^2/2 & (1-\Delta T/2\tau)\,\Delta T \\ 0 & 0 & 1-\Delta T/\tau + \Delta T^2/2\tau^2 \end{bmatrix} ; K_R \triangleq \begin{bmatrix} K_R \\ K_{\dot{R}} \\ K_a \end{bmatrix}$$

GP74-0122-19

2.5 ATS DIRECTOR SIGHT EQUATIONS

The basic principles of the ATS director sight equations are illustrated in Figure 7. There are four basic computations involved: 1) the time-of-flight (T_F) computation; 2) the future bullet position computation; 3) the future target position computation; and 4) the pipper (sight reticle) position computation. A summary of these computations, their inputs and their interface with each other are presented in Figure 8. Each computation is considered in detail in the following subsections.

33

$\overline{D}_{EA}$	=	Pilot Eye Location Relative to Aircraft
$\overline{D}_{TE}$	=	Target LOS Relative to Pilot Eye
$\overline{D}_{PT}$	=	Target Motion During T_F
$\overline{D}_{FT}$	=	Range Vector to Future Target
$\overline{V}_B$	=	Initial Bullet Velocity Vector
$\overline{D}_{FB}$	=	Range Vector to Future Bullet
$\overline{D}_{FTB}$	=	Vector Miss Distance of Future Target wrt Future Bullet
$\overline{\epsilon}$	=	Angular Miss of Future Target wrt Future Bullet
$\overline{D}_P$	=	Vector Defining Pipper LOS
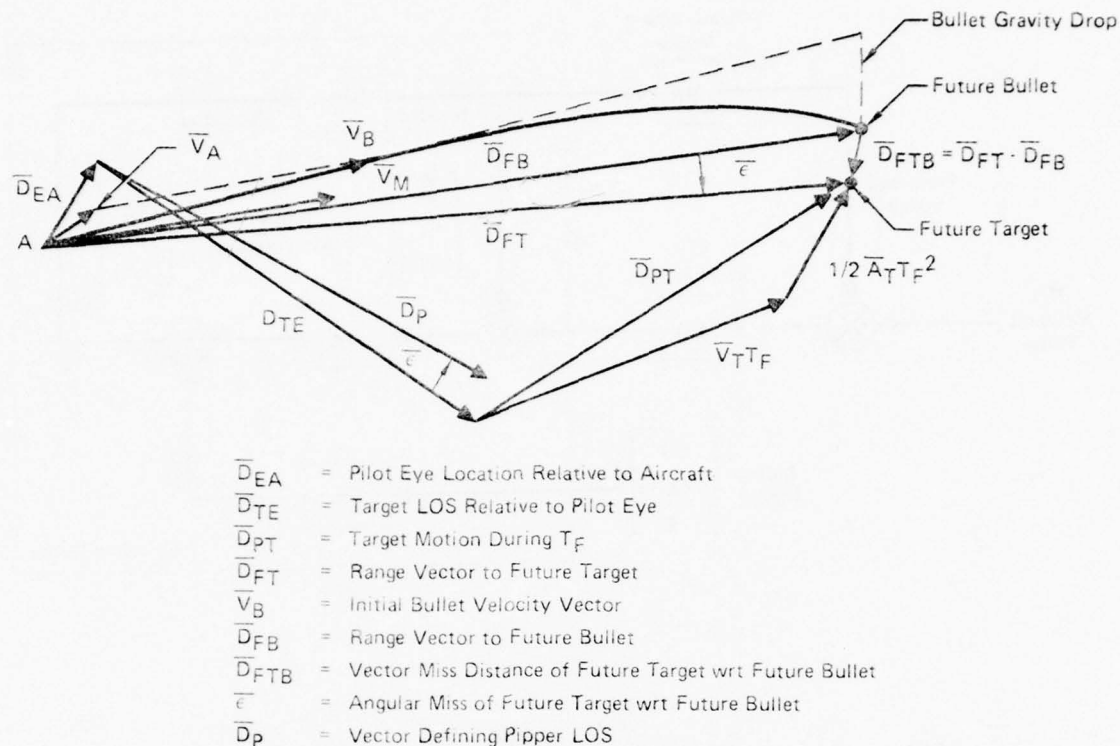
FIGURE 7
BASIC PRINCIPLES OF THE ATS DIRECTOR SIGHT EQUATIONS

GP74-0122-92

2.5.1 Time-of-Flight Computation

The time-of-flight (T_F) computation used in Figure 8 is developed in Figure 9. This computation is based on equating an approximate equation for predicted future target range D_{FT}, Equation (1), and predicted future bullet range D_{FB}, Equation (2), and then solving simultaneously for T_F. The resulting quadratic equation is solved for T_F by using the quadratic formula with the smaller root giving the value of T_F. The ballistic fit equation used to predict future bullet range uses a ballistic drag coefficient K_B which accounts for range shortening due to drag. K_B is calculated as a function of attacker true air speed and altitude. The constants C_1, C_2, C_3 and C_4 in the equation for K_B were selected to minimize the error in the overall time-of-flight equation when compared to standard ballistic tables for the 20mm bullet. In such a comparison, using the selected values of these constants, a root mean square time-of-flight error of only .015 second was obtained over altitudes of 500 to 30,000 feet and times-of-flight of .5 to 2 seconds.

T_F is limited to a maximum of 1.9 seconds by computing an equivalent maximum target range for comparison with the present target range. This approach is computationally efficient and insures sufficient bullet impact

34

ATS DIRECTOR SIGHT COMPUTATIONS

Attacker Velocity Vector

Predicted Target Position

$$\overline{D}_{FT} = \overline{D}_{TR} + (\overline{V}_A + \overline{V}_{TR})\,T_F + 0.5\,\overline{A}_T\,T_F^2$$

Future Bullet Position

$$\overline{V}_B = \overline{V}_M + \overline{V}_A$$

$$|\overline{D}_{FB}| = |\overline{V}_B|\,|T_F|\,T_F/(1 + K_B T_F)$$

$$\overline{D}_{FB} = |\overline{D}_{FB}|\,\overline{V}_B/|\overline{V}_B|$$

Pipper Position

$$\overline{D}_P = \overline{D}_{TE} - (\overline{D}_{FT} - \overline{D}_{FB})$$

Transform $\overline{D}_P$ to HUD Coordinates

$$X_p = 1000\ \overline{D}_{PY}/\overline{D}_{PX}$$

$$Y_p = -1000\ \overline{D}_{PZ}/\overline{D}_{PX}$$

To HUD: X_p, Y_p

T_F Computation

$$K_B = C_1 + (C_2 + C_3\,VTAS)e^{-C_4 H_A}$$

$$K_1 = (\dot{R} + VTAS)\,K_B$$

$$K_2 = \dot{R} + R K_B - V_M$$

$$T_F = \frac{-K_2 - \sqrt{K_2^2 - 4 K_1 R}}{2 K_1}$$

ADC: α, β, VTAS

Range and Angle Tracking Filters: $\overline{D}_{TR}$, $\overline{V}_{TR}$, $\overline{A}_T$, R, $\dot{R}$, H_A

All Vectors Expressed in Body Coordinates Unless Specified

VTAS	-	True Air Speed
α	-	Angle of Attack
β	-	Sideslip Angle
$\overline{V}_A$	-	Attacker Velocity Vector
$\overline{D}_{TR}$	-	Target Position Relative to Attacker
$\overline{V}_{TR}$	-	Target Velocity Relative to Attacker
$\overline{A}_T$	-	Target Non-Inertial Acceleration Vector
R, $\dot{R}$	-	Range, Range Rate
H_A	-	Attacker Altitude
T_F	-	Bullet Time of Flight
$\overline{V}_M$	-	Bullet Velocity Vector Relative to Attacker
K_B	-	Ballistic Drag Coefficient
$\overline{V}_B$	-	Bullet Initial Velocity Vector with Respect to Air Mass
$\overline{D}_{FB}$	-	Predicted Bullet Position with Respect to Attacker
$\overline{D}_{FT}$	-	Predicted Target Position with Respect to Attacker
$\overline{D}_{TE}$	-	Target Displacement with Respect to Pilot's Eye
$\overline{D}_{EA}$	-	Displacement of Pilot's Eye
X_p, Y_p	-	Pipper Position

FIGURE 8

ATS DIRECTOR SIGHT COMPUTATIONS

35

Geometry, $D_{FT} = R + (\dot{R} + V_A) T_F$ $\hspace{2cm}$ (1)

Ballistic Fit, $D_{FB} = \dfrac{(V_A + V_M) T_F}{1 + K_B T_F}$ $\hspace{2cm}$ (2)

Equation (1) and (2),

$$R + (\dot{R} + V_A) T_F = \dfrac{(V_A + V_M) T_F}{1 + K_B T_F} \hspace{2cm} (3)$$

Solving (3) for T_F,

$$(\dot{R} + V_A) K_B T_F^2 + (\dot{R} - V_M + K_B R) T_F + R = 0 \hspace{2cm} (4)$$

Employing the Quadratic Formula,

$$T_F = \dfrac{-K_2 - \sqrt{K_2^2 - 4K_1 R}}{2K_1} \hspace{2cm} (5)$$

Where $K_1 = (\dot{R} + V_A) K_B$

$\hspace{1.2cm} K_2 = \dot{R} - V_M + K_B R$

D_{FT}	Predicted Future Target Range	T_F	Bullet Time-of-Flight
D_{FB}	Predicted Future Bullet Range	V_A	Attacker Velocity
R	Present Range	V_M	Bullet Muzzle Velocity
$\dot{R}$	Present Range Rate	K_B	Ballistic Drag Coefficient

FIGURE 9
BASIC PRINCIPLES OF THE TIME-OF-FLIGHT COMPUTATION
GP74-0122-90

velocity over a large regime of the air combat environment. Exceptions occur at high opening range rates. An additional check in computing T_F is required to accommodate "beam type" attack conditions. In this geometry condition, the attacker airspeed is approximately the negative of the range rate and, as a result, the quadratic equation for T_F reduces to a linear equation.

2.5.2 Future Bullet Position Computation

The future bullet position (T_F seconds from the present) is based on the bullet's initial velocity vector and the range shortening caused by drag acting on the bullet. Gravitational acceleration acting on the bullet is accounted for by using accelerometer measurements as aiding inputs to the Range and Angle Tracking Filters. As a result, the target acceleration state estimates from these filters correspond to target accelerometer measurements which are used in computing the predicted target position to be described in the next paragraph. The bullet's initial velocity vector is the vector sum of the muzzle velocity, airspeed and velocity due to body rates at the gun muzzle in body coordinates. Computing the airspeed vector in body coordinates uses Air Data Computer (ADC) outputs of airspeed, angle-of-attack and sideslip angles. The future bullet position in body coordinates is the initial velocity vector multiplied by a modified time-of-flight, $T_F/(1+K_B T_F)$,

where K_B is the ballistic drag coefficient described above with the T_F calculation. This denominator term $(1+K_B T_F)$ accounts for drag retardation force acting on the bullet.

2.5.3 Future Target Position Computation

The predicted future target position (T_F seconds from the present) is based primarily on target state estimates from the Range and Angle Tracking Filters and ADC outputs of airspeed, angle-of-attack and sideslip angle. Since the filter state estimates are with respect to the sensor location, the small velocity due to body rates acting at the sensor location is also included for completeness. Sensitivity analyses conducted in conjunction with the complete AGFCS design phase may indicate that the effect of neglecting the velocity due to body rates at the gun muzzle and sensor locations will cause little error in the pipper position computation. This would permit neglecting these velocities in computing the future bullet and target positions. The terms are included in the ATS design for completeness. The predicted target position due to the filter states alone is computed in filter coordinates and then transformed to body coordinates. Then, the airspeed resolved into body coordinates, velocity due to body rates at the sensor location and the sensor location are accounted for in computing the future target position with respect to the attacker center of gravity (CG).

2.5.4 Pipper Position Computation

The displacement of the future target position with respect to the future bullet position, each referenced to the attacker CG, is first computed. This displacement, the predicted bullet miss distance, is transformed to gunline coordinates, and the components normal to the gun muzzle are computed. These components divided by bullet range give the angles through which the gun must be rotated to zero the predicted miss distance. These angles, called the command gun error angles, are subtracted from the target LOS angles, estimated by the Range and Angle Tracking Filters, to compute the pipper position. The subtraction of the command gun error angles accounts for the proper sign convention in displaying the pipper with respect to the LOS. Assuming the utilization of a HUD for ATS flight test, the pipper HUD position computation uses the angle between the HUD centerline and the body X axis to transform from body coordinates to HUD coordinates. The lead angles are the angles of the pipper with respect to the gunline.

2.6 ATS ERROR BUDGET

The ATS error budget is developed in Section 4 in conjunction with ATS sensor modeling, error analysis and performance sensitivity studies. Error budget considerations for each of the principal hardware subsystems are summarized in the following paragraphs.

37

2.6.1 Range Sensor Error Budget

The selected ATS range sensor design is basically on adaptation of a General Electric Solid State Range-Only Radar (SSR-1) development. The long history of the use of radar in air-to-air combat conditions and of the design and testing experience of General Electric Company has resulted in the selection of the anticipated values of the SSR-1's error sources as the ATS range sensor's error budget. These error sources and their values are tabulated in Section 4 (Table 10). Briefly summarizing this error budget: 1) bias errors should be less than 40 feet (1σ) with appropriate compensation for receiver time gain stability error at short range; 2) short-range (less than 6000 feet) random errors should be less than 15 feet/second (1σ); and 3) long-range (24,000 feet) random errors should be less than 125 feet (1σ).

Performance and sensitivity analyses have indicated that the ATS range sensor error budget summarized above, in combination with the ATS Kalman Range Tracking Filter and 4-sample prefiltering, should result in range tracking accuracies which meet air-to-air system performance requirements. As determined by the ATS sensitivity analysis, the effect of degraded range sensor performance per foot of random measured-range error is: 0.22 feet of estimated range; 0.36 feet/second of estimated range rate; and 0.2 feet/second^2 of estimated range acceleration. The effect of range bias error is to: 1) bias the estimated range by an equal amount; and 2) bias the estimated relative velocity normal to the LOS in the Angle Tracking Filter by an amount proportional to the LOS rate.

2.6.2 Angle Sensor Error Budget

In comparison to the range sensor the ATS angle sensor is in the early stages of its development. For this reason, many of its principal error sources have not been quantified and, conversely, those error sources which have been quantified analytically may not be significant contributors to the overall error budget. For example, error contributors which have been quantified analytically are tracking video receiver noise and atmospheric noise. However, an analysis presented in Section 4 indicates that these two noise sources in combination will not exceed the effect of a glint error of only 0.5 feet. Glint error is defined here as the displacement between measured contrast centroid and the target's center of gravity. Although the selected ATS angle sensor, the BASD ASCOT, is specifically designed to minimize glint error, its performance in this respect has not been quantified and it is reasonable to expect glint error in excess of .5 feet, 1σ.

These considerations have emphasized the need for both laboratory and flight test experimental evaluation of ASCOT error sources and have resulted in a conservative design policy in the ATS Angle Tracking Filter design. The parameters for the Angle Tracking Filter have been selected on the basis of the overall angle tracking loop performance and reflect the uncertain state-of-the-art knowledge of angle sensor noise. In like manner, the ATS angle sensor error budget was established as an upper bound on acceptable measurement errors. The error budget should not be interpreted as a design goal

38

but as a maximum acceptable design limitation. The angle sensor error budget selected was the equivalent of 2.5 milliradians of random pointing error (1σ) at maximum firing range (3000 ft) and throughout the sensor's operating field-of-view.

Performance and sensitivity analyses have indicated that the selected ATS angle sensor error budget, in combination with the ATS Kalman Angle Tracking Filter and 10-sample prefiltering, should result in angle tracking accuracies which meet air-to-air attack system performance requirements. As determined by the ATS sensitivity analysis the effect of degraded angle sensor performance per milliradian of random error in measured pointing error is: 0.6 feet of estimated pointing error; 2 feet/second of estimated relative velocity normal to the LOS; and 2.5 feet/second^2 of estimated target acceleration normal to the LOS.

2.6.3 SGAP Error Budget

The ATS SGAP error budget is presented in Section 4, Tables 11, 12 and 13. Table 11 presents the rate-integrating gyro specifications, Table 12 presents the accelerometer specifications and Table 13 presents the SGAP analog-to-frequency converter specifications. Each of these specifications is representative of presently available medium-quality strapdown gyro/accelerometer packages.

SECTION 3   ATS SUBSYSTEM DESIGN AND INTERFACE

3.1   GENERAL

The principal ATS subsystem hardware and software elements were identified in Figure 1. The subsystems selected for the ATS angle sensor and range sensor were the Bendix Aerospace Systems Division (BASD) ASCOT and the General Electric (GE) SSR-1 radar, respectively. Detailed design and operational features of the ASCOT are presented in VOLUME II , a summary of ASCOT's characteristics and its design status is contained in Subsection 3.2. Subsection 3.3 presents a summary of the SSR-1's characteristics and design status with a detailed description presented in VOLUME III. The ATS computer and SGAP are considered in Subsection 3.4 which also presents a detailed consideration of the interface of the sensor subsystems with the ATS computer.

3.2   ASCOT DESIGN

3.2.1   Development Background

The development of the ASCOT was initiated by the Bendix Aerospace Systems Division (BASD) as an Independent Research and Development (IRAD) effort in 1965. Government support was obtained in late 1965 from the Corona Laboratories for the development of two breadboard ASCOT units. These units were to be used for laboratory and field test evaluation of the basic concepts. In 1967, BASD provided two Guidance Test Vehicle seekers under contract for evaluation in the Modular Air-to-Surface Missile (ASM) program.

The basic ASCOT was subsequently modified for both air-to-air fire control and air-to-air missile applications. In 1969-1970 the ASCOT system was selected for use in an exploratory development program at the Naval Weapons Center, China Lake, for potential use in a Short Range Weapons Control System. The system was reconfigured to fit in an existing Sidewinder pod and test flown in 1970 with encouraging results. Engineering modifications were made under a BASD IRAD program in 1971. Fly-over tests, performed at a local air field, indicated improved tracking performance. The ASCOT was selected for comparative test and evaluation by the NAVMISCEN at Pt. Mugu. The objectives of this program were to determine likely candidate EO seekers for the Navy AGILE program. The ASCOT system was considered to be one of the higher performance systems by the NAVMISCEN test personnel.

At the time of selection for the ATS, ASCOT was considered an already fabricated, experimental subsystem. The ATS ASCOT design phase consisted in some design modifications to the experimental ASCOT system both for the purpose of performance improvements and for interface compatibility with the ATS computer, i.e., with the ATS Angle Tracking Filter. In parallel with the ATS ASCOT design, the BASD IRAD program continued the development of ASCOT for short-range, air-to-air missile applications. This design effort provided cross-fertilization with the ATS design and led to the inclusion of several advanced features not in the original ASCOT experimental system.

The ATS ASCOT flight system can be fabricated, assembled, and tested by the BASD Engineering Laboratory with support from the Experimental Machine Shop for mechanical parts and the Environmental Test Laboratory for environmental testing. Figure 10 presents the flight system plan and schedule. The following paragraphs briefly describe each line item:

o Image Dissector Procurement - This tube supplied by ITT, Fort Wayne, Indiana, is the only significantly long lead item to be procured. ITT quotes 120 days for delivery. Earlier procurement of this item could reduce the total ASCOT schedule time required from five to four months.

o Electronic Parts Procurement - None of these parts selected for the flight system have significant lead time. Most of them are expected to be 4-6 weeks for delivery. A production design incorporating high reliability parts would require a much longer lead time.

o Mechanical Parts Fabrication and Assembly - This is the fabrication and assembly of the housings and associated bracketry for the sensor and electronics assemblies. This work would be performed in the Experimental Machine Shop.

o Electronics Assembly - This is the wiring and assembly of the electronics circuit boards by the technicians in the Engineering Laboratory. These technicians are completely familiar with ASCOT and can perform this work with a minimum of documentation and supervision.

o Electronics Checkout - As the individual circuits are completed they will be tested. Formalized test procedures will be used and all test data will be documented.

o Assembly and Checkout - During this time period, the sensor and electronics processor will be completely assembled and performance tested. A substitute image dissector tube from the existing ASCOT breadboard hardware will be used until the tube ordered from ITT is available. This work will be performed in the Engineering Laboratory.

o Environmental Tests - Although experience has shown that ASCOT should not have in-flight environmental problems, the flight system hardware should be subjected to environmental testing to insure its flight-worthiness. Tests will include vibration, temperature and pressure, the latter being for the sensor assembly only. Specific test limits cannot be established until the test aircraft has been selected and the complete test environment has been defined. These tests will be conducted in the Environmental Test Laboratory.

o Final Checkout and Delivery - This will be the complete performance tests to be conducted on the system as a final acceptance for delivery.

Activity	Months after Go-Ahead				
	1	2	3	4	5
Image Dissector Procurement					
Electronic Parts Procurement..............					
Mechanical Parts Fabrication and Assembly......					
Electronics Assembly........................					
Electronics Checkout					
Assembly and Checkout					
Environmental Tests					
Final Checkout and Delivery..............					
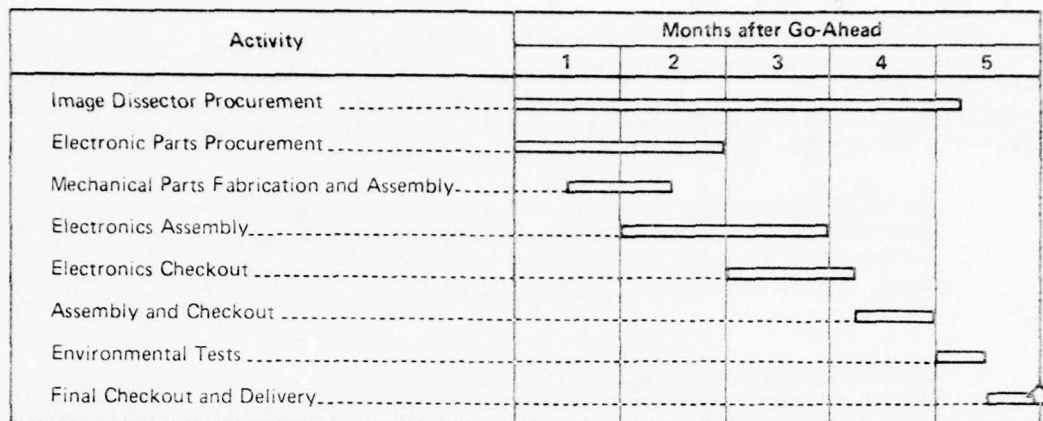
FIGURE 10
ASCOT FLIGHT SYSTEM SCHEDULE

GP74-0122-46

3.2.2 ASCOT Description

The ASCOT consists of two hardware units: the ATS ASCOT Sensor Assembly
and Electronics Assembly. Two-view outline drawings of each of these units
are included as Figure 11. Also presented in Figure 11 are relevant instal-
lation data. These units do not reflect mounting provisions since these must
be designed for the specific aircraft selected for flight testing; however
the additional weight will be minimal. System mounting restrictions are ap-
plicable to aircraft/sensor field-of-view requirements only. Thus the EO
sensor lens location will be the only significant installation item which
must be considered. Normal access will be provided for maintenance actions.

ASCOT inputs and outputs are handled through special interface circuits
that interconnect to the ATS system interface. Inputs include commands from
the ATS computer, and gain and parameter changes from the ASCOT control panel.
The outputs are signals required for total system operation and signals for
test recording. Interfaces have been designed to reduce as much as possible
any system problems, such as ground loops and noise pickup, that generally
occur in system interconnection. This has been done by using differential
inputs and outputs on all signal interfaces. This provides for system con-
nections without exchanging signal grounds. The use of shielded twisted
pairs for interconnection greatly reduces noise pickup on system interconnec-
tions. For the gain and tolerance commands all internal functions are
switched using relays. This also isolates circuits from aircraft ground
noise. All the relays operate between aircraft +28 VDC and aircraft ground.

Several of the ASCOT inputs allow for changing circuit gains or thresh-
olds without the need for component change, for example gain changes in the
tracking and scan-size control loops. Others control search field size and
tracking window width bias. These selectable functions represent circuits

30°

3.6 in. Dia

Strap
Clamp

16.7 in.

Sensor Assembly

4.5 in.

7.625 in.

12.562 in.

13.75 in.

2.25 in.

Electronics Assembly
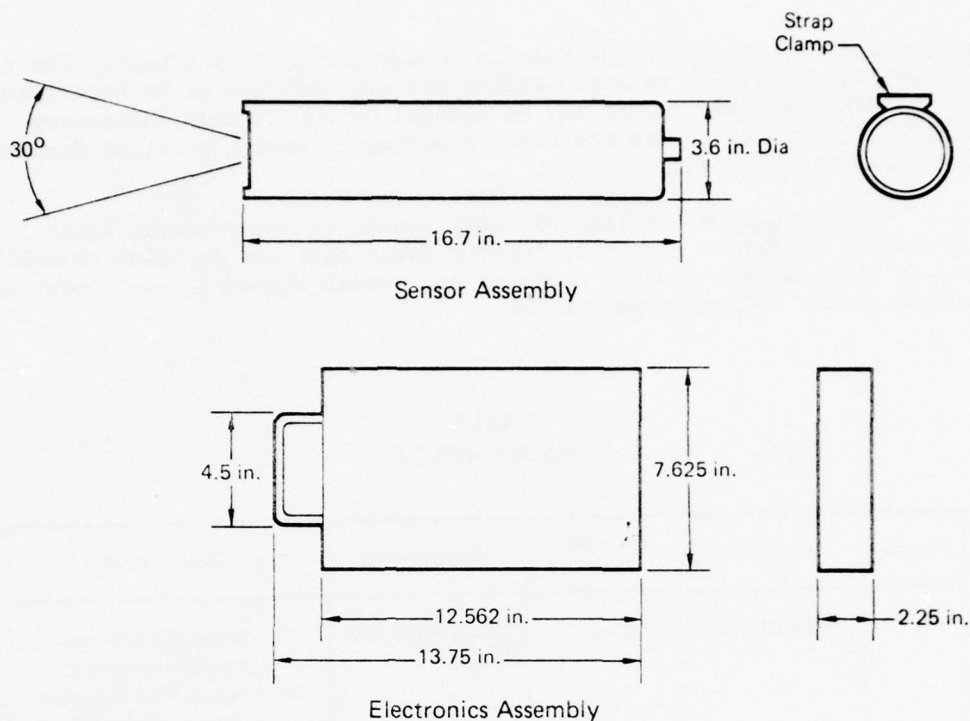
Weight	12.2 lb
Dimensions	
Sensor Assembly.	7.4 lb
Length	16.7 in.
Diameter	3.6 in.
Electronics Assembly	4.8 lb
Length	12.562 in.
Width	2.250 in.
Height	7.625 in.
Cooling Air	None
Pressurization	(Sealed to
Operating Altitude	Sea Level)
Power	50 W, +28 VDC
Mounting	Fixed
Operating Temperature	0°C to 45°C
Mounting Provisions	To be Determined

Installation Data

FIGURE 11
ATS ASCOT OUTLINE DRAWINGS AND INSTALLATION DATA

GP74-0122-52

whose gains or thresholds might require change during flight test. The gains
and thresholds have been selected either through analysis or by experimenta-
tion. All the selected values may be changed during further laboratory
testing or flight test. The electronics packaging design provides for making
such changes in the field.

3.2.2.1 ASCOT Inputs - The list of ASCOT inputs is presented in Table 1.
There are two different groups of input signals that are supplied to ASCOT.
These are signals from the ATS computer and manual signals. Each input is
described in the following paragraphs.

TABLE 1
ASCOT INPUTS

Inputs	Function	Software Name	Voltage Range	Scale Factor	
1	Track Discrete	ITRKA	T^2L Compatible	Hi:	Search Field Detection Voltages Connected
				Lo:	Search Field Detection Voltages Disconnected
2	Horiz. Pointing Command	EVTSSC(2)	−5 to +5 VDC	$0.333V/^O$:	Plus — Right Minus — Left
3	Vert. Pointing Command	EVTSSC(3)	−5 to +5 VDC	$0.333V/^O$:	Plus — Down Minus — Up
4	Target Subtense	EVTSOR	0 to 5 VDC	24 mr/Volt:	5 V=120 mr 0 V=0 mr
5	Standby/ Operate Select		T^2L Compatible	Hi: Standby Lo: Operate	
6	Search Field Select		Open, +28 VDC	+28 VDC: $2^O \times 2^O$ Open: $5^O \times 5^O$	
7	Tracking Loop Gain Select		Open, +28 VDC	+28 VDC: 66 Gain Open: 33 Gain	
8	Scan Size Loop Gain Select		Open, 28 VDC	+28 VDC: 0.3 Gain Open: 0.4 Gain	
9	Scan Reference Radius Select		Open, +28 VDC	+28 VDC: 0.7 Open: 0.8	
10	Duty Cycle Tolerance Select		Open, +28 VDC	+28 VDC: ±15% Open: ±10%	
11	Window Width Bias Select		Open, +28 VDC	+28 VDC: Narrow Open: Wide	

Note: All 5V signals are on shielded twisted pairs.

GP74-0122-50

44

ATS Computer Inputs - These inputs are controlled by the software program of the ATS computer:

   o Track Discrete - Input from the ATS computer that removes the search field detection voltage from the deflection coil. This is generated after the detection discrete is generated by ASCOT and the ATS Angle Tracking Filter is initialized.

   o Horizontal Pointing Command - Input to the horizontal deflection coil of ASCOT to initially point ASCOT or to maintain the center of search on target in the event of loss of track during search; or to provide reference pointing commands during track.

   o Vertical Pointing Command - Input to the vertical deflection coil of ASCOT either to initially point ASCOT or to maintain the center of search on target in the event of loss of tracking during search; or to provide reference pointing commands during track.

   o Target Subtense - Input to the ASCOT acquisition circuitry to aid acquisition of a valid target and rejection of an invalid target (false alarm) based upon radar range measurements and target size. Zero target subtense provides the "range unavailable" indication.

Manual Inputs - The signal discretes listed in this paragraph are manually controlled to select either of two values for selected ASCOT modes, gains and thresholds. These options have been provided to allow flexibility in evaluating design alternatives during laboratory and flight tests without physically changing components. Whether these inputs will be controlled by the test operator in-flight or pre-established before each flight will depend upon the test aircraft's configuration and detailed flight test planning. At present, only the Standby/Operate Select will be controlled by the in-flight operator.

   o Standby/Operate Select - This command when in Standby mode inhibits ASCOT from acquiring or will cause ASCOT to unlock from the target it is tracking. The ASCOT will search but will ignore detection signals.

   o Search Field Select - This command changes the size of the search field.

   o Tracking Loop Gain Select - This command changes the gain of the tracking loop integrators.

   o Scan-Size Loop Gain Select - This command changes the gain of the scan-size control loop.

   o Scan Reference Radius Select - This command varies the scan reference radius of the scan region discriminator.

   o Duty Cycle Tolerance Select - This command selects the duty cycle tolerance limits employed in the duty cycle comparator. Its

45

output, under normal operation, controls the state of the ASCOT acquisition discrete, i.e., determines whether a lock-on has been achieved and the ATS tracker should remain in its tracking mode or convert to its extrapolation mode.

o Window Width Bias Select - This command selects the tracking window width bias.

Each of these design parameters is discussed in detail in Appendix A.

3.2.2.2 ASCOT Outputs

The list of ASCOT outputs is presented in Table 2. Each output is described in the following paragraphs:

o Detection Discrete - This signal informs the ATS computer that the ASCOT has detected a potential target, i.e., that the detection video has exceeded its threshold.

o Acquisition Discrete - This signal informs the computer that ASCOT has acquired. The signal is derived from the Duty Cycle Monitor.

o Horizontal and Vertical Position - These signals transmit the location of a detected potential target with respect to the ASCOT bore-sight. They are used to initialize the filter coordinate system along the detected target line-of-sight.

o Horizontal and Vertical Pointing Error - These signals transmit the difference between the measured target location and the ATS computer pointing commands (inputs 2 and 3 of Table 1), i.e., the pointing error. They are obtained from the outputs of the ASCOT's internal tracking loop integrators and are used to update the Kalman Angle Tracking Filter after acquisition.

o Scan Size - This signal is derived from the scan size control circuit. As well as a measurement of target size, it is also a measure of the tracking performance.

o Duty Cycle - The duty cycle is an average measure of the ratio of the scan-on-target time to the total scan period. The output is derived from integration of the window discriminator. This signal is also an indication of tracking performance.

o Positive and Negative Target Levels - These signals measure, respectively, the average target video level greater than and less than the established background level.

o Scene Brightness - This is a measure of the brightness of the portion of the scene scanned by the ASCOT. The source of the signal is the AGC voltage on the tracking video amplifier.

o <u>Background Noise</u> - This is the RMS value of the high frequency fluc-
tuations in the background level.

TABLE 2
ASCOT OUTPUTS

Outputs	Function	Software Name	Voltage Range	Scale Factor
1	Detection Discrete	IDETA	T^2L Compatible	Hi — Detection Lo — No Detection
2	Acquisition Discrete	IACQA	T^2L Compatible	Hi — Acquired Lo — Not Acquired
3	Horizontal Position	EVTSSM(2)	−5 to +5 VDC	3°/V: Plus — Right Minus — Left
4	Vertical Position	EVTSSM(3)	−5 to +5 VDC	3°/V: Plus — Down Minus — Up
5	Horizontal Pointing Error	XDVSM(2)	−5 to +5 VDC	3°/V: Plus — Right Minus — Left
6	Vertical Pointing Error	XDVSM(3)	−5 to +5 VDC	3°/V: Plus — Down Minus — Up
7	Scan Size	XSCSZM	+5 to −5 VDC	TBD
8	Duty Cycle	XDUTYM	+5 to −5 VDC	10%/V: +5V — 0% −5V — 100%
9	Positive Target Level	XPTLVM	0 to +5 VDC	TBD
10	Negative Target Level	XNTLVM	0 to −5 VDC	TBD
11	Scene Brightness	XSCBRM	0 to +5 VDC	TBD
12	Background Noise	XBGNSM	0 to +5 VDC	TBD

3.3 SSR-1 DESIGN

3.3.1 Development Background

The ATS radar design drew heavily on the General Electric Solid State
Range-Only Radar (SSR-1) development effort. The SSR-1 was developed as a
simple, single-package radar suitable for use with guns or short-range
missiles. The basic radar parameters (frequency, power output, etc.) fit the
ATS application and the ATS SSR-1 design mainly concerned adaptation of the
basic radar to interface with the ATS computer. Several interface concepts
were evaluated for suitability. What evolved is a design in which the ATS
radar has two modes: 1) an Augmented Mode in which the ATS computer controls
the radar tracking loop via the Kalman Range Tracking Filter, providing
optimum filtering of the radar data as well as introducing data from other
sensors (ownship motion, for example) in order to provide accurate prediction
of range and range rate; and 2) an Autonomous Mode in which the SSR-1 tracks
the target, measuring present range and range rate without assistance from

the ATS computer. The Autonomous Mode allows check-out of the radar as a separate subsystem and provides a direct comparison of the advantages of optimum filtering in a central computer with more conventional radar filtering.

Development of the basic radar has progressed in parallel with this study. Detailed design and testing for MIL-E-5400 environments is in process and completed units of this design are scheduled for June 1974. Due to this parallel effort, long-lead parts in inventory will allow delivery of a flightworthy ATS SSR-1 six months after receipt of an order.

As an additional fall-out of this parallel development, a breadboard of the range tracker can be made available to demonstrate and evaluate detailed interface with a computer in a laboratory environment.

3.3.2 ATS SSR-1 Description

The ATS SSR-1 radar is self-contained in one line replaceable unit (LRU) and uses a six inch, fixed-horn antenna to provide a conical sector coverage of 15 degrees. It is an X-band, noncoherent, pulsed radar. Its principal parameters and performance characteristics are listed in Table 3. It has a detection capability of 2.65 nautical miles on a 2 square meter target located along the axis of the radar antenna beam.

The SSR-1 is comprised of the following subassemblies:

Microwave Assembly
Magnetron
Modulator
AFC
IF Amplifier
Range Tracker
Power Supply
Self-Test/Control

The antenna for the SSR-1 radar is a 6-inch horn-lens type. The installation configuration and data are shown in Figure 12. Although the horn antenna and radar LRU can be separated and connected by a waveguide if desired, it is suggested that such a waveguide run be no greater than 18 inches.

The standard input power is +28 VDC and the power drain is approximately 30 watts. Alternative primary sources such as 115 volt 400 Hz can be utilized. External cooling air is not required if the SSR-1 is operated within the environmental temperature limits of MIL-E-5400K from -55° to +71°C. Provisions for pressurization are not required and a time-totalizing meter (MIL-M-7193) on the radar unit indicates the total number of power-on hours accumulated by the radar.

Provisions are made on the radar display to light a malfunction lamp whenever a radar malfunction is sensed by built-in test circuitry. These

TABLE 3
ATS SSR-1 RANGE-ONLY RADAR DESIGN FEATURES

Antenna	6 in. Horn · Lens
Beamwidth	15° at 3dB
Gain	21 dB
Transmitter	
Frequency	9375 MHz
Peak Power	8 KW
PRF	1024 Hz
Pulsewidth	0.45 Microsecond
Receiver	
Intermediate Frequency	30 MHz
Bandwidth	4 MHz
Noise Figure	8 dB
MDS	−98 dBm
Processor	
Outputs	
Detection Discrete	
Lock On Discrete	
Range	Digital, 16 Bits
Range Rate	Digital, 8 Bits
Lock On	−91 dBm
Search Range	To 24,000 ft
Search Rate	24,000 ft/sec
Autonomous Tracking Accuracy	± 50 ft
Velocity Memory	2 sec

GP74-0122-58

circuits monitor key radar functions such as the modulator overload circuits, the AFC lock-on signal, and feed inputs to the self-test logic board. Loss of any signal will activate the malfunction indicator.

The radar incorporates a meter and test switch, which permits rapid check of crystal currents, magnetron current, power supply voltages, etc. Preflight or taxi checks can be made by locking onto a natural target or a corner reflector located at a known range. Where more precise testing is desired, a signal generator is used to check minimum discernible signal, and a precise range and range-rate target generator is used to check tracking performance. Since the radar consists of only one LRU, the matter of fault isolation is almost academic, but the test meter does provide the capability of verifying that the output signals are present. A BNC connector on the radar provides a sync pulse for use by an AGE equipment. Other signals, including the received video, are also brought out to external test points.

25.30

16.25

10.25

6.50

6.00 Dia

Aircraft Mounting Rack
with Retaining
Hardware and Guide Pins
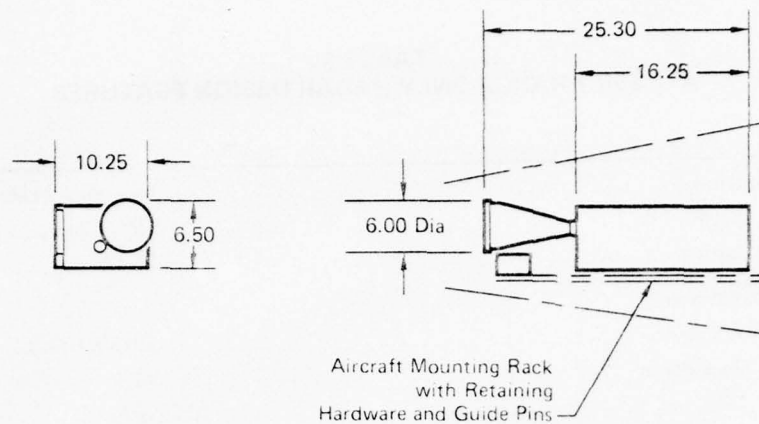
Note: All Dimensions in Inches

Installation Data

Weight . . . . 23 lb (Including Antenna)

Dimensions (Radar)
    Length . . . . 16.15 in.
    Width . . . . 9.06 in.
    Height . . . . 5.91 in.

Cooling Air . . . . None

Pressurization . . . . 15 psia (Waveguide Only)

Operating Temperature . . . . −55 to 71°C

Operating Altitude . . . . 0 to 50,000 ft

Electrical Power Input . . . . +28 VDC 1.0 Amp
115 V, 400 Hz, 1 Amp

Mounting . . . . Hard Mount

Vibration Level . . . . MIL-STD-810B, Curve A

FIGURE 12
ATS SSR-1 RADAR OUTLINE DRAWING AND INSTALLATION DATA

GP74-0122-57

The radar is entirely solid state except for the 2J42H Magnetron. This magnetron utilizes a rugged tungsten cathode. Due to the low power of the magnetron and the resulting low current density, this cathode is operated several hundred degrees lower in temperature than is common with higher power magnetrons. As a result of this, the tube life is in the thousands of hours. A primary failure mode of magnetrons is open circuits of the heater. For this reason a simple circuit to monitor the presence of heater current can provide a high level of self-test confidence for the transmitter.

The SSR-1 has been designed for high reliability, ease of fault isolation and ease of maintenance. Except for the magnetron, the radar is entirely solid state and has no moving parts. It uses fewer than 600 electrical parts and has a predicted MTBF in excess of 2000 hours. This prediction is based on reliability experience gained with production radars such as the APQ-113, -114 and -144, which utilize similar components and design techniques as have been employed in this radar. Modular construction techniques are utilized with all subassemblies except the harness since it is easily removable from the chassis. The unit is designed to the environmental levels of MIL-E-5400, Class 2, with vibration levels to MIL-STD-810B, Method 514, Curve A.

3.3.2.1 SSR-1 Inputs - The list of ATS SSR-1 inputs is presented in Table 4. There are two different groups of input signals that are supplied to the SSR-1. These are signals from the ATS computer and manual signals. Each input is described in the following paragraphs.

TABLE 4
ATS SSR-1 INPUTS

Inputs	Function	Software Name	Quantization			
			Length	Units	MSB	LSB
1	Command Word	JIOR	8 Bits	NA	—	—
2	Range Command	GPTSFP(1)	16 Bits	ft	12,000	0.36
3	Range-Rate Command	GVTSFP(1)	8 Bits	ft/sec	23.4	0.36
4	Off-Standby-Radiate Select	Pilot Controls				
5	Range Select					
6	Target Reject					
7	Self-Test Select					

GP74-0122-88

ATS Computer Inputs - These inputs are controlled by the software program of the ATS computer:

o Command Word - Input from the ATS computer that transfers commands and data between the ATS computer and the SSR-1.

o Range Command - Input to the SSR-1 range register to establish range gate position during Augmented mode operation.

o Range-Rate Command - Input to the SSR-1 range-rate register during Augmented mode operation. Serves to provide initial range-rate value if Autonomous mode is commanded.

Manual Inputs - These inputs to the SSR-1 are controlled by the operator from the SSR-1 control panel.

o OFF - STANDBY - RADIATE - This is the basic power-on control. In
   STANDBY position, bias voltages are applied along with magnetron fila-
   ment voltage. After a warm-up period, RADIATE select is enabled and
   its selection will initiate transmission of RF power.

o RANGE SELECT - Provides for selection of a 3000, 6000, or 24000 foot
   maximum search range.

o TARGET REJECT - Allows for breaking lock on presently acquired
   targets.

o SELF-TEST SELECT - Initiates generation of an internal test target
   for preflight or taxi checks.

3.3.2.2 SSR-1 Outputs - The list of ATS SSR-1 outputs is presented in Table
5. There are two different groups of output signals. These are a group of
digital signals transmitted to the ATS computer on request and a group of
pilot display signals. Each output is described in the following paragraphs.

TABLE 5
ATS SSR-1 OUTPUTS

Outputs	Function	Software Name	Quantization			
			Length	Units	MSB	LSB
1	Range	GPTSXM	16 Bits	ft	12,000	0.36
2	Range Rate	GVTSXM	8 Bits	ft/sec	23.4	0.36
3	Range Register Correction	XRCOR	8 Bits	ft	23.4	0.36
4	Status Word	JFSWR	3 Bits	NA	NA	NA
5	Signal-to-Noise Ratio	XSNRM	4 Bits	d.b.	24	3
6	Self-Test Failure Discrete	IFAILR	1 Bit	NA	NA	NA
7	Self-Test Go/No Go Display	Pilot Displays				
8	Search Display					
9	Lock-on Display					
10	Thermal Overload Display					

GP74-0122-89

ATS Computer Outputs - These digital outputs are transmitted to the ATS com-
puter on request:

o Range - This output transmits the 16-bit contents of the SSR-1 range
   register to the ATS computer.

o Range Rate - This output transmits an 8-bit (7 magnitude bits plus a
   sign bit) range-rate measurement from the range-rate register.

52

o Range Register Correction - This output transmits the 8-bit (7 magnitude bits plus a sign bit) quantized range-register correction.

o Status Word - The status word is a 3-bit word representing the status of the SSR-1's DETECTED PULSE, LOCK-ON and COAST signals.

o Signal-to-Noise Ratio - This output transmits a 4-bit quantized, measured signal-to-noise ratio.

o Self-Test Failure Discrete - This bit represents a SSR-1 malfunction based upon its self-test circuitry.

Pilot Display Outputs - These outputs are displayed directly to the operator on the SSR-1 display panel:

o SELF-TEST GO/NO-GO DISPLAY - Provides GO or NO-GO indicator lamp condition based on self-test parameters. Consists of 2 separate lamps.

o SEARCH DISPLAY - Illuminates indicator lamp when in search.

o LOCK-ON DISPLAY - Illuminates indicator lamp when radar has acquired and locked-on (tracking) a target.

o THERMAL OVLD DISPLAY - Illuminates indicator lamp when internal LRU temperature has exceeded 160°F.

3.4 ATS SUBSYSTEM INTERFACE

The previous subsections have described the principal ATS subsystems; namely, the ASCOT angle sensor and the SSR-1 range sensor. Two additional subsystems are required for ATS operation, the ATS computer and the Strapdown Gyro/Accelerometer Package (SGAP). In the contracted Statement of Work (SOW) the ATS computer was anticipated to be a Kearfott SKC-2000 airborne digital computer. Likewise, it was anticipated that the computer and appropriate support software would be furnished, as required, by AFAL during the contract to determine preliminary assembly language programming requirements for implementing the ATS software design on the SKC-2000.

During the course of AGFCS Phase II the (SOW) anticipated emphasis on the SKC-2000 as the ATS computer did not materialize. Also, neither the use of a SKC-2000 nor the required software definition was available from AFAL. Accordingly, the ATS software definition was made sufficiently general to allow implementation in either the SKC-2000 or another computer in its class. The detailed ATS software description is presented in VOLUME IV .

As was discussed in Subsection 2.4.2 coordinate system transformation is updated through the use of a SGAP in the ATS design in lieu of a gimballed platform, as authorized in the contract SOW. However, the ATS software has the option of utilizing inertial inputs from an inertial platform such as the Singer-Kearfott ASN-90 (KT-73) as a secondary method. The SGAP selected for the ATS consists of medium-quality gyros and accelerometers. It is

believed that it, or an equivalent strapdown assembly, can be furnished at no-cost to the government for ATS flight test. Representative ATS SGAP performance specifications are presented in Subsection 4.2.3.3.

The overall ATS computer interface is diagramed in Figure 13. A summary of principal ATS computation and interface rates is presented as Figure 14. Interface consists in twisted pairs transmitting complementary TTL (Transistor-Transistor Logic) signals. Each subsystem is assigned a command word. The individual bits of the command word command the subsystem to either: 1) transition to a particular operating mode; 2) receive data; or 3) transmit data. The number of bits in the command word is adjusted to the particular requirements of its subsystem.
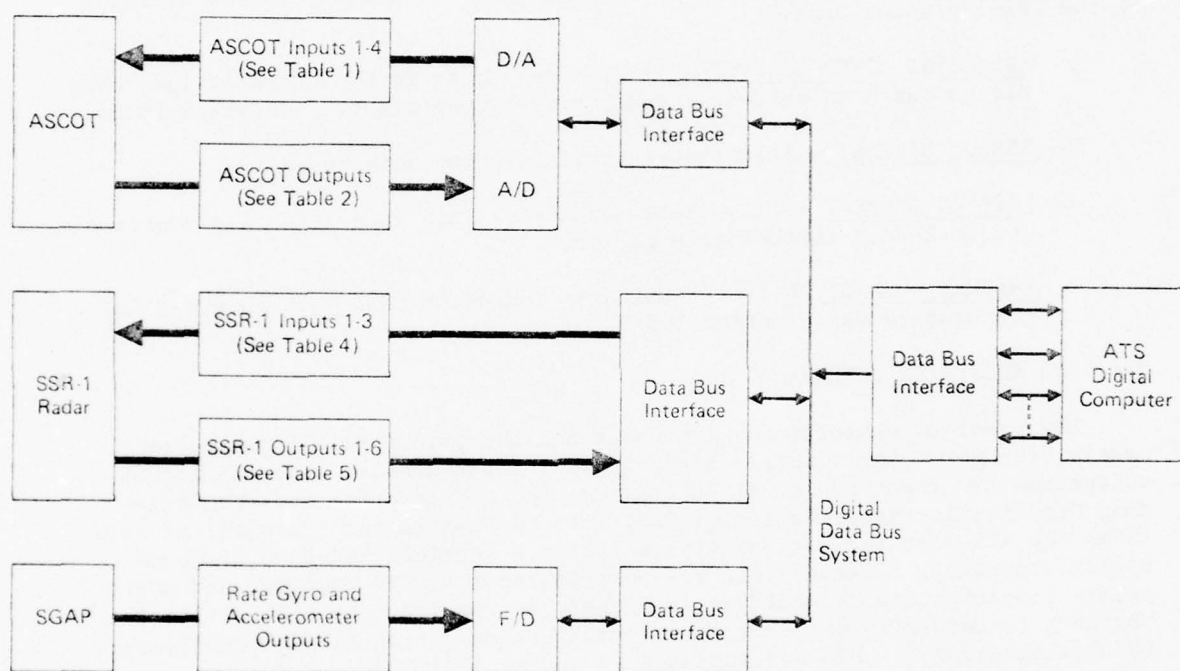
FIGURE 13
ATS COMPUTER INTERFACE DIAGRAM

GP74-0122-56

Data words are each 16 bits long with bit 1 being the least significant bit (LSB). To maintain efficient interface design data words are "packed" when possible. That is one 16-bit data word consists in several sub-words of less than 16 bit length. When the command is to "receive data", the ATS computer transmits the 16 data bits along with the computer clock pulses. An "Execute" pulse then follows the data word. When the command is to "transmit

54

```
┌─────────────────────────────────────────────────────────────────┐
│ SSR-1                                                             │
│                                                                   │
│    Transmission Pulse Rate ............................ 1024 Hz (Discrete)  │
│    Tracking Loop Update Rate ......................... 64 Hz (Discrete)     │
│    SSR-1/ATS Computer Interface Rate .................. 64 Hz (D/D)         │
│                                                                   │
│ ASCOT                                                             │
│    Tracking Loop Bandwidth ........................... Variable             │
│    Scan Frequency .................................... 1000 Hz (Continuous) │
│    ASCOT/ATS Computer Interface Rate .................. 160 Hz (A/D)        │
│                                                                   │
│ ATS Computer                                                      │
│    Angle Tracking Filter Update Rate ...................... 16 Hz (Discrete) │
│    Range Tracking Filter Update Rate ...................... 16 Hz (Discrete) │
│    Filter Coordinate System Update Rate ................... 160 Hz (Discrete)│
│    ATS Computer/SSR-1 Interface ........................ 64 Hz (D/D)        │
│    ATS Computer/ASCOT Interface ........................ 160 Hz (D/A)       │
│ SGAP                                                              │
│    Gyro Loop: Analog-to-Frequency Converter .............. 0-6250 pps (A/F) │
│    Accelerometer Loop: Analog-to-Frequency Converter....... 0-6250 pps (A/F)│
│    SGAP/ATS Computer Interface......................... 160 Hz (F/D)        │
└─────────────────────────────────────────────────────────────────┘
```

FIGURE 14

SUMMARY OF ATS COMPUTATION AND INTERFACE RATES

GP74-0122-53

data", the ATS computer follows the command transmission with an "Execute"
pulse. The 16 computer clock pulses follow and the data is entered into the
ATS computer. The "Execute" pulses represent parallel data transfers into
and out of the Input/Output (I/O) registers. The clock pulses provide for
serial transfer into the I/O registers or the ATS computer.

The ASCOT and SSR-1 command words are presented in Table 6. Each sub-
system command word is assigned 8 bits in a packed 16 bit ATS computer com-
mand word. At present both the ASCOT and the SSR-1 command words utilize
only 7 bits with one unassigned bit available for future use.

Because of its digital design it was convenient to describe the quanti-
zation of the SSR-1 inputs and outputs in the previous subsection concerned
with the SSR-1 design summary. SSR-1 digital inputs were quantized in Table
4; while Table 5 quantized the digital output data. Range and range-rate
data are transmitted and received in 16-bit words. Since range-rate data are
quantized with an 8-bit word (7 bits plus sign), the extra unassigned 8 bits
of the range-rate word are available for future use. The range register cor-
rection (8 bits), status word (3 bits), signal-to-noise ratio (4 bits) and
self-test failure discrete (1 bit) are packed into one 16-bit word.

As shown in Figure 13 ASCOT input and outputs require Digital-to-Analog
(D/A) and Analog-to-Digital (A/D) conversion prior to direct interface with
the ATS computer via the data bus. Tables 1 and 2 summarize the analog ASCOT
inputs and outputs, respectively. The quantized digital ASCOT inputs prior
to D/A conversion are presented in Table 7. Word 1 is packed. It consists
in the 8-bit ASCOT command word, target subtense (7 bits) and the track dis-
crete. Words 2 and 3 are the horizontal and vertical pointing commands.

55

TABLE 6
ASCOT AND SSR-1 COMMAND WORDS

ATS Computer Command Word Structure		
	Bit	Command
ASCOT CMD Word	1	Receive Target Subtense
	2	Receive Horizontal and Vertical Pointing Commands
	3	Transmit Status, Scan Size and Duty Cycle
	4	Transmit Horizontal and Vertical Position
	5	Transmit Horizontal and Vertical Pointing Errors
	6	Transmit Target Levels
	7	Transmit Scene Brightness and Background Noise
	8	Unassigned
SSR-1 CMD Word	9	Transmit Range Register Correction, Status and Signal-to-Noise Ratio
	10	Autonomous Mode
	11	Augmented Mode
	12	Transmit Range Data
	13	Receive Range Data
	14	Transmit Range-Rate Data
	15	Receive Range-Rate Data
	16	Unassigned

GP74-0122-93

TABLE 7
DIGITAL ASCOT INPUTS

Input Words	Function	Software Name	Quantization			
			Length	Units	MSB	LSB
Word 1	Command Word	JIOA	8 Bits	NA	NA	NA
	Target Substance	EVTSOR	7 Bits	Volts	2.5	0.0195
	Track Discrete	ITRKA	1 Bit	NA	NA	NA
Word 2	Horizontal Pointing Command	EVTSSC(2)	15 Bits + Sign	Volts	2.5	0.000153
Word 3	Vertical Pointing Command	EVTSSC(3)	15 Bits + Sign	Volts	2.5	0.000153

GP74-0122-96

56

ASCOT output quantization is presented in Table 8. Word 1 is composed of a 2-bit Status word derived from the ASCOT's Detection and Acquisition Discretes, a 5-bit Scan Size word and a 6-bit Duty Cycle word. The Status word is defined by Table 9. Words 2 through 5 are self-explanatory. Words 6 and 7 transmit target levels, scene brightness and background noise measurements. The quantization of these outputs is to be determined upon scale factor selection.

TABLE 8
DIGITAL ASCOT OUTPUTS

Output Words	Function	Software Name	Quantization			
			Length	Scale Factor	MSB	LSB
Word 1	Status Word	JFSWA	2 Bits	NA	NA	NA
	Scan Size	XSCSZM	4 Bits + Sign	2.8 mr/V	2.5	0.3125
	Duty Cycle	XDUTYM	6 Bits	10%/V	2.5	0.078125
Word 2	Horizontal Position	EVTSSM(2)	15 Bits + Sign	3°/V	2.5	0.000153
Word 3	Vertical Position	EVTSSM(3)	15 Bits + Sign	3°/V	2.5	0.000153
Word 4	Horizontal Pointing Error	XDVSM(2)	15 Bits + Sign	3°/V	2.5	0.000153
Word 5	Vertical Pointing Error	XDVSM(3)	15 Bits + Sign	3°/V	2.5	0.000153
Word 6	Positive Target Level	XPTLVM	8 Bits	TBD	2.5	0.0195
	Negative Target Level	XNTLVM	8 Bits	TBD	2.5	0.0195
Word 7	Scene Brightness	XSCBRM	8 Bits	TBD	2.5	0.0195
	Background Noise	XBGNSM	8 Bits	TBD	2.5	0.0195

GP74-0122-95

TABLE 9
ASCOT STATUS WORD DEFINITION

ASCOT Status	ASCOT Output*				Status Word	
	1		2		Bit 1 IDETA	Bit 2 IACQA
	Hi	Low	Hi	Low		
Search		X		X	0	0
Acquisition	X			X	1	0
Track	X		X		1	1

*Reference Table 2

GP74-0122-94

SECTION 4 ATS PERFORMANCE ANALYSIS

4.1 GENERAL

The ATS performance analysis task included: 1) sensor system math model-
ing and validation methodology; 2) ATS Kalman filter design and development;
and 3) error budget determination and performance analysis. Each of these
principal subtasks is discussed in the following subsections.

4.2 ATS SENSOR MATH MODELS

The principal ATS sensors are the ASCOT angle tracking sensor and the
SSR-1 range tracking sensor. Also included in the ATS mechanization is a
strapdown gyro/accelerometer package, SGAP. Detailed functional descriptions
of the ASCOT and SSR-1 as well as a discussion of their principal error
sources are presented in VOLUMES II & III , respectively. In this subsection
selected portions of this data are collected to form ASCOT and SSR-1 math
models suitable for: 1) discussion of the principal error sources and methods
of validating the sensor model; 2) incorporation into the ATS digital computer
simulation used in performance analysis; and 3) utilization as measurement
models in the ATS Kalman tracking filters after appropriate modification.

4.2.1 ATS Angle Sensor (ASCOT) Math Model

The fundamental measurement geometry of the ASCOT is illustrated in
Figure 15. For simplicity, only the geometry of the horizontal measurement
plane is shown; similar considerations apply to the vertical measurement
plane. The actual target position, its line of sight (LOS) and the horizontal
position of the target in sensor coordinates, $P_{TS}(2)$, are shown. Also shown
are the estimated target position, the estimated LOS and the estimated hori-
zontal position of the target in sensor coordinates, $\hat{P}_{TS}(2)$. The ASCOT is
commanded to point at the estimated target position. The pointing error,
ΔP_{TS}, is then measured by closing the internal ASCOT tracking loop. Since the
internal tracking loop utilizes integral action, the output of the integrator
represents the pointing error.

Based upon the ASCOT design description of VOLUME II , the ATS angle
sensor model presented in Figure 16 was developed to represent the ASCOT in
its tracking mode. The model includes the principal ASCOT noise sources
(receiver noise, glint noise and atmospheric noise) as well as the geometric
relationship between target position and pointing command. Also included is
the ASCOT's integral-control internal tracking loop. Pertinent elements of
the ATS computer software (such as, the ASCOT pointing command, the measure-
ment averaging computations, and the interface data sampling rates) are also
included.

58

4.2.1.1 ASCOT Tracking Loop Bandwidth - The ASCOT tracking loop due to its integral action has a bandwidth equal to the forward gain, K_I, in radians/second. From Appendix A,

$$K_I = \frac{K_{ES}}{T} \cdot K_{TF} * K_{DA}$$

where

$\frac{K_{ES}}{T} \triangleq$ Pointing error sensor gain, volts/degree

$K_{ES} = .26$

$T \triangleq$ Target subtense, degrees

$K_{TF} \triangleq$ Tracking filter integrator gain, volts/second/volt

$\quad = 33$ or 66 (See Table 1, Input 7)

$K_{DA} \triangleq$ Deflection amplifier gain, degrees/volt

$\quad = 6.9$

GCSF $\triangleq$ Filter to sensor direction cosine matrix

$P_{T_S} \triangleq$ Target position (sensor coordinates)

$\hat{P}_{T_S} \triangleq$ Estimated target position (sensor coordinates)

$\Delta P_{T_S} \triangleq$ Error in estimated target position (sensor coordinates) $P_{T_S} - \hat{P}_{T_S}$
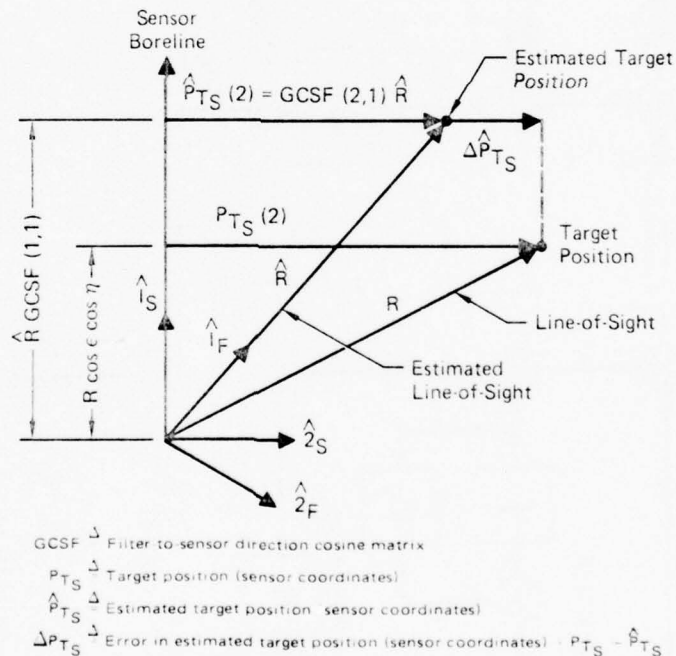
FIGURE 15
ANGLE SENSOR GEOMETRY

GP 74-0122-8

59

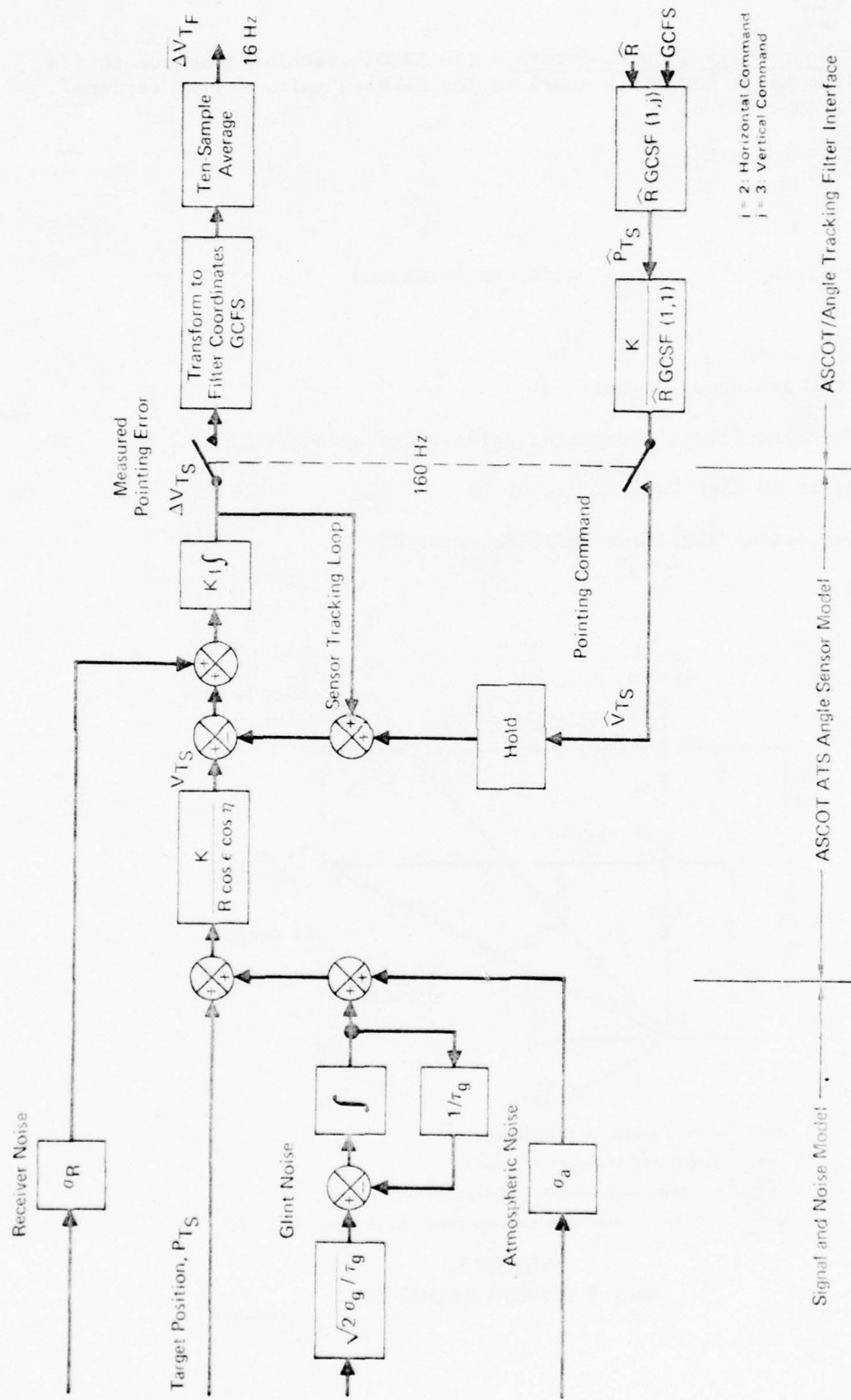**FIGURE 16**

ATS ANGLE SENSOR (ASCOT) MATH MODEL - TRACKING MODE

Figure 17 illustrates the variation in the ASCOT tracking loop bandwidth as a
function of range, target size (aspect) and the selectable tracking filter
gain. Extreme conditions provide minimum and maximum ASCOT bandwidths. For
example, a minimum bandwidth of approximately 2.5 Hz is obtained at short
range (500 feet), large target (32 feet) conditions using the lower tracking
filter gain option (33). On the other hand, a maximum bandwidth of approxi-
mately 330 Hz is obtained at long range (6000 feet), small target (6 feet)
conditions using the higher tracking filter gain option (66).
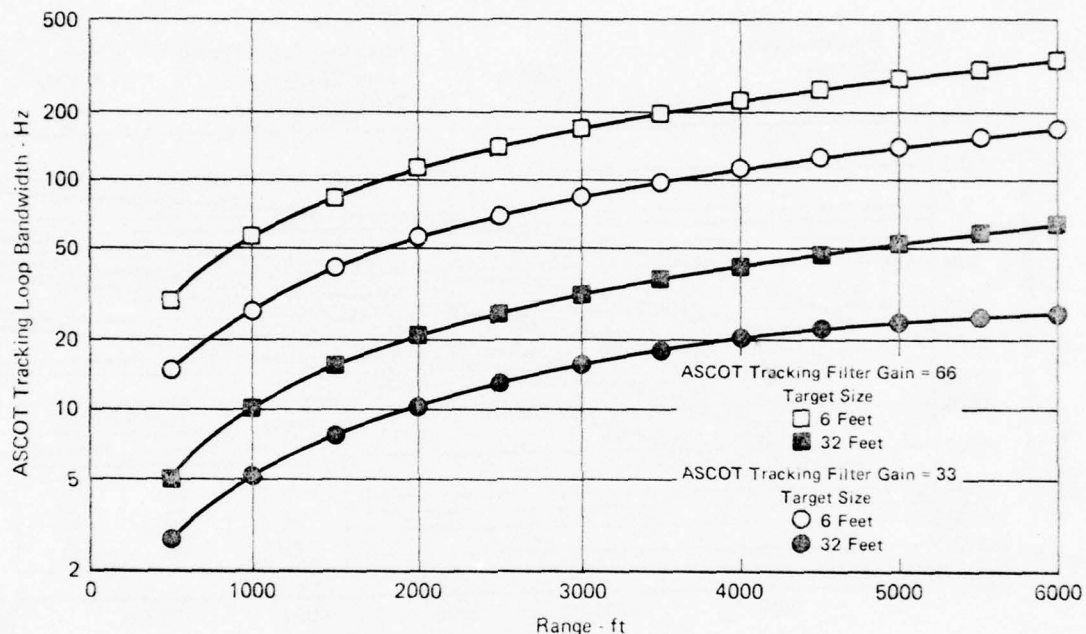

FIGURE 17
ASCOT TRACKING LOOP BANDWIDTH VARIATION

GP74-0122-68

It is apparent that the ASCOT tracking loop dynamics will color the
noise corrupting the measured pointing error. The noise correlation time
will vary from approximately 3 to 400 milliseconds. However, the ATS Kalman
Angle Tracking Filter bandwidth is on the order of 0.6 Hz. Thus for filter
design purposes the ASCOT measurement noise is considered white.

4.2.1.2 ASCOT Measurement Noise - The principal ASCOT measurement noise
sources which can be modeled analytically are atmospheric noise, receiver
noise and glint. ASCOT atmospheric and receiver noise models are presented
in VOLUME II. The term glint is used here to denote the ASCOT measurement
error due to a lack of correspondance between the target's center of gravity
and the measured target contrast centroid. The ASCOT is designed to minimize
this error source; however, it has not been quantified experimentally.

61

Figure 18 presents the combined effect of atmospheric and receiver noise on the ASCOT's measurement error in terms of feet at target range. Figure 19 presents the same information in terms of measured voltage. Since range is of particular significance, the measurement error standard deviation is presented as a function of range for various levels of scene brightness and target size. The measurement error due to atmospheric and receiver noise reaches a maximum of about .2 feet (.7 millivolts) for maximum range and target size and minimum scene brightness conditions.
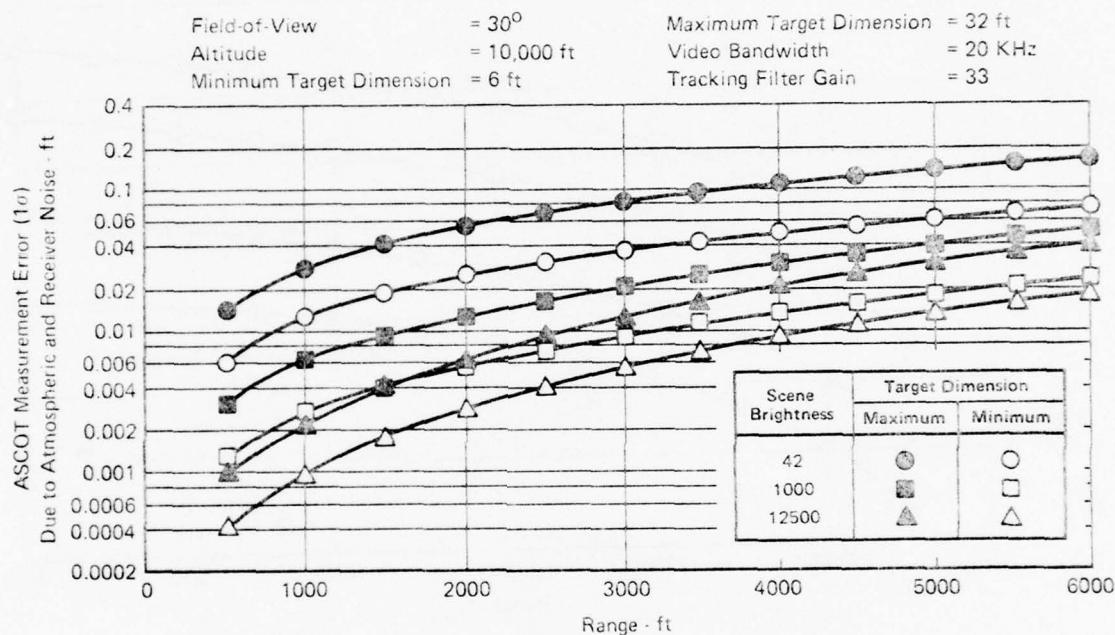

FIGURE 18
COMBINED EFFECT OF ATMOSPHERIC AND RECEIVER NOISE IN FEET

GP74-0122-66

The data of Figures 18 and 19 were computed based upon the lower value of selectable tracking filter gains (33 volts/second/volt) and an ASCOT video bandwidth of 20 KHz. The effect of increasing the tracking filter gain and decreasing the video bandwidth is illustrated in Figures 20 and 21. Worst case conditions only (low scene brightness, large target) are illustrated. The point of interest here is that, even under the worst set of conditions, the combined effect of atmospheric and receiver noise is less than .5 feet (1.5 millivolts).
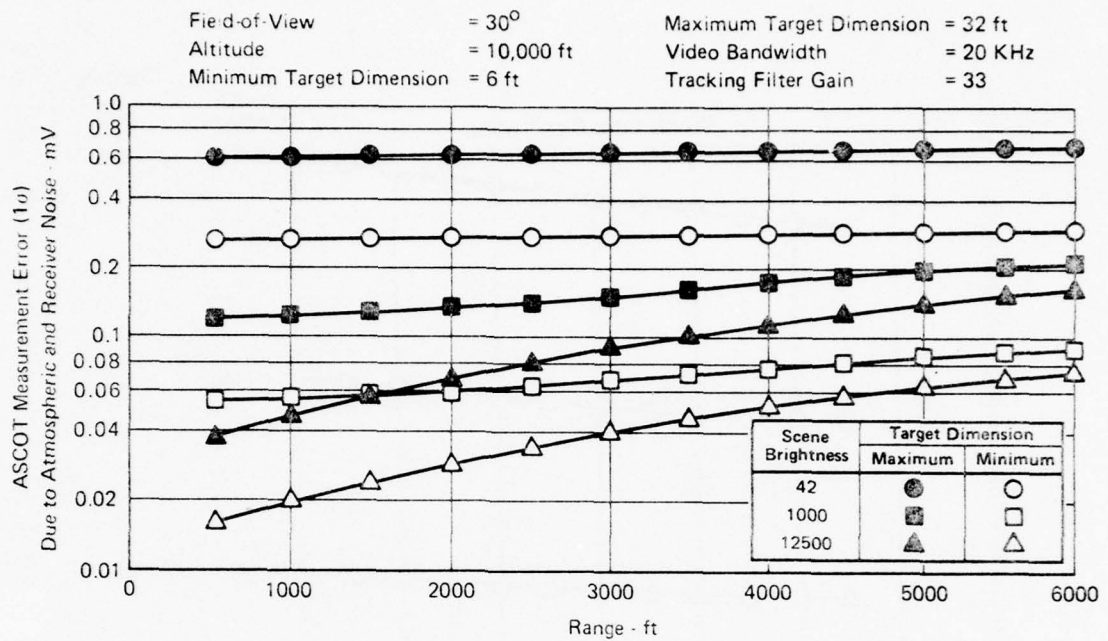
FIGURE 19
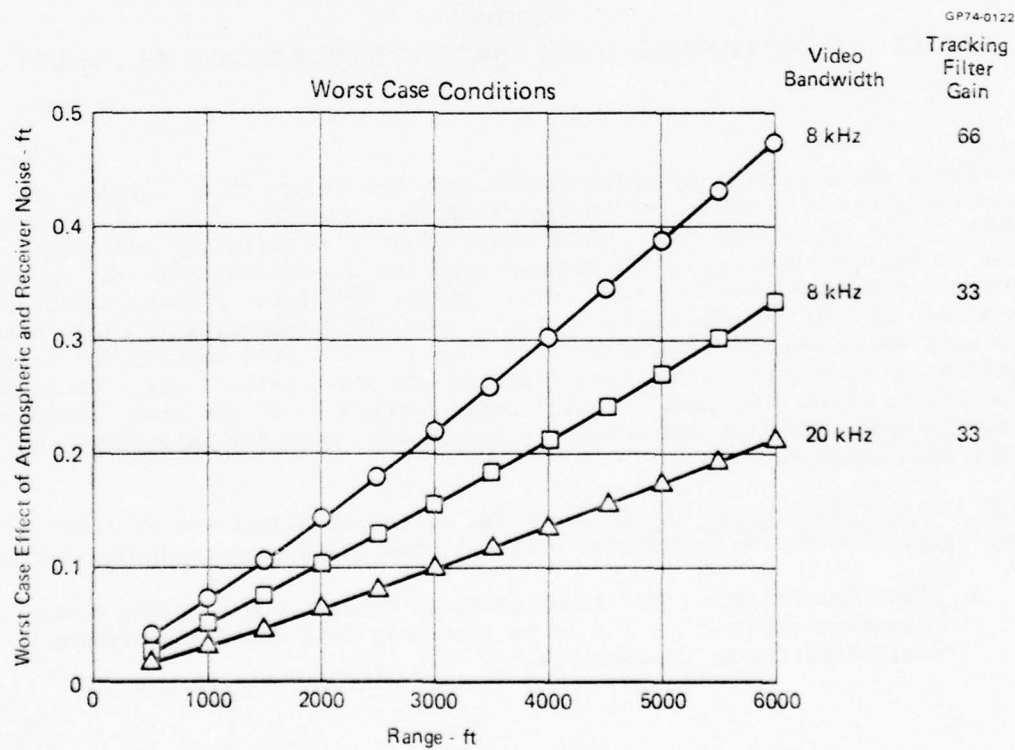COMBINED EFFECT OF ATMOSPHERIC AND RECEIVER NOISE IN MILLIVOLTS

GP74-0122-67

FIGURE 20
EFFECT OF VIDEO BANDWIDTH AND TRACKING FILTER GAIN IN FEET
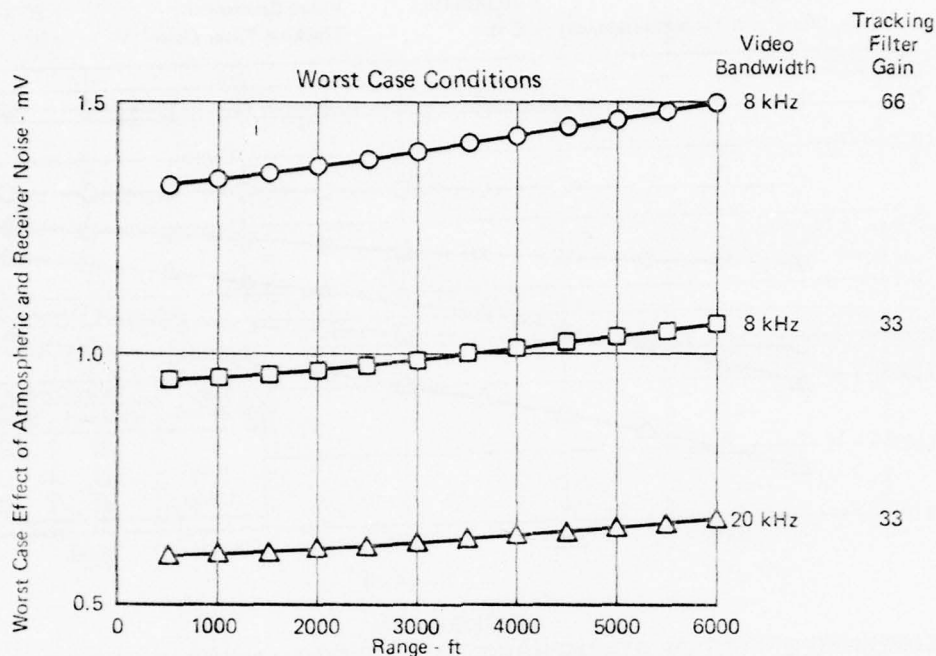
GP74-0122-65

63

FIGURE 21

EFFECT OF VIDEO BANDWIDTH AND TRACKING FILTER GAIN IN MILLIVOLTS

GP74-0122-64

Since the magnitude of glint is unknown, its effect in millivolts of measurement error is presented in Figure 22 for glint amplitudes of .5, 1 and 5 feet (1 σ). Note that for a glint error of only .5 feet, the measurement noise in millivolts exceeds the maximum expected from atmospheric and receiver effects for ranges less than 6000 feet. Inside 3000 feet (gunnery conditions) the effect of glint predominates. Even if the ASCOT successfully minimizes glint, it seems probable that errors in excess of 0.5 feet between the target's center of gravity and the contrast centroid are inevitable. Thus, the as yet unquantified glint component of ASCOT noise appears to be the most important factor in noise modeling and should be a principal item for laboratory and flight test investigation.

4.2.1.3 <u>ASCOT Math Model Validation</u> - The principal objectives of ASCOT math model validation during subsequent phases of the AGFCS program should include:

o ASCOT Calibration - The ASCOT pointing command and pointing error measurement circuitry should be precisely calibrated identifying nonlinearities or distortions.

64

o Pointing Error Measurement Noise – The total pointing error measure-
  ment noise should be quantified. This includes bias and systematic
  errors, random errors and their correlation period.

o Angle Glint Error – A thorough experimental study should be conducted
  to specify the ability of the ASCOT to track the geometric controid
  of a target under dynamic conditions.

o Miscellaneous Errors – Design testing of the ASCOT circuitry should
  be conducted to determine such miscellaneous error sources as scale
  factor accuracy, scale factor variation with temperature, amplifier
  gain variations, noise pickup in tracking circuits, etc.

o ASCOT Detection Performance – Analysis and experimental studies
  should be performed to determine ASCOT detection performance for
  various conditions of range, scene brightness, search field size, etc.

These validation studies require the use of appropriate experimental test
facilities and procedures which could be performed in conjunction with hot
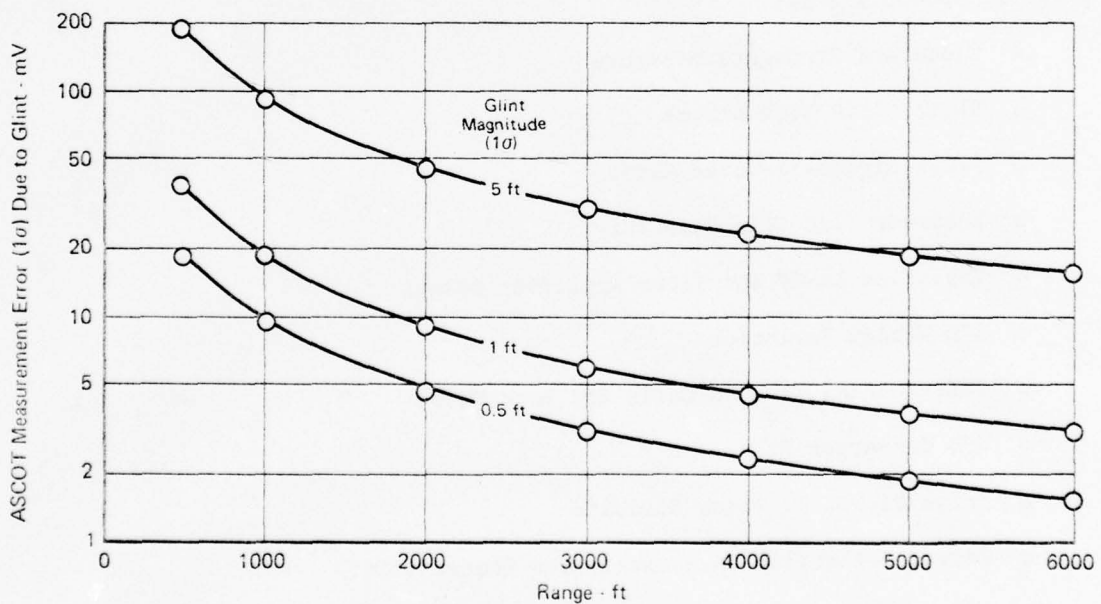mock-up testing prior to flight test.

FIGURE 22
EFFECT OF GLINT MAGNITUDE ON ASCOT MEASUREMENT ERROR

GP74-0122-63

65

4.2.2   ATS Range Sensor (SSR-1) Math Model

Based on the SSR-1 design description of VOLUME III, the ATS range sensor model presented in Figure 23 was developed. When operating in its Augmented tracking mode, the SSR-1's autonomous tracking loop is opened by: 1) loading the range register by external (ATS computer) command with estimated range from the Range Tracking Filter; and 2) setting $\alpha = 1$ and $\beta = 0$. The nine most significant bits of the range register are used to position range gates 4 and 5 about the filter's estimated range so that Fine ΔR represents the error in estimated range smoothed over 16 returns, plus the seven least significant bits of the range register. The measured range register correction is, therefore, the difference between Fine ΔR and the seven least significant bits of the range register. The measured range register correction is then added to the range register contents to provide a total range measurement every 1/64 second. Four consecutive range measurements are averaged in the ATS computer to obtain radar measurements at the 16 Hz rate required by the Range Tracking Filter.

This model includes the principal SSR-1 noise sources, receiver noise and range glint. Also shown are radar pulse rates and pertinent elements of the ATS computer software, such as, interface sampling rates and measurement averaging computations.

4.2.2.1   SSR-1 Measurement Noise - Sources of range error in the SSR-1 are given in Appendix B as:

- o   Clock and Propagation Errors

- o   RF to Clock Time Errors

- o   Radar Signal-To-Noise Ratio

- o   Reciever Time Gain Stability

- o   Variation in IF and Video Amplifier Delays

- o   A/D Window Variations

- o   Differential Gain in Early and Late Video

- o   A/D Converter Bias

- o   Noise Pickup in Video Circuits

- o   Target Reflection Characteristics (Range Glint)

- o   ATS Digital Computer Interface Quantization

Each of these sources is discussed in detail in the addendum; their magnitudes are summarized in Table 10. Table 10 also classifies each error source as either random or bias. This classification is based on the anticipated correlation time of each error. Errors which have a long correlation time in
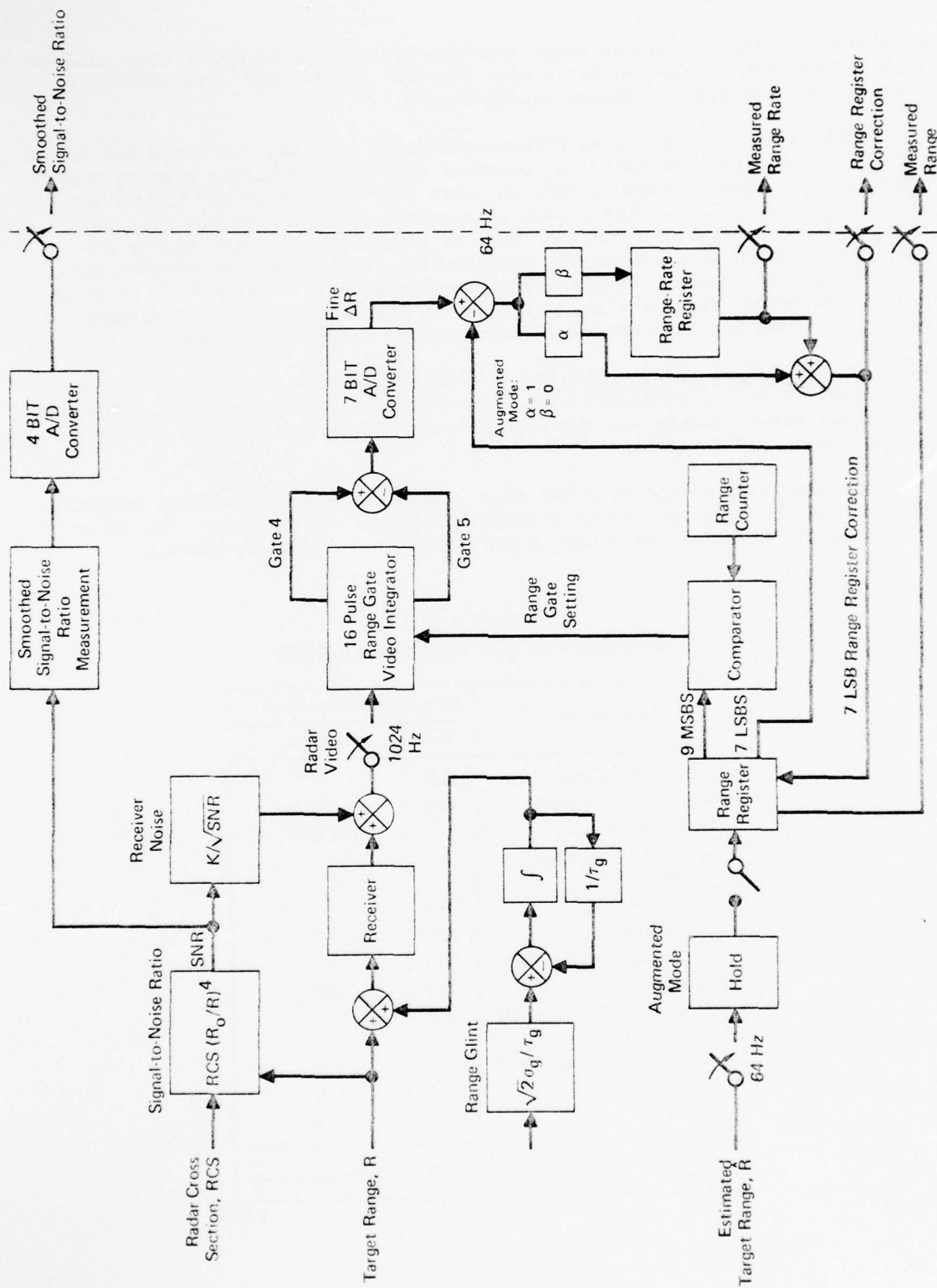
FIGURE 23

ATS RANGE SENSOR (SSR-1) MATH MODEL - TRACKING MODE

GP74-0122-10

67

comparison to the ATS Kalman Range Tracking Filter's predominant time constant (2.4 second) are considered to be bias errors. Errors with a relatively short correlation time are considered random errors.

Table 10 identifies three predominant error sources: 1) error due to the radar's signal-to-noise ratio; 2) receiver time gain stability errors; and 3) range glint. Each of these errors is taken into account in the Kalman Range Tracking Filter design. The effect of receiver time gain stability error is minimized by compensating for the error as a function of range in the ATS computer. Figure 24 presents the compensation formula and the compensation as a function of range. Errors due to signal-to-noise ratio and range glint are random errors which are accounted for in the Kalman filter measurement model as a function of measured signal-to-noise ratio (see Subsection 4.3.3.1).

4.2.2.2 *SSR-1 Math Model Validation* - Unlike the ASCOT math model, the SSR-1 math model is well established based upon previous subcontractor experience in similar radar designs and the long history of the use of radar in the air-to-air combat environment.

The magnitude of the receiver time gain stability errors after compensation in the ATS computer can be established during hot mock-up. The error due to signal-to-noise ratio can be measured by experimental testing.

TABLE 10
SUMMARY OF SSR-1 ERROR SOURCES

| Error Source	Error Standard Deviation - ft	
	Bias	Random
Clock and Propagation Error	0.8	—
RF to Clock Time Error	10.0	3.0
Signal-to-Noise Errors	—	$57/\sqrt{SNR}$
Receiver Time Gain Stability (Range 500 ft)		
Uncompensated	80.0	—
Compensated	35.0	—
IF and Video Amplifier Delay	13.0	—
A/D Window Variations	13.0	6.5
Differential Gain in Early and Late Video	3.0	—
A/D Converter Bias and Offset	3.0	1.3
Video Circuits	—	2.0
Range Glint	—	10.0
Total RSS Error with Compensation	41.0	$\sqrt{12.5^2 + 57^2/SNR}$
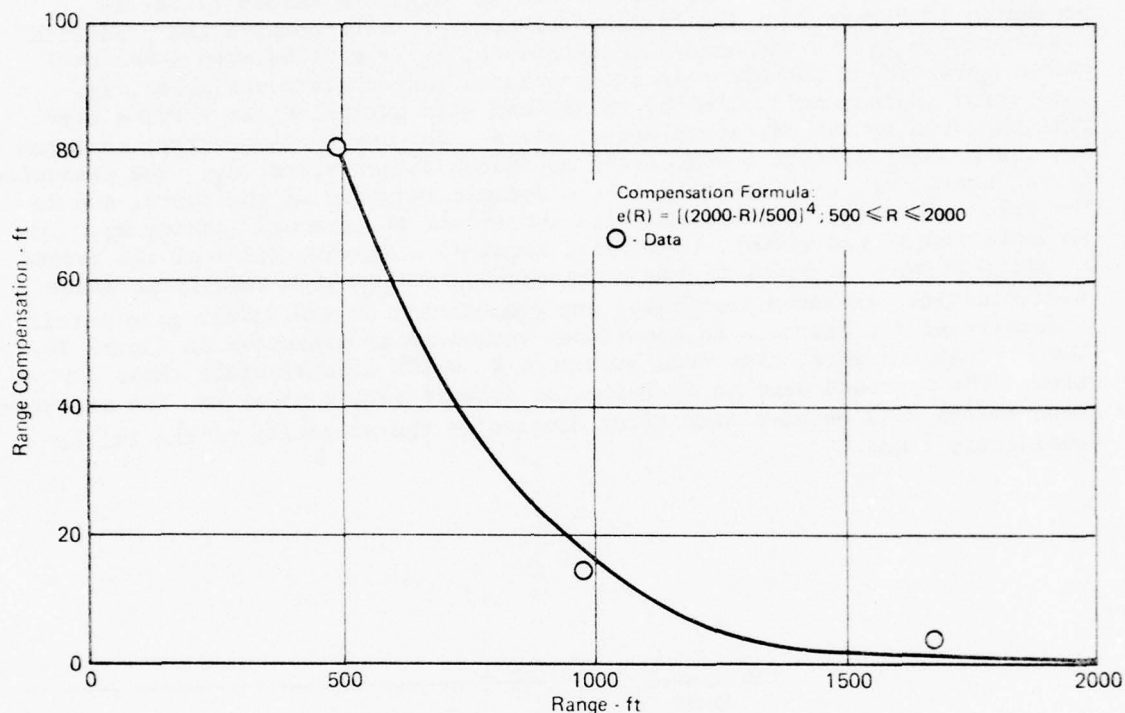
FIGURE 24
RECEIVER TIME GAIN STABILITY COMPENSATION

GP74-0122-101

4.3 ATS KALMAN FILTER DESIGN

This subsection reviews the ATS Kalman tracking filter design. Included
are discussions related to the overall filter design approach utilized for
the ATS, as well as the specific designs selected for the ATS Range Tracking
Filter and Angle Tracking Filter. The ATS tracking filter design employs
optimal Kalman filtering and prediction methods. The word optimal is used
here with reservation. While optimal for the idealized linear system used
in its original derivation, the Kalman filter is not "optimal" in the real
world of air combat. This is due to the inevitable mismatch between the
actual operating environment and the hypothetical world of the theorist.
Nevertheless, the approach is useful and valid because it provides a system-
atic method of incorporating known target dynamic equations and knowledge of
the degree of uncertainty in sensor measurements into the data processing.
Care must be taken, however, to minimize the sensitivity of the equations to
any mismatch between operating conditions and design assumptions. ATS track-
ing filter sensitivities are discussed in Subsection 4.4.3.

The basic structure selected for the ATS discrete Kalman filter is presented in Figure 25. The fundamental concept is to compare the predicted measurements, $\bar{z}_i$, to the actual measurements, z_i; the difference (residual) being a measure of the error in the predicted target state variables, $\bar{x}_i$. This error is then multiplied by the Kalman gain matrix, K, to provide correction terms to the predicted target state. The sum of the correction terms and the predicted state provides the estimated target state, $\hat{x}_i$. The predicted target state, $\bar{x}_{i+1}$, is composed of the dynamic response of the system due to the prior estimated target state plus the effect of external inputs, w_i. Implementation of the filter, therefore, requires a dynamic model of the target in discrete form, a model of the measurement process which transforms state variables into measured variables, and computation of the Kalman gain matrix. A summary of the discrete Kalman filter equations is presented in Figure 26. These equations were taken from Reference 2, which also presents their derivation. The approach used in deriving the dynamic target model and the measurement models will be presented after discussing the selection of the filter coordinate frame.
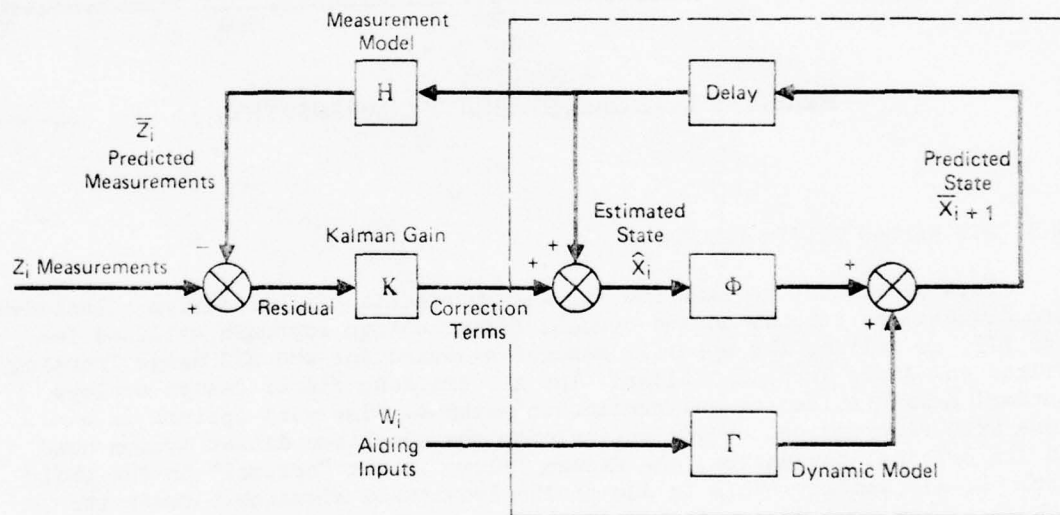

FIGURE 25
ATS KALMAN FILTER STRUCTURE

GP74-0122-11

70

Dynamic Model

$x_{i+1} = \phi_i x_i + \Gamma_i w_i, \; i = 0, \ldots, N-1,$

Where $\quad E(x_o) = \overline{x}_o$

$\qquad E(w_i) = \overline{w}_i$

$\qquad E(x_o - \overline{x}_o)(x_o - \overline{x}_o)^T = M_o$

$\qquad E(w_i - \overline{w}_i)(w_j - \overline{w}_j)^T = Q_i \delta_{ij}$

$\qquad E(w_i - \overline{w}_i)(x_o - \overline{x}_o)^T = 0$

Measurement Model

$z_i = H_i x_i + v_i, \; i = 0, \ldots, N,$

Where $E(v_i) = 0$

$E(v_i v_j^T) = R_i \delta_{ij}$

$E(w_i - \overline{w}_i)v_j^T = 0,$ and

$\qquad E(x_o - \overline{x}_o)v_i^T = 0$

Estimation Algorithm

$\hat{x}_i = \overline{x}_i + K_i(z_i - H_i \overline{x}_i), \; (i = 0, \ldots, k, \text{ Where } k \leq N).$

Where $\quad \overline{x}_{i+1} = \Phi_i \hat{x}_i + \Gamma_i \overline{w}_i, \; \overline{x}_o$ Given

$\qquad K_i = P_i H_i^T R_i^{-1}$

$\qquad P_i = (M_i^{-1} + H_i^T R_i^{-1} H_i)^{-1} = M_i - M_i H_i^T (H_i M_i H_i^T + R_i)^{-1} H_i M_i$

$\qquad M_{i+1} = \Phi_i P_i \Phi_i^T + \Gamma_i Q_i \Gamma_i^T$

Prediction Algorithm

$\hat{x}_{i+1} = \overline{x}_{i+1} = \Phi_i \hat{x}_i + \Gamma_i \overline{w}_i; \; i = m, m+1, \ldots, (m > N)$

FIGURE 26
SUMMARY OF DISCRETE KALMAN FILTER EQUATIONS

GP74-0122-12

4.3.1 Coordinate System Selection

An important consideration in connection with target state estimation and prediction techniques is the selection of the coordinate reference frame for system computations. Problems associated with many two-axis tracking systems, due to their use of non-roll-stabilized line-of-sight coordinates associated directly with the tracking device as their computation frame, were discussed in Subsection 2.4.1. As discussed in that subsection, a roll-stabilized line-of-sight coordinate system was selected for ATS Kalman filter design. In addition to avoiding the cited problems, the selection of this coordinate system for tracking loop computations yielded a more systematic variation of the corresponding target states, thereby contributing to improved target estimation and prediction. Other advantages in the use of the roll-stabilized line-of-sight system are: 1) the decoupling of the elevation and traverse tracking dynamics; and 2) its close physical correspondence to the measurements taken by the ASCOT angle sensor. ASCOT measurements are taken in a focal plane which maintains a fixed reference with respect to the aircraft body axes. Thus, a simple rotation matrix relates the non-roll-stabilized measurement plane to the roll-stabilized filter plane. This close physical correspondence also prompted the following selection of the Angle Tracking Filter state variables: 1) the error in estimated target position; 2) relative target velocity; and 3) total target acceleration. All are defined in a plane at target range normal to the estimated line-of-sight.

71

4.3.2 Target Dynamic Model

The basic target dynamics in roll-stabilized line-of-sight coordinates are derived in Figure 27. The basic target states in these coordinates are R and $\dot{R}$, $\omega(2)$ and $\omega(3)$ in the range, traverse and elevation coordinates respectively. The target acceleration relative to the attacker is unknown and must be modeled a priori as a random process. Modeling of the target acceleration will be discussed in more detail in subsequent paragraphs after first considering the nonlinear form of the target dynamic equations.

Kalman filter theory as originally published applied to linear systems only. It is conveniently (but not optimally) extended to nonlinear systems by linearizing the dynamic equations about the estimated state variables. This technique is particularly applicable to the target dynamic equations. By configuring independent range and angle tracking filters, the elevation and traverse filter coordinate system rates can be fed into the range equation resulting in a linear equation. Similarly, range and range-rate estimates can be fed into each of the angle equations giving them a linear structure. The resulting linear equations are:

$$\ddot{R} = (\omega^2(2) + \omega^2(3)) \; R + \Delta a(1)$$

$$\dot{P}(2) = V(2) - \omega(3) \; \hat{R}$$

$$\dot{V}(2) = -(\hat{\dot{R}}/\hat{R}) \; V(2) + \Delta a(2)$$

$$\dot{P}(3) = V(3) + \omega(2) \; \hat{R}$$

$$\dot{V}(3) = -(\hat{\dot{R}}/\hat{R}) \; V(3) + \Delta a(3)$$

Modeling the target accelerations colinear and orthogonal to the tracker LOS is a highly speculative process and one must exercise care in the choice of a model. Too elaborate a model can result in a mismatch between the filter design assumptions and the true operating environment and lead to filter instability. Because of the highly uncertain nature of the dogfight environment, target acceleration models with two levels of sophistication were considered. The more complicated model was a first-order Gauss-Markov process; while in the simplified model target acceleration was modeled as Gaussian, white noise. Use of the first-order Gauss-Markov process required augmenting the target state variables by the acceleration component in order to account for the hypothesized time correlation of the target acceleration dynamics. Although the more sophisticated model results in increased filter complexity, the tracker performance using the white noise model was unsatisfactory. Use of the total target acceleration instead of relative acceleration as a state in the target dynamic equations in Figure 27 requires including attacker acceleration in these equations. Digital computer analysis indicated that using total target acceleration results in improved Kalman filter state estimation accuracy. Thus, the ATS tracking filters utilize the first-order Gauss-Markov model of total target acceleration shown in Figure 28.

$(\hat{1}, \hat{2}, \hat{3}) \triangleq$ Filter Coordinate System Unit Vector Triad

$\underline{R} = R\,\hat{1}$

$\underline{\omega} = \omega(1)\,\hat{1} + \omega(2)\,\hat{2} + \omega(3)\,\hat{3}$

for Roll Stabilization, $\omega(1) = 0$.

$\dfrac{d}{dt}\,\underline{R} = \underline{\dot{R}} + \underline{\omega} \times \underline{R}$

$\dfrac{d^2}{dt^2}\,\underline{R} = \underline{\ddot{R}} + \underline{\omega} \times \underline{\omega} \times \underline{R} + 2\underline{\omega} \times \underline{\dot{R}} + \underline{\dot{\omega}} \times \underline{R}$

$\quad = \Delta a(1)\,\hat{1} + \Delta a(2)\,\hat{2} + \Delta a(3)\,\hat{3}$

Where $\Delta a(1)$, $\Delta a(2)$ and $\Delta a(3)$ are the Target Accelerations Relative to the Attacker Along and Orthogonal to the LOS.

Expanding in Roll Stabilized Filter Coordinates,

$\ddot{R} = (\omega^2(2) + \omega^2(3))\,R + \Delta a(1)$ Range Dynamics

$\dot{\omega}(2) = -2\,\dfrac{\dot{R}}{R}\,\omega(2) + \dfrac{-\Delta a(3)}{R}$ Elevation Dynamics

$\dot{\omega}(3) = -2\,\dfrac{\dot{R}}{R}\,\omega(3) + \dfrac{\Delta a(2)}{R}$ Traverse Dynamics

Selecting target position and velocity orthogonal to the LOS as state variables, the Traverse and Elevation Dynamics become:

$\dot{P}(2) = V(2) - \omega(3)\,R = 0$

$\dot{V}(2) = -\dfrac{\dot{R}}{R}V(2) + \Delta a(2)$ Traverse Dynamics

$\dot{P}(3) = V(3) + \omega(2)\,R = 0$

$\dot{V}(3) = -\dfrac{\dot{R}}{R}V(3) + \Delta a(3)$ Elevation Dynamics

FIGURE 27
TARGET DYNAMICS IN ROLL-STABILIZED LINE-OF-SIGHT COORDINATES

GP74-0122-13

$$\dot{a} = \dfrac{-1}{\tau_T}\,a + \sqrt{\dfrac{2}{\tau_T}}\;\sigma_T\,u$$

Where

$a \triangleq$ Target Acceleration (Colinear or Orthogonal to Tracker LOS)

$u \triangleq$ White, Gaussian Noise (Zero Mean, Unit Variance)

$\sigma_T \triangleq$ Steady State Standard Deviation of Target Acceleration

$\tau_T \triangleq$ Target Acceleration Correlation Time

FIGURE 28
FIRST-ORDER GAUSS-MARKOV TARGET ACCELERATION MODEL

GP74-0122-14

4.3.3 ATS Sensor Measurement Models

Math models of the principal ATS sensors, the ASCOT and SSR-1, were presented in Subsection 4.2. These models must be linearized and simplified for incorporation into the Kalman tracking filter equations. Linearization is required in order that the measurement models conform to the basic hypotheses used in deriving the Kalman filter equations; simplification is required so that a practical filter mechanization results from the design procedure. Thus, the primary consideration here is the development of simplified measurement models suitable for practical incorporation in the Kalman ATS filters. In addition to the ASCOT and SSR-1 measurement models, linear sensor models of the strapdown gyro/accelerometer package, SGAP, are required.

4.3.3.1 ASCOT Measurement Model - The simplified angle sensor model used in the ATS Kalman filter is presented in Figure 29. The reduction of the more complete model of Figure 16 to that of Figure 29 was accomplished by the following steps:

o Step 1 - Model all noise sources as Gaussian, white noise processes with a total standard deviation of σ_m volts. This standard deviation includes the combined effects of glint; atmospheric noise, receiver noise; quantization and A/D conversion; but not the effect of the 10-sample smoothing. This approach reflects our experience that, when modeling noise processes for Kalman filtering which are not well known statistically, a white noise model yields better performance than a colored noise model which does not perfectly match the operational environment.

Simplified ASCOT Measurement Model

$$\Delta V_{T_F} = H \Delta P_{T_F} + \sigma_m u$$
$$H \overset{\Delta}{=} K_{SF} / \hat{R} \ GCFS \ (1,1)$$
$$\Delta P_{T_F} \overset{\Delta}{=} \text{Angle tracking filter state variable,}$$
$$\text{Pointing error in filter coordinates}$$
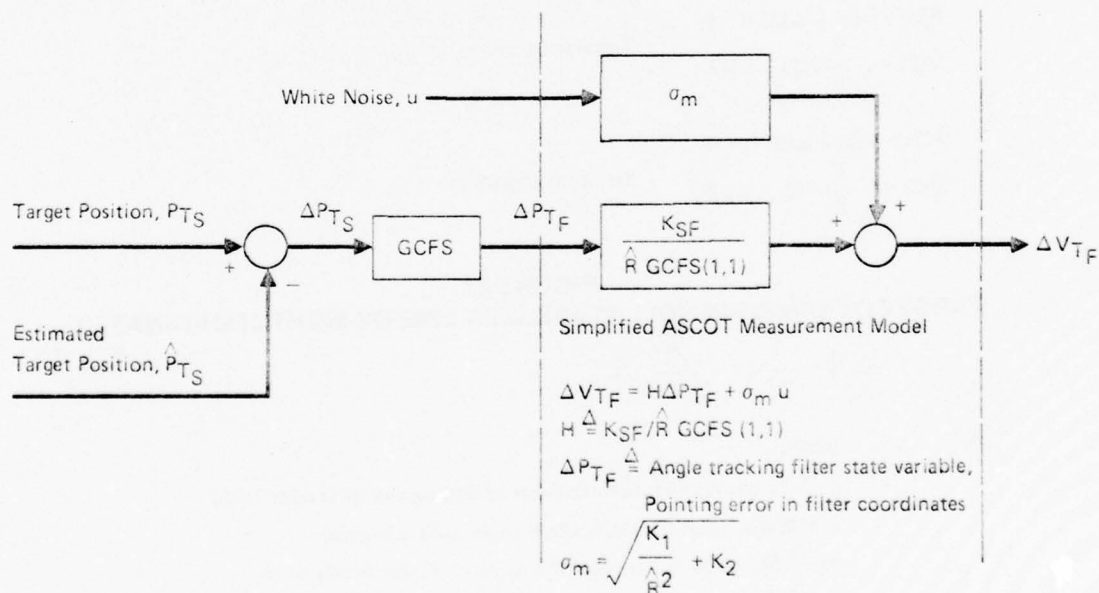$$\sigma_m = \sqrt{\frac{K_1}{\hat{R}^2} + K_2}$$

FIGURE 29
ATS KALMAN FILTER ANGLE SENSOR MODEL

GP74-0122-15

74

o   Step 2 - Neglect ASCOT internal dynamics. This approximation is based
    on the relatively high ASCOT tracking loop bandwidth (2.5 to 330 Hz)
    in comparison with the basic tracking geometry dynamics and on its
    wide variation with range and target aspect (see Figure 17). However,
    the effect of ASCOT bandwidth on σ_m was taken into account.

o   Step 3 - Neglect second-order effects in sensor/geometry transfer
    function, i.e.,

$$\frac{K}{R \cos \varepsilon \cos \eta} \approx \frac{K}{\hat{R} \text{ GCFS } (1,1)}$$

o   Step 4 - Manipulate block diagram to place sensor-to-filter coordinate
    transformation before the ASCOT model. This manipulation provides the
    desired Kalman filter measurement; i.e., it properly relates the
    transformed measurements to the filter state variable (pointing error
    in filter coordinates).

The angle sensor measurement error model used in the ATS Angle Tracking
Filter is presented in Figure 30. The error model was selected principally
on the basis of Angle Tracking Filter performance analysis rather than on the
basis of ASCOT error analysis. The main reasons for this selection method
were:

o   The ASCOT error analysis was based only on theoretical predictions
    and did not include experimental test results.

o   The magnitude of a potentially significant ASCOT error source, angle
    glint, is unknown.

o   Since the ASCOT/ATS Angle Tracking Filter interface utilizes the
    combined internal/system feedback structure discussed in Subsection
    2.4.1.3, the selected values of the angle sensor measurement error
    model parameters can significantly affect the overall angle tracking
    loop performance.

Therefore, at this stage of the ATS development a conservative approach was
followed and an error model with pessimistically large noise was used to
design the ATS Angle Tracking Filter. The ATS software design, however, per-
mits the measurement model parameters to be supplied to the ATS computer as
input data. This will allow optional refinement of the filter design in
later phases based upon experimental results.

4.3.3.2 SSR-1 Measurement Model - The simplified range sensor model used in
the Kalman Range Tracking Filter is presented in Figure 31. The reduction of
the more complicated model of Figure 23 to that of Figure 31 was accomplished
by the following steps:

75

o   Step 1 – Model all noise sources as Gaussian white noise processes
    with a total standard deviation of σ_R feet. This standard deviation
    reflects the combined effect of: range glint, receiver noise as a
    function of measured signal-to-noise ratio, quantization, A/D con-
    version, and the 16-pulse smoothing. It does not include the effect
    of 4-sample averaging. As in the case of the angle sensor filter
    model, uncertainty in the exact nature of the statistical behavior of
    the noise prompted the use of the white noise model.

o   Step 2 – With $\alpha = 1$, $\beta = 0$ and the range register set at $\hat{R}$,

$$\Delta R_S = R_S - \hat{R}$$

subscript S denoting the 16-pulse smoothing of the range-gate video
integrator, so that

$$R_m = \hat{R} + \Delta R_S = R_S = R + \sigma_R u$$

The anticipated variation in σ_R as a function of range (signal-to-noise
ratio) is shown in Figure 32. (See Table 10 for σ_R equation.) As indicated
by the figure, no particular benefit should be realized by adapting σ_R to
radar signal-to-noise ratio at ranges less than 6000 feet. It is only at
long range conditions that σ_R is substantially affected. However, the capa-
bility was provided in the ATS design for flight test evaluation, as it might
aid long range acquisition and provide improved performance during head-on-pass
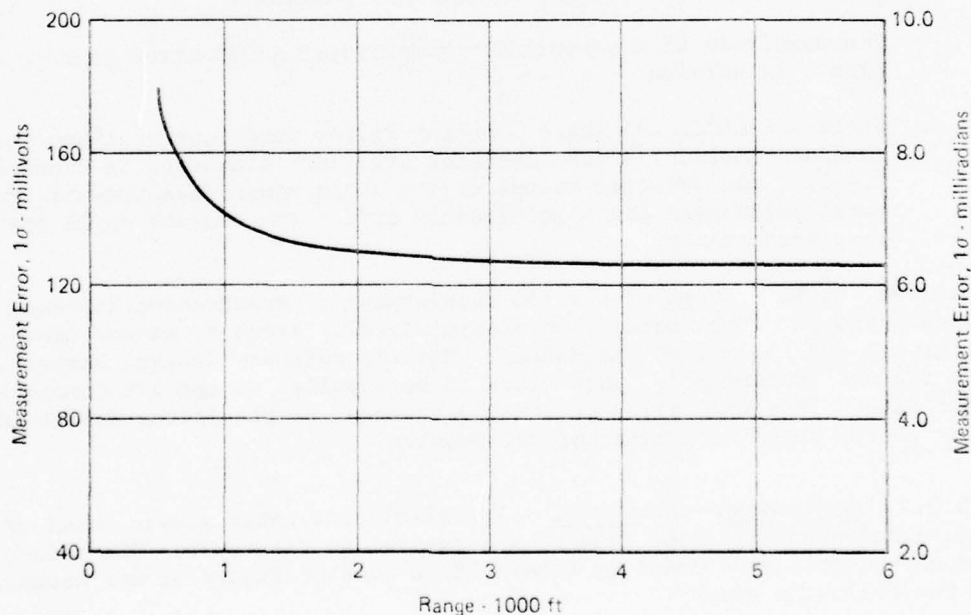encounters.

FIGURE 30

ATS KALMAN FILTER ANGLE SENSOR MEASUREMENT ERROR MODEL

GP74-0122-138
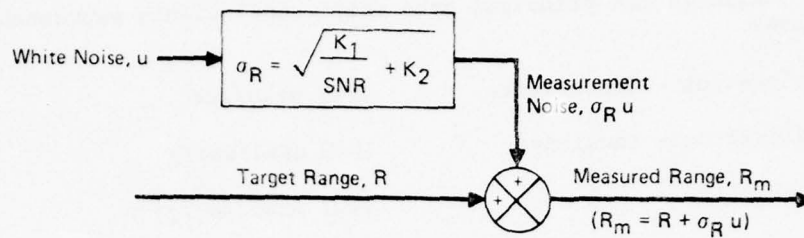
FIGURE 31
ATS KALMAN FILTER RANGE MEASUREMENT MODEL

GP74-0122-139
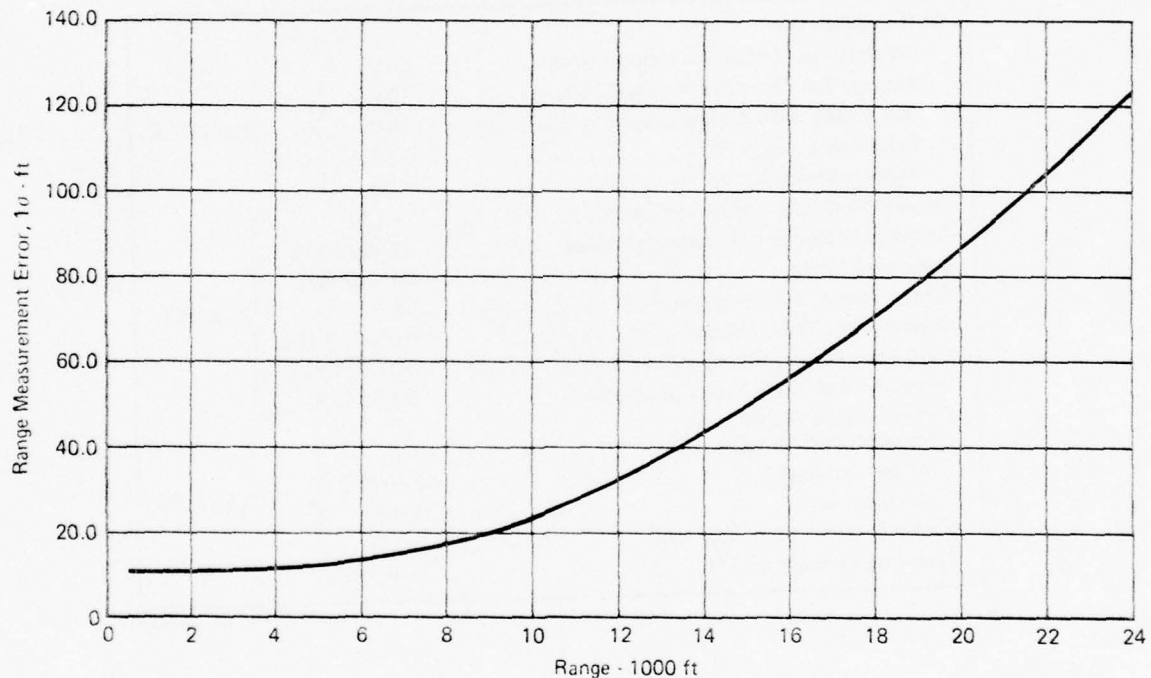
FIGURE 32
ATS KALMAN FILTER RANGE SENSOR MEASUREMENT ERROR MODEL   GP74-0122-99

4.3.3.3 <u>Strapdown Gyro/Accelerometer Measurement Models</u> – Tables 11 and 12 summarize representative performance specifications for the medium-quality ATS Strapdown Gyro/Accelerometer Package (SGAP). In addition to the basic rate gyro and accelerometer specifications, the analog-to-frequency converter characteristics must also be considered in the measurement model. The converter characteristics are specified in Table 13.

77

From Table 11 the principal gyro drift coefficients expressed in milli-radians are:

Acceleration - Insensitive	.145 mrad/sec
Acceleration - Sensitive	.040 mrad/sec/g
Anisoelastic	.002 mrad/sec/g^2
Random	.002 mrad/sec

TABLE 11
REPRESENTATIVE ATS RATE INTEGRATING GYRO SPECIFICATIONS

```
Drift Coefficient
    Acceleration - insensitive (deg/hr) (Max)...........30.0      ⎫
    Acceleration - Sensitive (deg/hr/G) (Max)..........10.0      ⎪
    Day to Day Repeatability (deg/hr) (Total Max).....10.0       ⎬  0° to 175°F
    Anisoelastic (deg/hr/G²)......................0.50           ⎪
    Random (deg/hr) (1 σ) .......................0.35            ⎭
Angular Momentum, H (gm-cm²/sec) .............19,530            ⎫
Damping Coefficient, B (dyne-cm/rad/sec) ...........20,000 ±10%  ⎪
Damping Method....................................Derived Rate  ⎪
Gimbal Inertia, J (eff.) (gm-cm²).................55            ⎬  at R.T.
Characteristic Time, J/B (sec) .....................0.00275 ±10% ⎪
Gyro Scale Factor, H/B Kp (V rms/deg) ............0.215 ±10%    ⎪
Command Rate Scale Factor (deg/sec/ma)............0.75 ±4.5%    ⎭
Command Rate Scale Factor
    Temperature Sensitivity
    Uncompensated.............................±1.4%             ⎫
    Compensated ..............................±.15%             ⎬  0° to 175°F
Gimbal Freedom (deg) (Nominal) ..................±1.67
Operating Temperature (°F) .....................0 to +175
```

Another major error source is the temperature sensitivity of the command rate scale factor. Assuming compensation is used this error is ±.15%. From Table 13 the full scale gyro loop analog-to-frequency converter input corresponds to 175 deg/sec. (3.054 rad/sec.). Thus the command rate scale factor temperature sensitivity, assuming compensation, can produce a maximum error of ±4.58 mrad/sec. Additional errors introduced by the converter include the ±.01% FS scale factor trim resolution and the 3°/hr (.0145 mrad/sec) error due to bias trim resolution. All of these errors with the exception of the random drift error are deterministic errors. These deterministic errors can be further separated into bias (constant) errors and systematic errors. The systematic errors are found to be either g-sensitive errors or scale factor (ω-sensitive) errors. A summary of the principal gyro errors is given in Table 14.

Examination of Table 12 reveals that the principal accelerometer error source is the output noise. Assuming a full accelerometer range of ± 15 g the maximum rms noise is 7.5 milli-g's or about 0.24 fps^2. The analog-to-frequency accelerometer quantization given in Table 13 indicates about 2 milli-g's/pulse. Thus, for the ATS application the error associated with accelerometer measurements is considered negligible.

TABLE 12

REPRESENTATIVE ATS ACCELEROMETER SPECIFICATION

Range	$\pm$ 15g
Input Voltage	$\pm$ 15 VDC $\pm$ 10%
Output Current (Application Requires External Rebalance Current Reference)	1.35 ma $\pm$ 5% per g
Frequency Response	800 Hz, min
MTBF	30,000 hrs, min
Bias	$\pm$ 4 mg, max
Bias Repeatability Start to Start	$\pm$ 0.2 mg max
Bias Temperature Coefficient (50°F - 150°F)	0.05 mg per $^{\circ}$F, max
Scale Factor Temperature Sensitivity	$\pm$ 0.15% of Room Temperature, SF (0°F to + 175°F)
Scale Factor Nonlinearity	$\pm$ 0.05% FS
Cross Coupling	$\pm$ 1 x 10^{-4} g/g, max
Vibration Rectification	$\pm$ 3 x 10^{-4} g/g^2, max
Output Noise	0.05% of Full Range in rms volts, max
Input Axis to Mounting Surface Temperature Instability Over 0°F to + 175°F	0.3 milrad max
Temperature Range	
Operating	-65°F to + 200°F
Storage	-65°F to + 200°F
Vibration	
Operating } Survival }	MIL-E-5400, Class II
Shock	15g for 11 ms Along Each Major Axis

GP74-0122-26

79

TABLE 13
REPRESENTATIVE ATS ANALOG-TO-FREQUENCY
CONVERTER CHARACTERISTICS

	Gyro Loop	Acceleration Loop
Input Clock	100 kHz	100 kHz
Full Scale Output	6250 pps	6250 pps
Full Scale Input	6.95V (175 deg/sec)	6.95V (12.1G)
Scale Factor Temperature Co.	0.002%/°F	0.002%/°F
Temperature Operating	−65°F to 200°F	−65°F to 200°F
Scale Factor Trim Range	±6% FS	±6% FS
Scale Factor Trim Resolution	±0.01% FS (62 deg/hr)	0.01% FS (1.21 mg)
Bias Trim Range	0.04% FS (250 deg/hr)	0.04% FS (4.8 mg)
Bias Trim Resolution	0.0005% FS (3 deg/hr)	0.0005% FS (60 μg)
Bias Temperature Coefficient	0.10 PPM/°F (0.062 deg/hr/°F)	1 PPM/°F 1.2 μg/°F
Linearity	±0.05% (of Reading)	±0.05% (of Reading)
Out of Pulse Width (t)	1.5 < t < 5.0 ms	1.5 < t < 5.0 ms
Output Pulse Amplitude	5.0V ±10%	5.0V ±10%

Note: Each output pulse shall occur within 0.5 microseconds after a
rising edge of the 100 kHz reference. All output pulses shall
be synchronous with one internal 6250 kHz reference.

GP74-0122-24

TABLE 14
SUMMARY OF PRINCIPAL GYRO ERRORS

Gyro Error Source	Milliradians/second
Acceleration - Insensitive Drift	0.145
Acceleration - Sensitive Drift	0.040a
Anisoelastic Drift	$0.002a^2$
Command Rate Scale Factor Error	1.50 ω
Scale Factor Trim Resolution	0.30
Bias Trim Resolution	0.0145
A-F Converter Resolution	0.49

$\omega \overset{\Delta}{=}$ Ownship Body Rate, radians/sec - 3.054 Maximum

$a \overset{\Delta}{=}$ Ownship Acceleration, G's

GP74-0122-23

4.3.4 Discrete Kalman Tracking Filter Equations

The first steps in Kalman filter design have considered coordinate system selection, modeling the dynamic process, and modeling the measurement systems. The final steps of the design process are concerned with establishing the specific elements of the discrete Kalman filter equations previously given in Figure 26. These final steps can be separated into: 1) establishing the discrete state transition matrix, Φ, and the discrete driving matrix, Γ; 2) establishing the covariance matrices of the error in the aiding inputs, Q, and the error in the measurements, R; and 3) establishing an initialization procedure to establish the initial state variable extimates, $\bar{x}_0$, and the covariance matrix of the error in the initial estimates, M_0. Each of these steps will be covered for the ATS Angle and Range Tracking Filter designs in subsequent subsections, after some general discussion on the discretization procedure.

In the preceding subsections continuous, linearized models of the range and angle dynamics have been developed which take the form,

$$\dot{x} = \hat{A} x + \hat{w} + G \sigma_w u$$

where x represents the state vector

$\hat{w}$ represents the estimated aiding vector

$\hat{A}$ represents the linearized coefficient matrix

G represents the aiding vector error sensitivity matrix

σ_w represents a vector of aiding variable standard deviations

u represents a zero mean, unit variance white noise process.

For example, consider the target traverse dynamics in roll-stabilized line-of-sight coordinates derived in Figure 27 in combination with the target acceleration model presented in Figure 28. Collecting the pertinent equations,

$$\dot{P}(2) = V(2) - \omega(3) \hat{R}$$

$$\dot{V}(2) = - (\hat{\dot{R}}/\hat{R}) V(2) + a_T(2) - a_A(2)$$

$$\dot{a}_T(2) = -(1/\tau_T) a_T(2) + \sqrt{2/\tau_T} \sigma_T u$$

Now by: 1) defining the traverse state vector as

$$x^T = [P(2) \; V(2) \; a_T(2)]$$

and 2) linearizing about the estimated range, $\hat{R}$, range rate, $\hat{\dot{R}}$, and measured ownship acceleration, a_A; the following linearized model of the traverse dynamics is obtained:

$$\frac{d}{dt}\begin{bmatrix} P(2) \\ V(2) \\ a_T(2) \end{bmatrix} = \begin{bmatrix} 0 & 1 & 0 \\ 0 & -\hat{\dot{R}}/\hat{R} & 1 \\ 0 & 0 & -1/\tau_T \end{bmatrix}\begin{bmatrix} P(2) \\ V(2) \\ a_T(2) \end{bmatrix} + \begin{bmatrix} -\omega(3)\,\hat{R} \\ -a_A(2) \\ 0 \end{bmatrix}$$

$$+ \begin{bmatrix} -\omega(3) & 0 & 0 \\ 0 & -1 & 0 \\ 0 & 0 & 1 \end{bmatrix}\begin{bmatrix} \sigma_R \\ \sigma_a \\ \sqrt{2/\tau_T}\,\sigma_T \end{bmatrix} u$$

Similar dynamic equations obtained for the elevation dynamics and the range dynamics are presented in later subsections.

Returning to the general form of the continuous model, its differential form is:

$$dx = \hat{A}\, x\, dt + \hat{w}\, dt + G\, \sigma_w\, dv$$

where $dv = u\,dt$ is the unit differential white noise process, that is,

$$E\{dv\} = 0$$

$$E\{dv\,dv^T\} = I\, dt$$

$$E\{dv\,dv^T\} = 0.$$

The differential covariance matrix of the state variable estimates is therefore

$$d\Sigma_x = E\{(dx - Edx)(dx - Edx)^T\}$$

$$= \hat{A}\, \Sigma_x\, dt + \Sigma_x\, \hat{A}^T\, dt + G\, \sigma_w\, I\, \sigma_w^T\, G^T\, dt.$$

A discrete model is desired which: 1) provides solutions to the state equations at discrete time intervals, ΔT, which agree (approximately) with the continuous solutions; and 2) has the same steady-state covariance matrix as the continuous model. Specifically a discrete model of the form,

$$x_{i+1} = \phi\, x_i + \Gamma\, w_i$$

is sought to agree with the format of Figure 26. Obviously ϕ is the state transition matrix, $e^{A\Delta T}$, or some close approximation to it. (It has been found that the first three terms of its power series definition provides suitable accuracy for the ATS Kalman filter design, i.e., $\phi = I + \hat{A}\,\Delta T + 1/2\,\hat{A}^2\,\Delta T^2$.) Γ, on the other hand, will be selected to properly account for the effect of aiding signals on the state estimates and to establish the desired correspondance between the steady state covariance matrices.

Separating Γ into a driving matrix associated with the estimated aiding inputs, Γ_A, and a sensitivity matrix associated with the (zero mean, unit variance) errors in the aiding inputs, Γ_E,

$$x_{i+1} = \phi \, x_i + \Gamma_A \, \hat{w}_i + \Gamma_E \, \varepsilon w_i$$

Thus the average state variable is given by the discrete model as,

$$\bar{x}_{i+1} = \phi \, \bar{x}_i + \Gamma_A \, \hat{w}_i$$

while the continuous model is

$$\dot{\bar{x}} = \hat{A} \, \bar{x} + \hat{w}$$

or solving,

$$\bar{x} \, (t + \Delta T) = \phi \, (\Delta T) \, \bar{x} \, (t) + \int_t^{t + \Delta T} \phi \, (t + \Delta T - \tau) \, \hat{w} \, (\tau) \, d\tau$$

where

$$\phi \, (\lambda) = \exp \{\hat{A} \, (\lambda)\}.$$

Since the estimated aiding signals are constant over the interval ΔT

$$\bar{x} \, (t + \Delta T) = \phi \, (\Delta T) \, \bar{x} \, (t) + \int_t^{t + T} \phi \, (t + \Delta T - \tau) \, d\tau \cdot \hat{w} \, (t)$$

Equating coefficients,

$$\phi = \phi \, (\Delta T) = \exp \{\hat{A} \, \Delta T\}$$

and

$$\Gamma_A = \int_t^{t + \Delta T} \exp \{\hat{A} \, (t - \Delta T - \tau)\} \, d\tau = \hat{A}^{-1} \{\phi \, (\Delta T) - I\}.$$

Now, to determine Γ_E the discrete covariance equation is formed

$$\Sigma_{x_{i+1}} = E \{(x_{i+1} - \bar{x}_{i+1}) \, (x_{i+1} - \bar{x}_{i+1})^T\}$$

$$= \phi \, \Sigma_{x_i} \, \phi^T + \Gamma_E \, I \, \Gamma_E^T$$

Expanding to first-order terms in ΔT,

$$\Sigma_{x_{i+1}} = \Sigma_{x_i} + (\hat{A} \, \Sigma_{x_i} + \Sigma_{x_i} \, \hat{A}^T) \, \Delta T + \Gamma_E \, I \, \Gamma_E^T$$

Comparing this result to the continuous equation for the covariance equation results in the following equation for Γ_E,

$$\Gamma_E = G \, \sigma_w \, \sqrt{\Delta T}$$

83

In summary, the following equations describe the discrete model:

$$\Phi = \exp \{\hat{A} \, \Delta T\} \approx I + \hat{A} \, \Delta T + 1/2 \, \hat{A}^2 \, \Delta T^2$$

$$\Gamma_A = \hat{A}^{-1} \{\Phi - I\} \approx \Delta T + 1/2 \, \hat{A} \, \Delta T^2$$

$$\Gamma_E = G \, \sigma_w \, \sqrt{\dot{\Delta T}}$$

These equations will be used in the next subsections to derive the discrete Kalman ATS Range and Angle Tracking Filters.

4.3.4.1 <u>Angle Tracking Filter Equations</u> – The linearized continuous model of the traverse dynamics were derived in the preceding subsection. This model together with that of the elevation dynamic model and the ASCOT measurement model are presented in Figure 33. The discrete Kalman angle tracking filter structure, which results from the discretization process previously derived, is presented in Figure 34. (This figure is identical to Figure 5 and is repeated here for convenience.) The remaining steps in the Kalman filter design are to establish: 1) the aiding input covariance matrix, Q, and the measurement convariance matrix, R; and 2) to establish the Angle Tracking Filter initialization procedure, $\bar{x}_o$, and its error covariance matrix, M_o.

The aiding input covariance matrix is, from the previous discussion,

$$Q = G \, \sigma_w \, I \, \sigma_w^T \, G^T \, \Delta T$$

Substituting,

$$Q_a(2) = \begin{bmatrix} \omega^2(3) \, \sigma_R^2 & 0 & 0 \\ 0 & \sigma_a^2 & 0 \\ 0 & 0 & 2\sigma_T^2/\tau_T \end{bmatrix} \Delta T$$

Similarly,

$$Q_a(3) = \begin{bmatrix} \omega^2(2) \, \sigma_R^2 & 0 & 0 \\ 0 & \sigma_a^2 & 0 \\ 0 & 0 & 2\sigma_T^2/\tau_T \end{bmatrix} \Delta T$$

Since Q (2) differs from Q (3) the traverse angle tracking filters Kalman gains will differ from those of the elevation filter. This lack of symmetry would double the number of computations involved in computing the Kalman gains from those required if the Q matrix were equal in both channels. Thus, an approximation is made to select a Q matrix common to both channels in order to reduce the Kalman gain computational requirements. The element to be approximated is Q (1,1).

Target Dynamic Model

$$\frac{d}{dt} \begin{bmatrix} P(j) \\ V(j) \\ a_T(j) \end{bmatrix} = \begin{bmatrix} 0 & 1 & 0 \\ 0 & -\dfrac{\hat{\ddot{R}}}{\hat{R}} & 1 \\ 0 & 0 & -\dfrac{1}{\tau_T} \end{bmatrix} \begin{bmatrix} P(j) \\ V(j) \\ a_T(j) \end{bmatrix} + \underline{W}(j) + \begin{bmatrix} 0 \\ 0 \\ \sqrt{\dfrac{2}{\tau_T}}\,\sigma_T \end{bmatrix} U$$

where $j = 2 \Rightarrow$ Traverse Dynamics

$j = 3 \Rightarrow$ Elevation Dynamics

Angle Sensor Measurement Model

$$W(2) \overset{\Delta}{=} \begin{bmatrix} -\omega(3)\,\hat{R} \\ -a_A(2) \\ 0 \end{bmatrix} \; ; \; W(3) \overset{\Delta}{=} \begin{bmatrix} \omega(2)\,\hat{R} \\ -a_A(3) \\ 0 \end{bmatrix} \; ; \; P_m = \frac{K_{SF}}{\hat{R}\;GCFS(1,1)} P + \frac{\sigma_m}{\sqrt{N}} U$$

P   — Target Position Orthogonal to Estimated LOS (Pointing Error)

V   — Relative Target Velocity Orthogonal to Estimated LOS

a_T — Target Acceleration Orthogonal to Estimated LOS

a_A — Attacker Acceleration Orthogonal to Estimated LOS

ω — Filter Coordinate System Rate

$\hat{R}$ — Estimated Range

$\hat{\dot{R}}$ — Estimated Range Rate

τ_T — Target Acceleration Correlation Time

σ_T — Steady State Standard Deviation of Target Acceleration

U   — Unit White, Gaussian Noise Process (Zero Mean, Unit Variance)

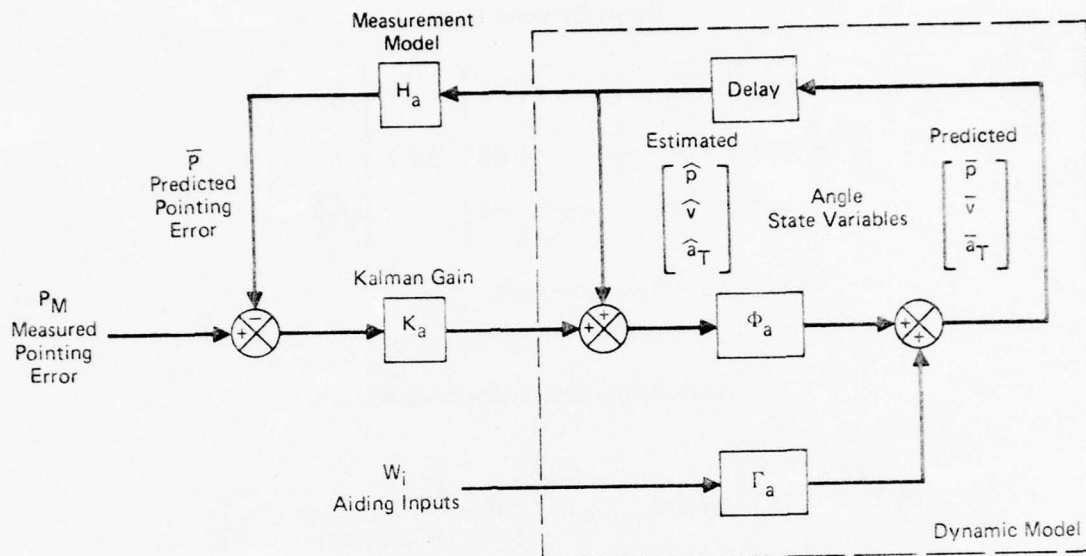σ_m — Standard Deviation of Pointing Error Measurement $= \sqrt{\dfrac{K_1}{\hat{R}^2} + K_2}$

P_m — Pointing Error Measurement

N   — Number of Samples in the Averaging Process (Nominal Value of 10)

K_{SF} — Sensor Scale Factor

FIGURE 33
TARGET TRAVERSE AND ELEVATION DYNAMIC MODELS AND ANGLE SENSOR MEASUREMENT MODEL

GP74-0122-16

85

Measurement Model

H_a

Delay

Estimated $\begin{bmatrix} \widehat{p} \\ \widehat{v} \\ \widehat{a}_T \end{bmatrix}$

Predicted $\begin{bmatrix} \bar{p} \\ \bar{v} \\ \bar{a}_T \end{bmatrix}$

Angle State Variables

$\bar{P}$ Predicted Pointing Error

P_M Measured Pointing Error

Kalman Gain K_a

Φ_a

W_i Aiding Inputs

Γ_a

Dynamic Model

Traverse Aiding Inputs $\begin{bmatrix} -\omega(3)\widehat{R} \\ -a_A(2) \\ 0 \end{bmatrix}$; Elevation Aiding Inputs $\begin{bmatrix} \omega(2)\widehat{R} \\ -a_A(3) \\ 0 \end{bmatrix}$

$$\Gamma_a = \begin{bmatrix} \Delta T & 1/2\Delta T^2 & 0 \\ 0 & [1-1/2\,(\widehat{R}/R)\,\Delta T]\,\Delta T & 1/2\Delta T^2 \\ 0 & 0 & [1-1/2\Delta T/\tau]\,\Delta T \end{bmatrix} ; H_a = \begin{bmatrix} \dfrac{K_{SF}}{\widehat{R}\,GCFS(1,1)} & 0 & 0 \end{bmatrix} ; K_a = \begin{bmatrix} K_p \\ K_v \\ K_a \end{bmatrix}$$

$$\Phi_a = \begin{bmatrix} 1 & [1-1/2(\widehat{R}/\widehat{R})\,\Delta T]\,\Delta T & 1/2\Delta T^2 \\ 0 & 1-(\widehat{R}/\widehat{R})\Delta T + 1/2\,(\widehat{R}/\widehat{R})^2\,\Delta T^2 & \{1-1/2\,[(\widehat{R}/\widehat{R}) + 1/\tau]\,\Delta T\}\,\Delta T \\ 0 & 0 & 1-\Delta T/\tau + 1/2\,(\Delta T/\tau)^2 \end{bmatrix}$$

FIGURE 34
KALMAN ANGLE TRACKING FILTER

GP74-0122-17

86

It is assumed that the total filter coordinate system rate is equally distributed between channels, that is, $\omega(2)$ and $\omega(3)$ are approximated by $\sqrt{(\omega^2(2) + \omega^2(3))}/2$. Thus,

$$Q_a \approx \begin{bmatrix} (\omega^2(2) + \omega^2(3))\,\sigma_R^2/2 & 0 & 0 \\ 0 & \sigma_a^2 & 0 \\ 0 & 0 & 2\sigma_T^2/\tau_T \end{bmatrix} \Delta T$$

where

σ_R is obtained from the Range Tracking Filter covariance matrix,

σ_a is the standard deviation of the accelerometer measurement error, and

σ_T is the assumed standard deviation of the target acceleration model.

The measurement variance, R_a, is obtained directly from the ASCOT model (Figure 33) as,

$$R_a = \sigma_m^2/N$$

where N is the number of samples in the averaging process (nominal value of 10).

Initialization of the ATS Angle Tracking Filter is accomplished as follows:

o Position State: The sensor-to-filter direction cosine matrix is initialized to point at the measured target position at ASCOT detection. Thus, the estimated initial pointing error is zero. The initialization error can be as large as the physical extent of the target. Therefore, $M_{a_o}(1,1)$ has been specified as $25^2/12$ ft^2.

o Velocity State: The velocity state is initialized by assuming ownship body rates equal to the line-of-sight rates. Thus, the initial target velocity normal to the LOS is: $\bar{v}_o(2) = \omega_A(3)\,\hat{R}$ and $\bar{v}_o(3) = -\omega_A(2)\,\hat{R}$. The error in this initialization procedure is difficult to estimate since the correspondence between ownship body rate and line-of-sight rate at initialization depends to a great extent on pilot procedure. For the ATS filter σ_{v_o} was selected to be ± 50 ft/sec. This corresponds to about $\pm 1.5°$/sec LOS rate error at 2000 ft and $\pm 3°$/sec at 1000 ft.

o Acceleration State: The acceleration state is initialized by assuming target acceleration equal to ownship acceleration. Thus, initial target acceleration normal to the LOS is: $\bar{a}_{T_o}(2) = a_A(2)$ and $\bar{a}_{T_o}(3) = a_A(3)$. The error in acceleration initialization is also dependent upon pilot acquisition procedure. For the ATS angle filter σ_{a_o} was selected equal to σ_T in the angle target acceleration model, that is, $\sigma_{a_o} = \pm 3$ g.

87

Summarizing the initial angle filter state vectors and initial covariance matrix,

$$\bar{x}_{a_O}(2) = \begin{bmatrix} 0 \\ \omega_A(3)\ \hat{R} \\ a_A(2) \end{bmatrix} \qquad \bar{x}_{a_O}(3) = \begin{bmatrix} 0 \\ -\omega_A(2)\ \hat{R} \\ a_A(3) \end{bmatrix}$$

$$M_{a_O} = \begin{bmatrix} (25/\sqrt{12})^2 & 0 & 0 \\ 0 & (50)^2 & 0 \\ 0 & 0 & (3g)^2 \end{bmatrix}$$

4.3.4.2 <u>Range Tracking Filter Equations</u> – The linearized continuous model of the range dynamics are derived in the same manner as the angle dynamics model. The range dynamic model together with the SSR-1 range measurement model are presented in Figure 35. The discrete Kalman Range Tracking Filter structure which results from the discretization process is presented in Figure 36. (This figure is identical to Figure 6 and is repeated here for convenience.)

Since the only aiding term is ownship acceleration along the LOS, the Q matrix takes the form

$$Q_R = \begin{bmatrix} 0 & 0 & 0 \\ 0 & \sigma_a^2 & 0 \\ 0 & 0 & 2\sigma_T^2/\tau_T \end{bmatrix} \Delta T$$

In like fashion the measurement variance, R, has the form

$$R_R = \sigma_R^2/N$$

where N is the number of samples in the averaging process (nominal value of 4).

Initialization of the ATS Range Tracking Filter is accomplished as follows:

o Range State: The filter range state is initialized at the value of SSR-1 measured range at the time of radar acquistion. Thus, the initialization error is the basic (no 4-sample averaging) SSR-1 range measurement error including the effect of acquisition signal-to-noise ratio.

o Range-Rate State: Range rate is initialized at the initial range-rate estimate of the SSR-1. This is obtained by accumulating scaled ΔR range register corrections for .25 seconds prior to issuing a radar lock-on discrete. The scaling is selected to provide a smoothed range-rate estimate at the end of the 0.25 second interval.

This interval represents 16 samples of range increments of accuracy σ_R taken at 1/64 second intervals. Thus the variance on the range-rate estimate will be $(16\sigma_R)^2$ $(\text{fps})^2$.

Target Dynamic Model

$$\frac{d}{dt}\begin{bmatrix} R \\ \dot{R} \\ a_T(1) \end{bmatrix} = \begin{bmatrix} 0 & 1 & 0 \\ (\omega^2(2)+\omega^2(3)) & 0 & 1 \\ 0 & 0 & -\frac{1}{\tau_T} \end{bmatrix}\begin{bmatrix} R \\ \dot{R} \\ a_T(1) \end{bmatrix} + \begin{bmatrix} 0 \\ -a_A(1) \\ 0 \end{bmatrix} + \begin{bmatrix} 0 \\ 0 \\ \sqrt{\frac{2}{\tau_T}}\,\sigma_{T_R} \end{bmatrix} U$$

Range Measurement Model

$$R_m = R + \frac{\sigma_R}{\sqrt{N}} U$$

R	—	Range
$\dot{R}$	—	Range Rate
$a_T(1)$	—	Target Acceleration Along LOS
$a_A(1)$	—	Attacker Acceleration Along LOS
$\omega(2), \omega(3)$	—	Filter Coordinate System Rates
τ_T	—	Target Acceleration Correlation Time
σ_{T_R}	—	Steady State Standard Deviation of Target Acceleration
U	—	White, Gaussian Noise (Zero Mean, Unit Variance)
σ_R	—	Standard Deviation of Range Measurement $= \sqrt{\dfrac{K_1}{SNR} + K_2}$
R_m	—	Range Measurement
N	—	Number of Samples in the Averaging Process (Nominal Value of 4)

FIGURE 35

TARGET DYNAMIC MODEL ALONG THE LINE-OF-SIGHT AND THE
RANGE MEASUREMENT MODEL

GP74-0122-18

89

o Acceleration State: The acceleration state is initialized by assuming target acceleration equal to ownship acceleration, that is, $a_{T_o}(1) = a_A(1)$. The error in **acceleration** initialization is dependent upon the pilot's acquisition procedure. For the ATS range filter σ_{a_o} was selected equal to σ_T in the range target acceleration model, that is, $\sigma_{a_o} = \pm\ 1$ g.
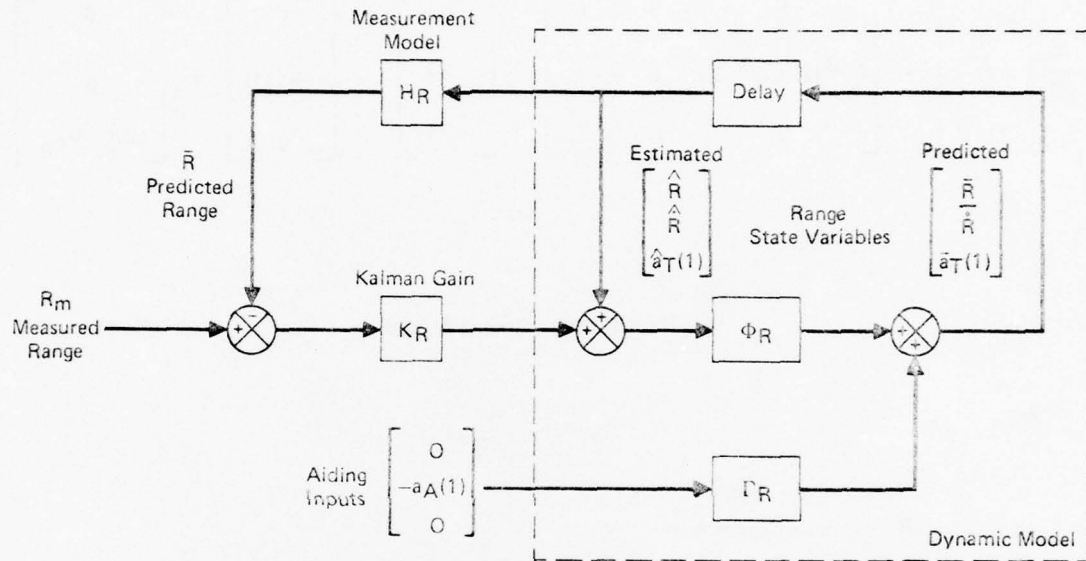
$$\Gamma_R \overset{\Delta}{=} \begin{bmatrix} \Delta T & \Delta T^2/2 & 0 \\ (\omega(2)^2 + \omega(3)^2)\,\Delta T/2 & \Delta T & \Delta T^2/2 \\ 0 & 0 & (1-\Delta T/2\tau)\Delta T \end{bmatrix} \; ; H_R \overset{\Delta}{=} [\,1\ 0\ 0\,]$$

$$\Phi_R \overset{\Delta}{=} \begin{bmatrix} 1 + (\omega(2)^2 + \omega(3)^2)\,\Delta T^2/2 & \Delta T & \Delta T^2/2 \\ (\omega(2)^2 + \omega(3)^2)\,\Delta T & 1 + (\omega(2)^2 + \omega(3)^2)\,\Delta T^2/2 & (1-\Delta T/2\tau)\,\Delta T \\ 0 & 0 & 1-\Delta T/\tau + \Delta T^2/2\tau^2 \end{bmatrix} \; ; K_R \overset{\Delta}{=} \begin{bmatrix} K_R \\ K_{\dot R} \\ K_a \end{bmatrix}$$

FIGURE 36
KALMAN RANGE TRACKING FILTER

GP74-0122-19

90

Summarizing the initial range filter state vector and the initial convariance matrix,

$$\bar{x}_{R_O} = \begin{bmatrix} R_m \\ \dot{R}_m \\ a_A(1) \end{bmatrix}$$

$$M_{R_O} = \begin{bmatrix} \sigma_R^{\,2} & 0 & 0 \\ 0 & (16\sigma_R)^2 & 0 \\ 0 & 0 & (1g)^2 \end{bmatrix}$$

4.4 ATS PERFORMANCE

4.4.1 ATS Performance Analysis Approach

ATS performance has been determined by various methods. A principal consideration in the ATS design was its performance under dynamic conditions. For the purposes of dynamic design and analysis a CDC 6600 digital computer simulation of the ATS Range and Angle Tracking Filters was programmed. This computer simulation represents the ATS at the 16Hz rate of the tracking filters and provides realistic relative geometry and variable noise conditions with which to test the filter using the MCAIR Terminal Aerial Gunnery Simulation (TAGS) program, Reference 4. Subsection 4.4.2 presents detailed results of the ATS dynamic performance analysis.

Another principal analysis consideration is the effect of the major ATS error sources on the overall system performance. The sensitivity of the ATS's performance with respect to its major error sources is presented in Subsection 4.4.3. These sensitivities are established both by means of the dynamic performance analysis program referred to above and by a special purpose program which solves the steady state Kalman filter equations.

The ATS sensor noise models are not well known at this time, as was postulated in the Phase II work statement. They will be completely defined only after the appropriate laboratory experimentation, hot mock-up testing, and flight test evaluation are conducted during later AGFCS phases. As a result, the ATS performance analysis task was pursued during the Phase II study principally as a design tool. As such it served to establish: 1) reasonable error budgets for the principal ATS sensors, including environmental effects; and 2) conservative ATS Kalman tracking filter designs which will function adequately even in the event of significantly degraded sensor performance due to severe environments. Thus, the ATS performance analysis at this stage of AGFCS development does not attempt to establish the specific predicted or anticipated ATS performance. Rather, it attempts to define a range of potential performance based on a conservative postulation of overall sensor/environment conditions.

The approach taken below to summarizing the Phase II performance analysis effort is to first present the performance of the finally evolved ATS design with the theoretically predicted sensor measurement random noise determined by the respective sensor subcontractors. These theoretical random-noise results are judged to be fairly representative in the case of the SSR-1/ Range Tracking Filter performance, disregarding the effects of ground clutter at low altitudes. However, these random-noise results are probably optimistic with regard to the ASCOT/Angle Tracking Filter performance, because they do not account for clutter related environmental noise which, under many tracking conditions, is apt to be the predominant error source. Because these theoretical results represent a somewhat optimistic performance, which will serve primarily as a reference for later experimental-oriented analysis, they are referred to herein as the ATS reference performance.

After the reference performance is presented, the results of the sensitivity studies are summarized. Their purpose was to determine the effect of degraded measurement accuracies on the reference ATS performance. Based on the sensitivity studies, error budgets, which could reasonably be expected to encompass a broad range of sensor/environment conditions, were established for each of the sensors. Finally, these error budgets and the ATS performance (using the budgeted error source magnitudes) are presented. These performance results show that the conservative ATS filter design approach taken results in highly acceptable ATS performance for the established "reasonable" error budgets.

4.4.2 ATS Dynamic Performance Analysis

The key dynamic performance parameters are the accuracies and dynamic characteristics of the estimated target states as obtained by the ATS Kalman tracking filters. These parameters include: 1) the estimated target range, range rate and acceleration along the LOS by the Range Tracking Filter; and 2) the estimated target position, relative velocity and acceleration normal to the LOS by the Angle Tracking Filter. For convenience the dynamic performance analysis results are separated into results pertaining to the Range Tracking Filter performance and the Angle Tracking Filter performance.

Results are presented for three dynamic conditions: 1) a constant 3g turn at a nearly constant (2000 ft.) range ; 2) a 3g reversal; and 3) a subsonic head-on pass. The constant turn condition represents the type of conditions to be expected during ATS testing. The reversal and head-on pass conditions represent difficult dynamic conditions for acquiring and maintaining ATS tracking. For convenience the 3g constant turn and reversal are combined into one encounter which will be called the Reversal encounter. The constant turn is maintained for the first six (6) seconds (which is sufficiently long to attain steady state filter performance) and then a two second reversal is performed after which the target again maintains a constant 3g turn.

4.4.2.1 <u>Range Tracking Filter Performance</u> - The dynamic variations in the
three range variables to be estimated by the Range Tracking Filter during
the Reversal encounter are shown in Figure 37. Note that range varies
slowly throughout the encounter with low values of both range rate and acceler-
ation. Thus, this encounter does not provide a particularly difficult test
of the range filter's dynamic performance. It does, however, provide a
measure of the range filter's accuracy during relatively benign range condi-
tions. The accuracy of the ATS Range Tracking Filter during the Reversal
encounter is illustrated by the estimation errors presented in Figures 38
through 41.
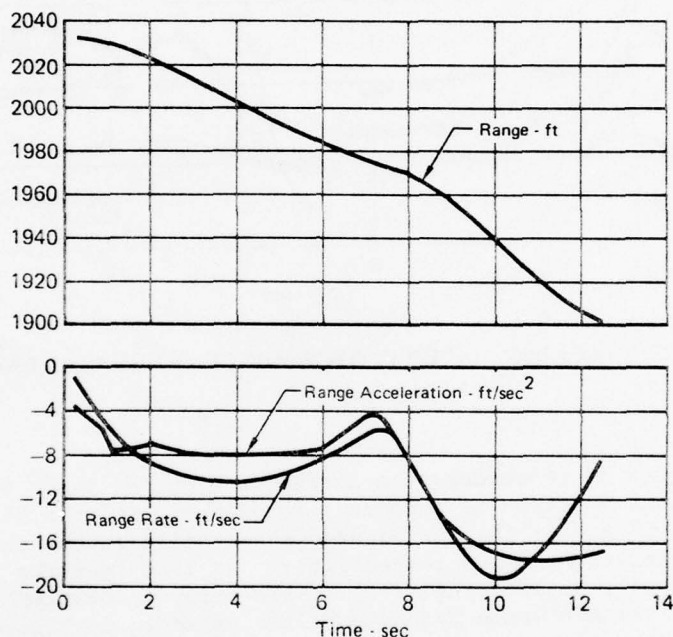
FIGURE 37
RANGE DYNAMICS - REVERSAL ENCOUNTER

GP74-0122-97

Figure 38 illustrates only the dynamic accuracy of the range filter in
that the results were obtained with ideal (no noise) radar measurements.
There are two time periods of particular interest in Figure 38. The first
occurs just after initialization and lasts about 3 seconds. The initiali-
zation transient is particularly evident in the error in estimated range
acceleration since the acceleration state is initialized at ownship acceler-
ation. The acceleration error peaks at about one second after initialization
(9 feet/second^2) and reaches a steady-state condition (2 feet/second^2) at
3 seconds. This acceleration error feeds into the estimated range-rate and
range errors, even though they are initialized perfectly, causing a 3 second
transient in these filter states also. The second period of interest occurs
during and after the two second reversal (time 6 to 8 seconds). The range
error is insignificant due to the accuracy of the ideal measurements. Range-
rate and range-acceleration errors can be directly correlated to the dynamic
variation of range rate and acceleration during this period (see Figure 37).
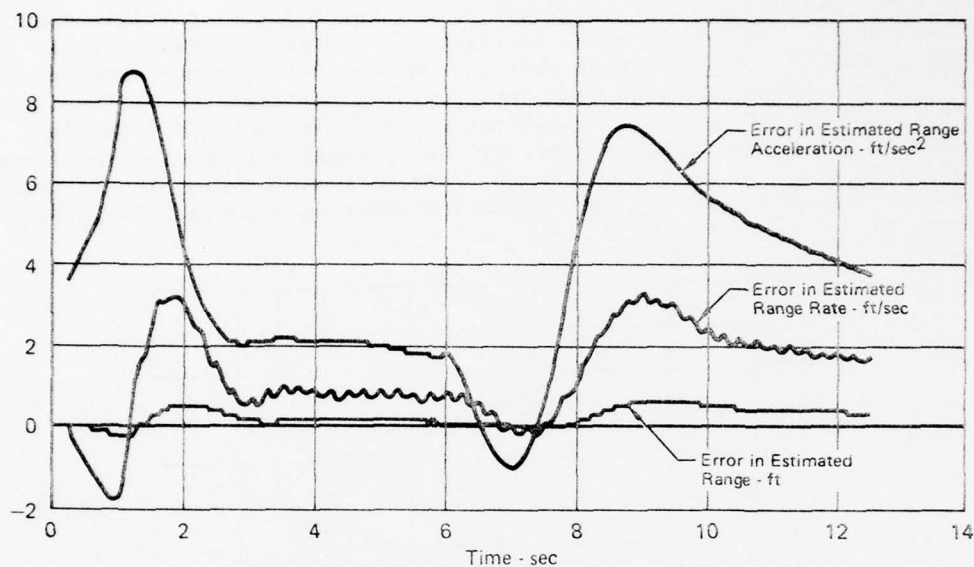
93

FIGURE 38
IDEAL RANGE TRACKING FILTER PERFORMANCE - REVERSAL ENCOUNTER

GP74-0122-107

While Figure 38 represents the performance of the range filter under dynamic but ideal (perfect measurement) conditions, Figures 39, 40 and 41 illustrate the effect of the anticipated SSR-1 noise on the range, range-rate and range-acceleration errors respectively. At 2000 feet the error in measured range will be 12.5 feet (1σ). This error is reduced to less than 4 feet (1σ) by the ATS Range Tracking Filter as shown in Figure 39. Figure 40 illustrates that the effect of noisy measurements on range rate produces errors of about 11 feet/second (1σ). Peak acceleration errors of 28 feet/second^2 are experienced during transient conditions (see Figure 41) but are considerably smaller (9 to 20 feet/second^2) during steady-state conditions.

The accuracies exhibited by the Range Tracking Filter with anticipated SSR-1 measurement noise are considered more than satisfactory for air-to-air gunnery applications. The effect of degraded range measurement accuracy is treated in the sensitivity analysis, Subsection 4.4.3.

The dynamic variations in the three Range Tracking Filter state variables during the Head-on Pass encounter are shown in Figure 42. For this encounter range varies rapidly with a nearly constant closing rate of 1800 feet/second and zero acceleration along the LOS. The target is detected and acquired by the SSR-1 1.75 seconds after the start of the encounter at a range of nearly 11,100 feet. After an initial transient the ATS Range Tracking Filter tracks the target until the head-on pass occurs. Figures 43 and 44 present the tracking filter errors without and with radar measurement noise, respectively.
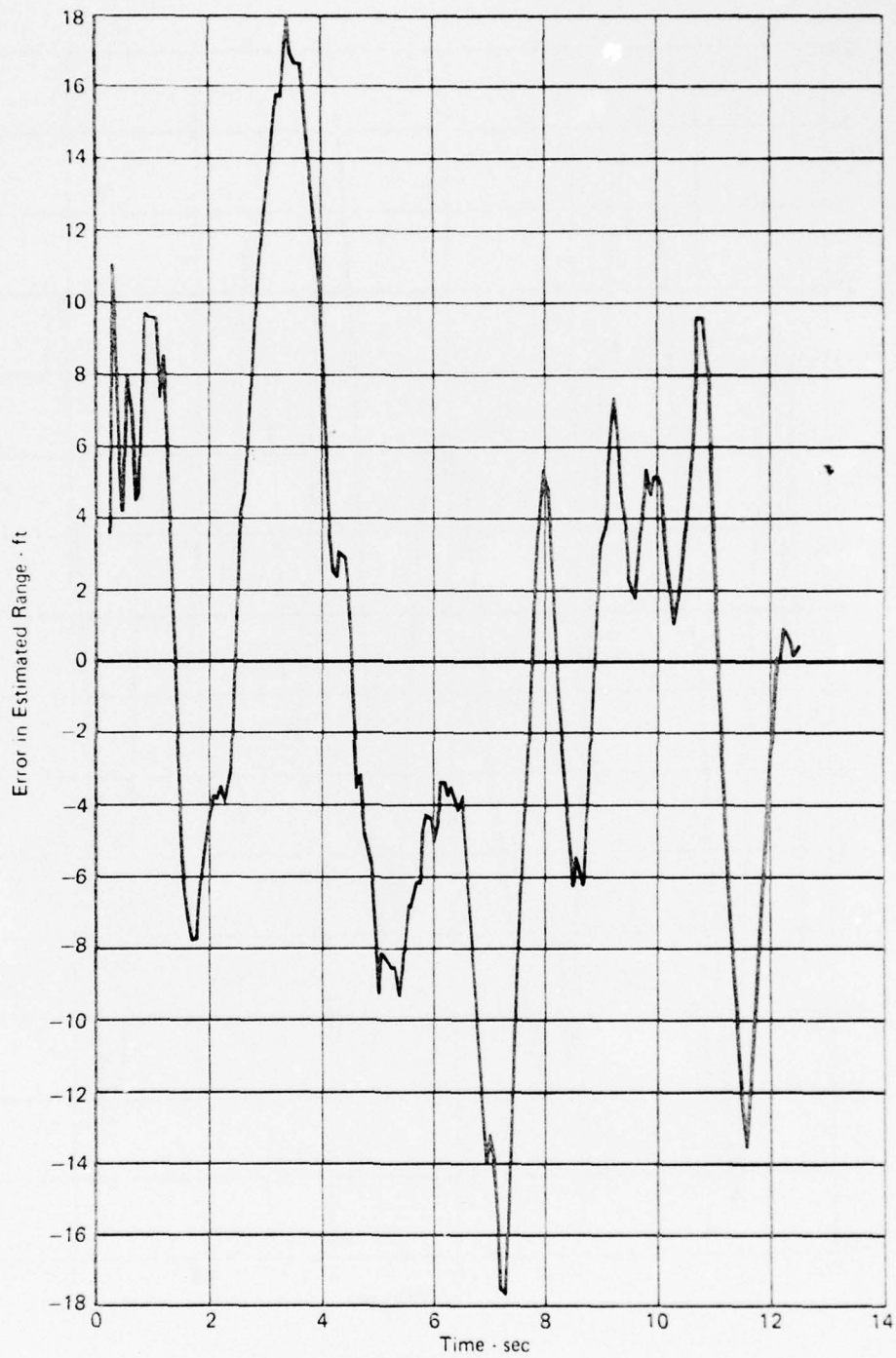
94

END

DATE
FILMED

7-77

FIGURE 39
ERROR IN ESTIMATED RANGE - REVERSAL ENCOUNTER
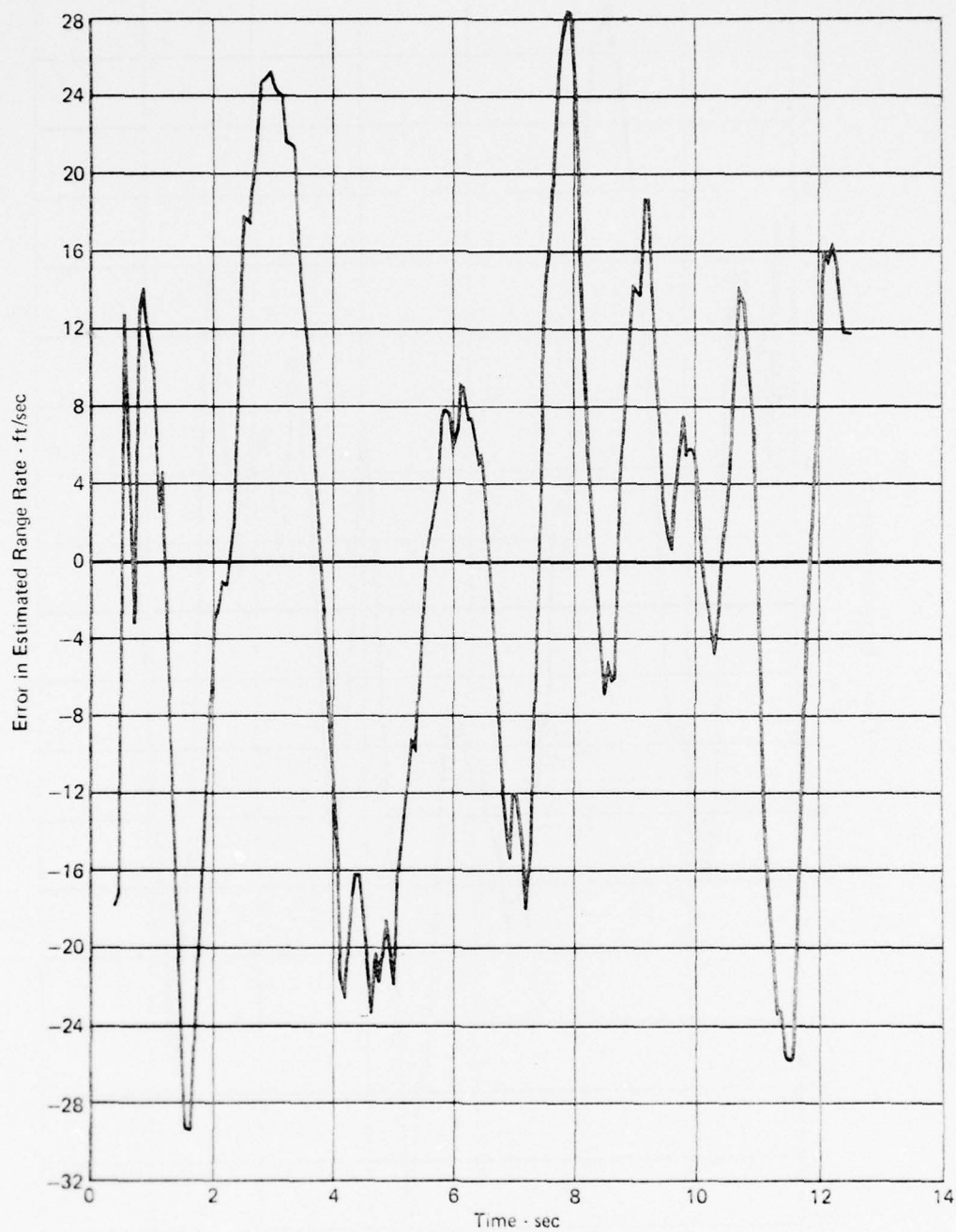
GP74-0122-106

FIGURE 40
ERROR IN ESTIMATED RANGE RATE - REVERSAL ENCOUNTER
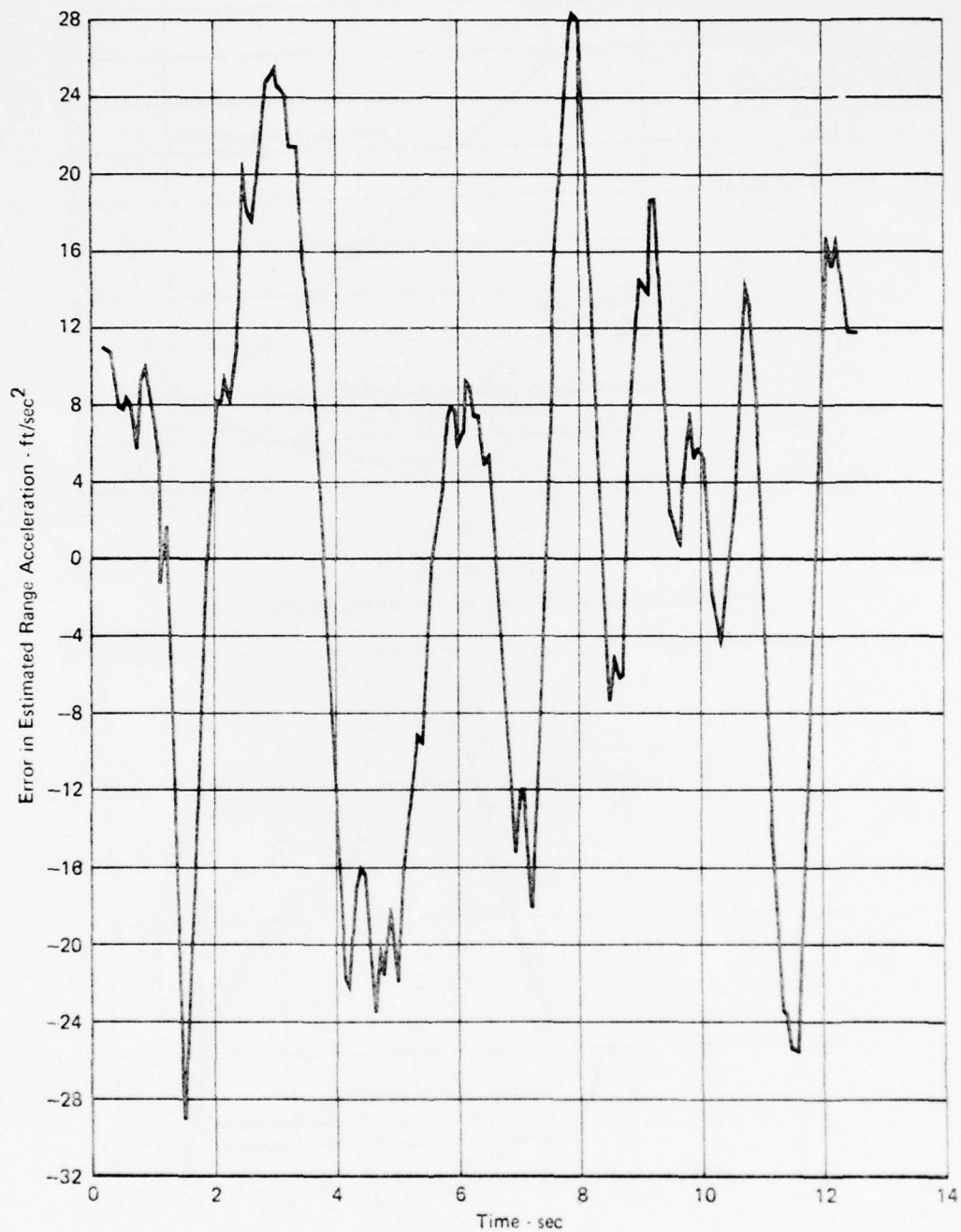
GP74-0122-109

96

FIGURE 41
ERROR IN ESTIMATED RANGE ACCELERATION - REVERSAL ENCOUNTER
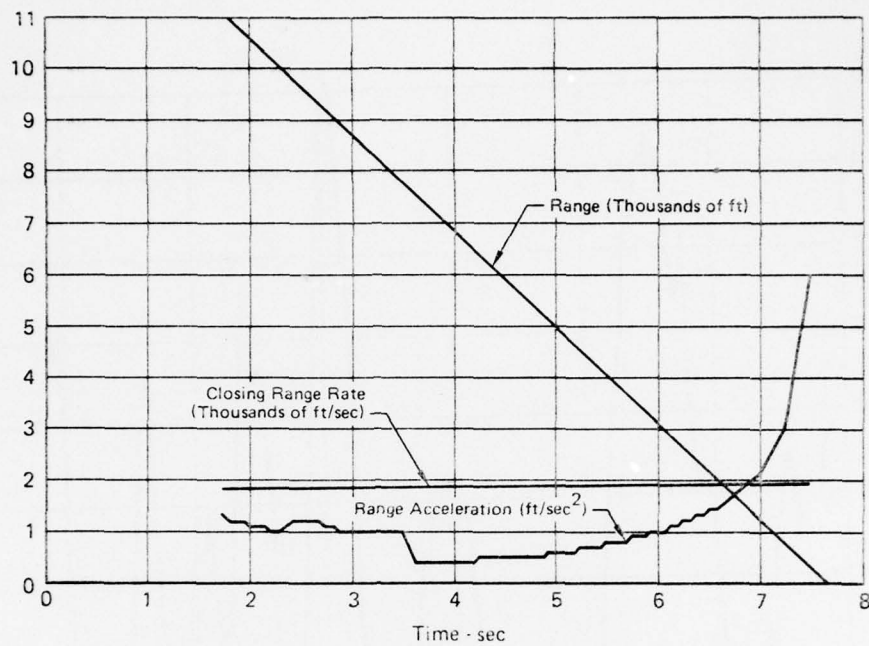
GP74-0122-110

97

FIGURE 42
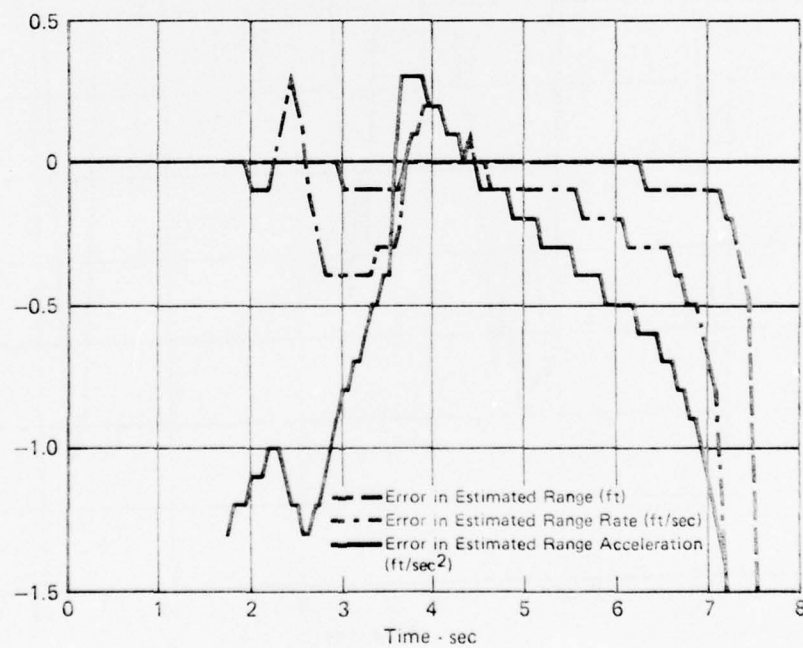RANGE DYNAMICS - HEAD-ON PASS ENCOUNTER

GP74-0122-111

FIGURE 43
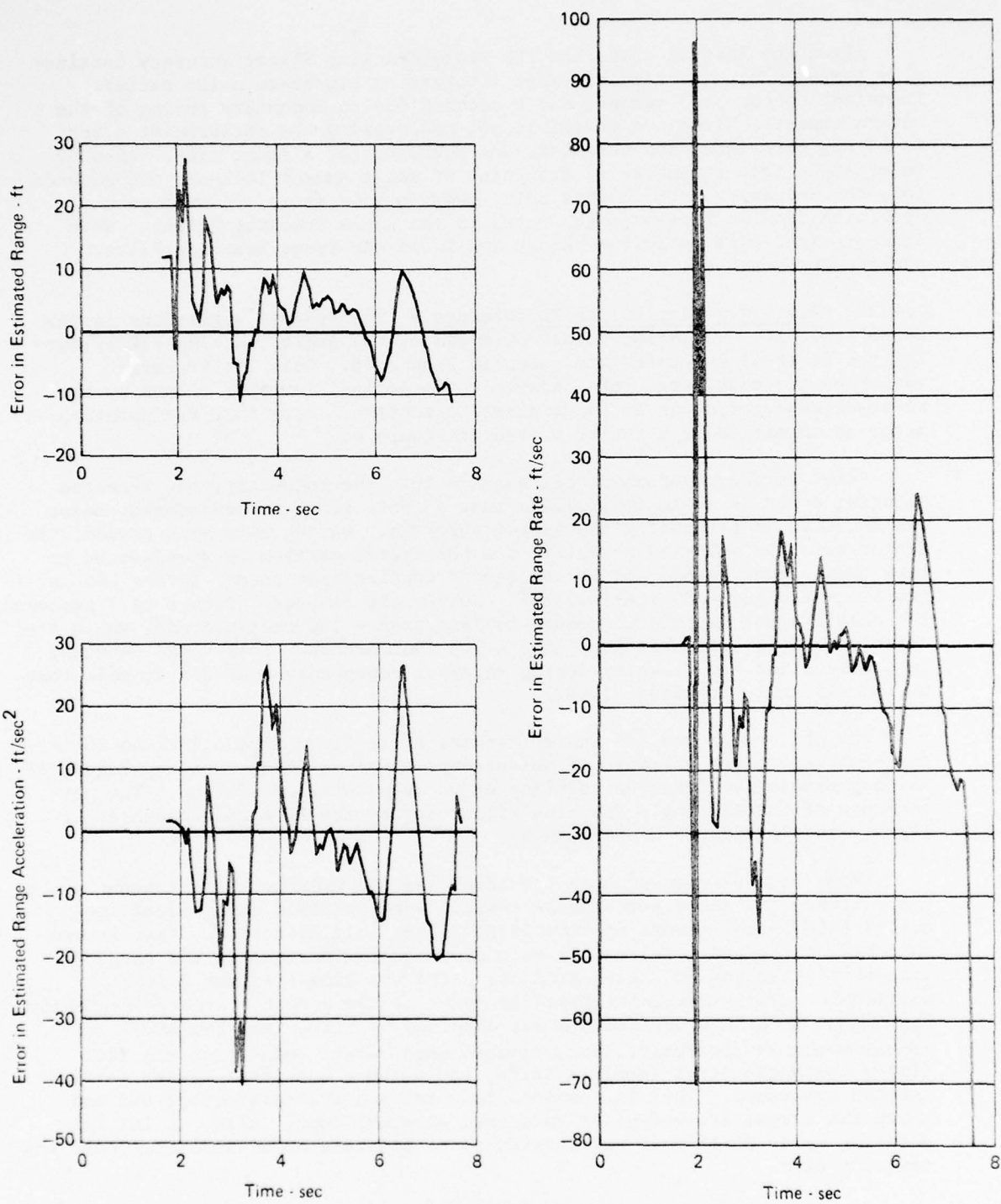IDEAL RANGE TRACKING FILTER PERFORMANCE - HEAD-ON PASS ENCOUNTER

GP74-0122-112

98

FIGURE 44
RANGE TRACKING FILTER PERFORMANCE - HEAD-ON PASS ENCOUNTER

GP74-0122-113

99

After the initial transient the Range Tracking Filter accuracy continually improves with decreasing range (increasing signal-to noise ratio). Transients occur at 3 seconds and 6 seconds due to momentary fading of the return signal. Since the target is not maneuvering the measurement error is highly correlated and this degrades accuracy for a short time. Also of interest in this encounter is the point of angle sensor lock-on, 4.6 seconds into the encounter. Up to this point ownship body rates are used as an approximation for line-of-sight rates in the Range Tracking Filter. When line-of-sight rate estimates become available the Range Tracking Filter performance improves.

4.4.2.2 <u>Angle Tracking Filter Performance</u> - The dynamic variations in the three traverse variables to be estimated by the Angle Tracking Filter during the Reversal encounter are shown in Figure 45. Only the traverse variables are considered here because the principal dynamics caused by the reversal maneuver occur in the traverse direction. Note that the pointing error is magnified by a factor of ten in Figure 45.

Prior to the reversal at six seconds into the encounter, the traverse pointing error is quite small (less than a foot) since no measurement noise was included in generating the dynamic profile. During this same period, the target relative velocity normal to the LOS decreases from 60 feet/second to less than 5 feet/second; while the target acceleration normal to the LOS is constant at about - 30 feet/second^2. During the reversal (from 6 to 8 seconds) the acceleration rapidly decreases to less than - 100 feet/second^2, while the relative velocity reaches less than - 100 feet/second. This rapid decrease in acceleration and velocity during reversal represents a severe dynamic test on the ATS Angle Tracking Filter.

The ability of the ATS Angle Tracking Filter to maintain lock-on during the reversal in the presence of measurement noise is illustrated by Figure 46 which presents the traverse pointing error as a function of time. The performance of the ATS Angle Tracking Filter during the Reversal Encounter is illustrated in Figures 47 through 49.

These figures present both the ideal and the reference performance of the filter. The ideal performance results were obtained using ideal (no noise) ASCOT measurements and idealized filter initialization. That is ownship body rates and acceleration were close approximations to the target line-of-sight rates and accelerations. Also the line-of-sight filter coordinate system was initialized to point at the target's center-of-gravity. The reference filter performance was obtained by corrupting the ASCOT measurements by theoretically determined measurement noise plus a 1 foot (1σ) glint angle error (nominal noise) and using a non-ideal filter initialization procedure. That is, ownship body rates and accelerations did not match the target line-of-sight rates and accelerations. Also, an initial pointing error of 16 feet was introduced to simulate ASCOT detection near the target's edge.

After the initial transients (about 2.5 seconds) the reference performance data closely tracks the ideal data. This is due to the low noise content of the ASCOT measurements. The effect of degraded ASCOT measurement accuracy is treated in the sensitivity analyses, Subsection 4.3.3.
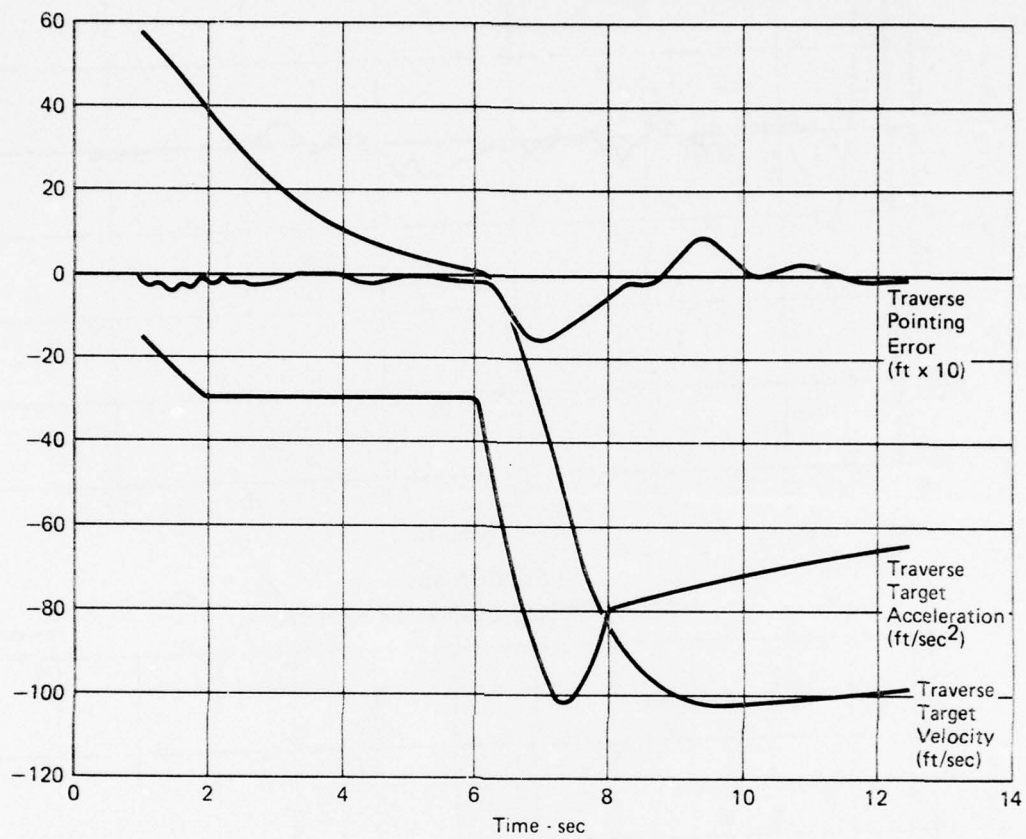
100

FIGURE 45
ANGLE DYNAMICS - REVERSAL ENCOUNTER
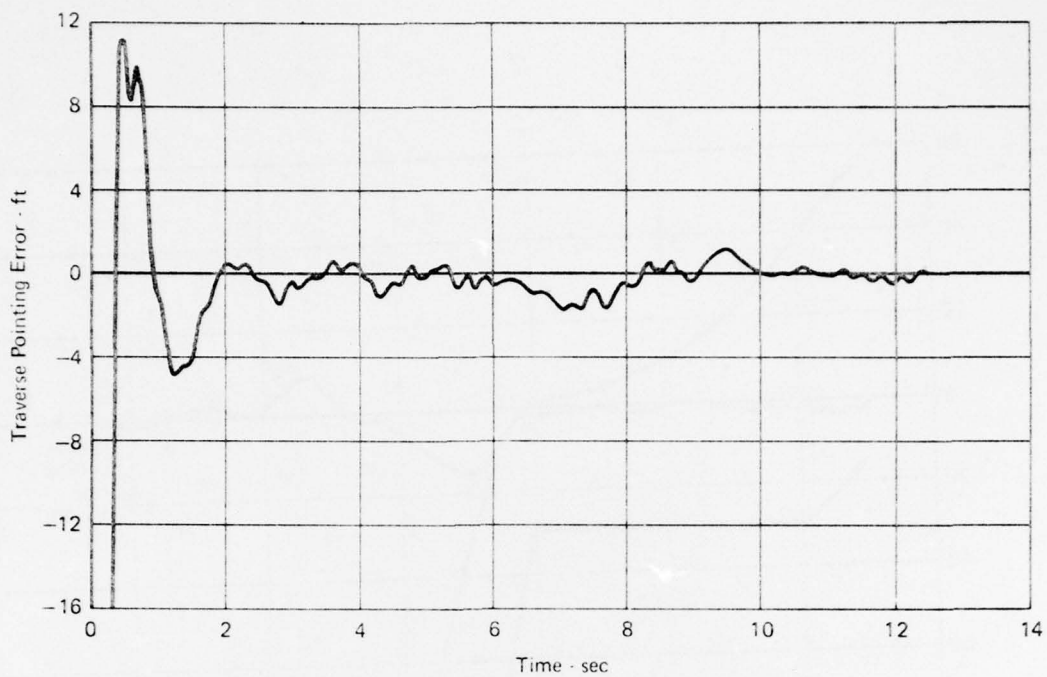
GP74-0122-115

101

FIGURE 46
ANGLE SENSOR POINTING ERROR
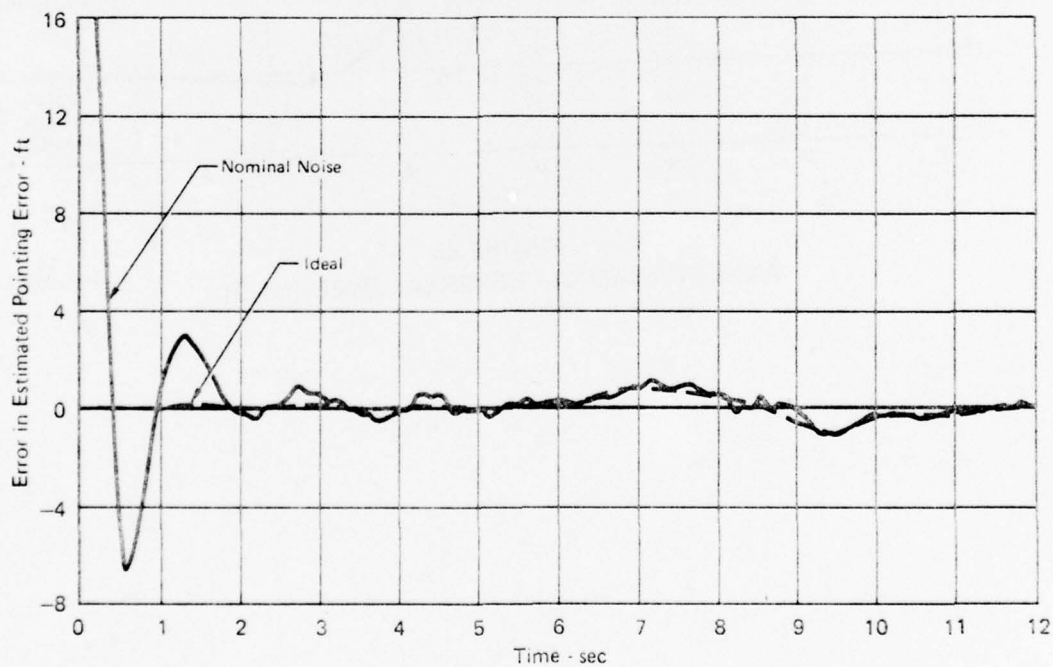
GP74-0122-114

FIGURE 47
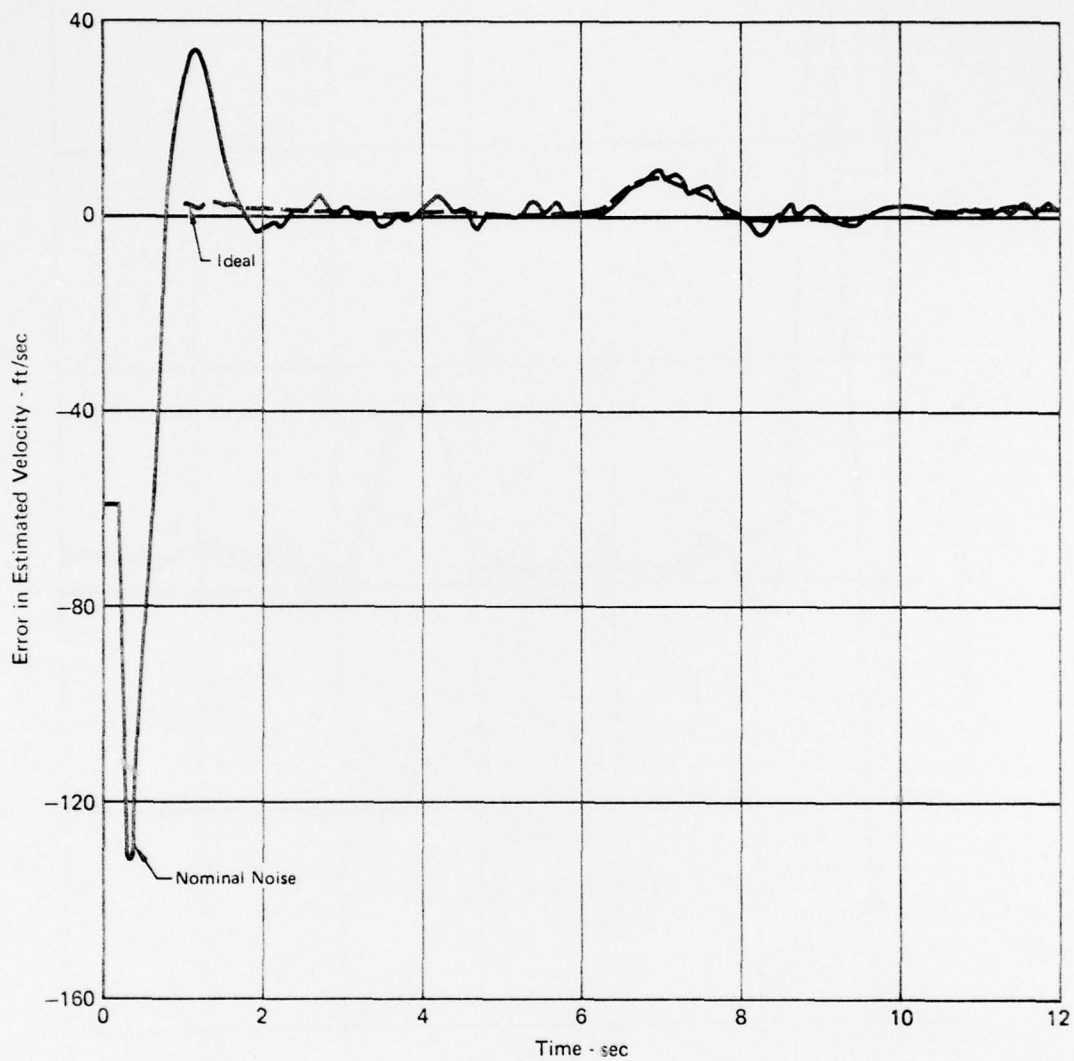ERROR IN ESTIMATED POINTING ERROR - REVERSAL ENCOUNTER

GP74-0122-116

102

FIGURE 48
ERROR IN ESTIMATED VELOCITY - REVERSAL ENCOUNTER
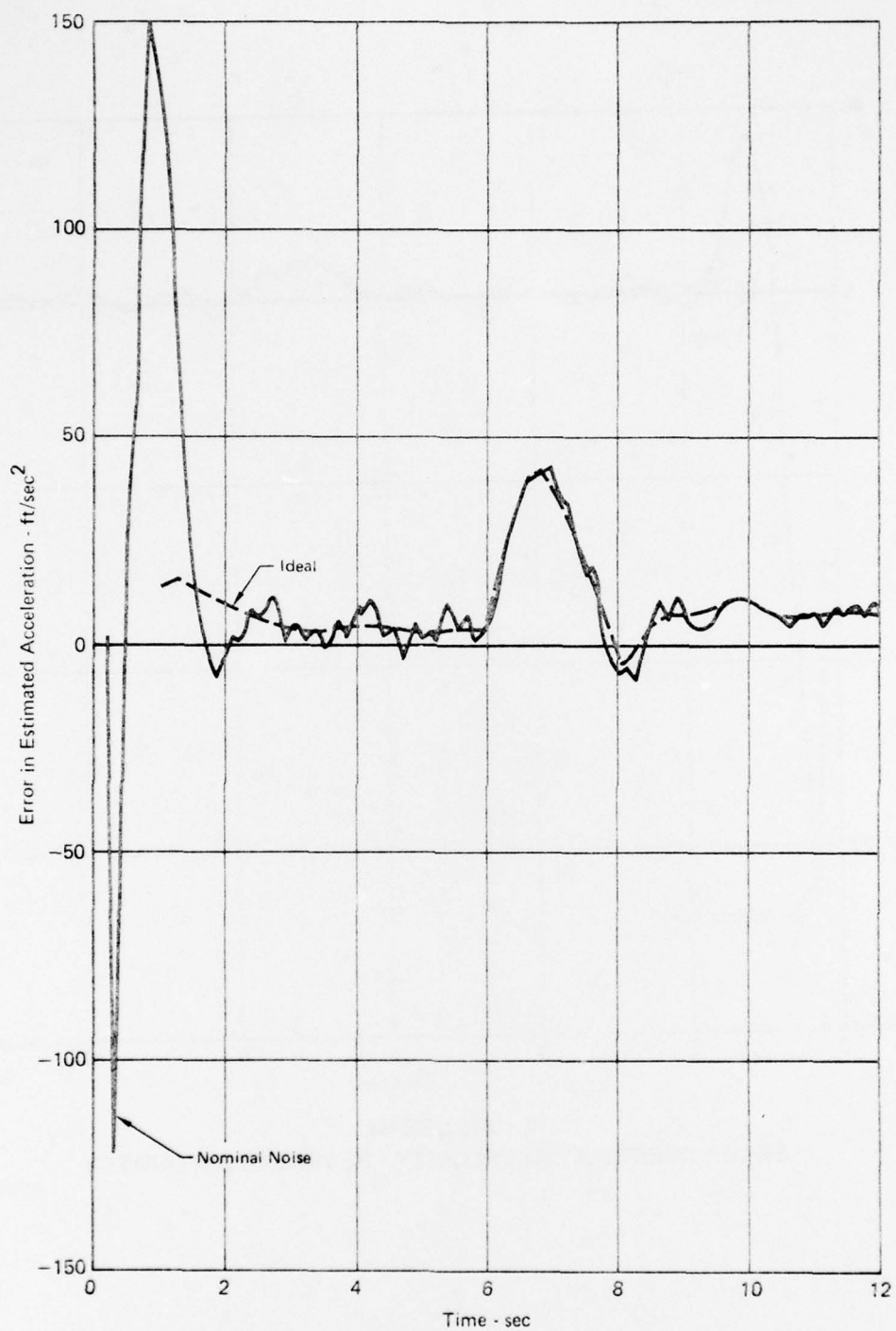
GP74-0122-117

103

FIGURE 49

ERROR IN ESTIMATED ACCELERATION - REVERSAL ENCOUNTER

GP74-0122-116

104

4.4.3 ATS Error Budget and Sensitivities

The error sources of each of the ATS subsystems and their magnitudes were discussed in Subsection 4.2. The principal error sources are: 1) SSR-1 range measurement error; 2) ASCOT measurement error; and 3) SGAP rate gyro bias error. The SSR-1 range measurement error consists in both a bias and a random component. The random component of ASCOT measurment error is of principal interest - bias errors will result in a constant offset between the estimated LOS and the true LOS.

The effect of degraded measurement accuracies in the random portions of the ATS sensor errors can be computed from the steady-state a posteriori standard deviations of the state variables in the Range and Angle Tracking Filters. This presumes, of course, that the degraded accuracies are accounted for in the filter design. The Range Tracking Filter's standard deviations are presented in Figure 50 as a function of measured range standard deviation. The range, range-rate and range-acceleration error sensitivities about the anticipated SSR-1 measurement accuracy are 0.22 feet, 0.36 feet/second, and 0.2 feet/second^2 per foot of measured range standard deviation.
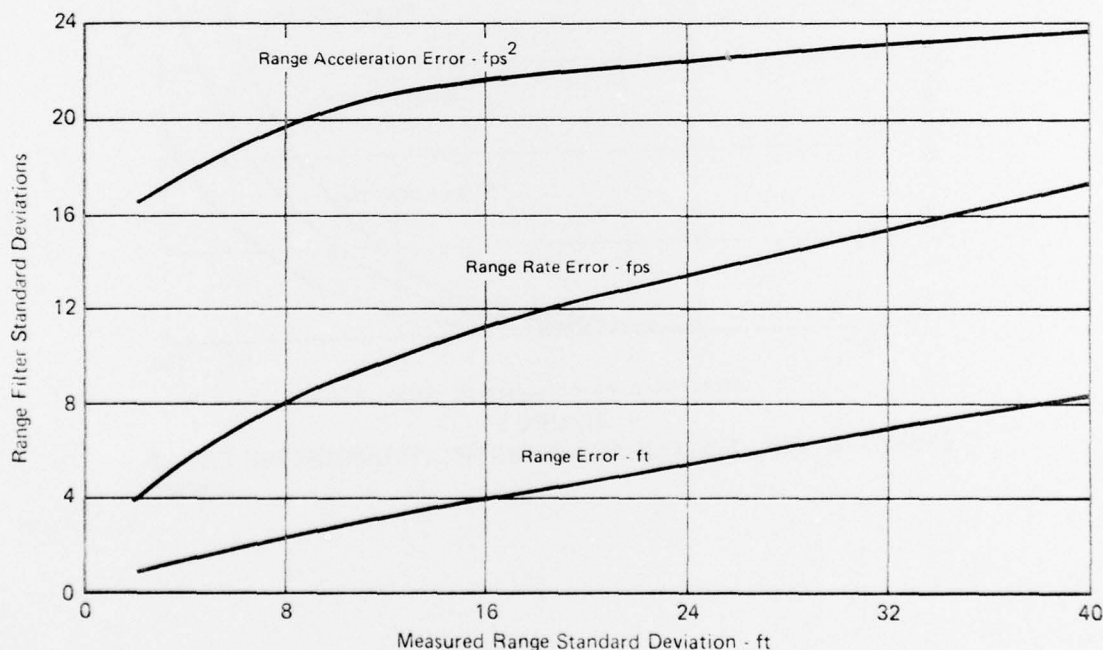
FIGURE 50
EFFECT OF MEASURED RANGE ACCURACY ON
RANGE FILTER ACCURACY

GP74-0122-98

105

The Angle Tracking Filter's standard deviations in estimated pointing error, velocity and acceleration are presented in Figures 51, 52 and 53 respectively for various gunnery ranges of interest. As noted previously, the ASCOT measurement error standard deviation is not well known. This analysis indicates that a measurement error standard deviation of as much as 50 millivolts (2.5 milliradians) could be tolerated for gunnery applications. The error sensitivities in estimated pointing error and velocity and acceleration normal to the LOS are 0.03 feet, 0.1 feet/second and 0.125 feet/second^2 per millivolt of ASCOT measurement standard deviation respectively.

FIGURE 51

EFFECT OF ASCOT ACCURACY ON ESTIMATED POINTING ERROR

GP74-0122-136

FIGURE 52
EFFECT OF ASCOT ACCURACY ON ESTIMATED TARGET RELATIVE VELOCITY

GP74-0122-135

FIGURE 53
EFFECT OF ASCOT ACCURACY ON ESTIMATED TARGET ACCELERATION

GP74-0122-134

107

Bias errors in both measured range and ownship body rates (SGAP rate gyro bias) affect the estimated target velocity normal to the LOS. This is illustrated in Figure 54. These data were obtained from the Reversal encounter which has a range of about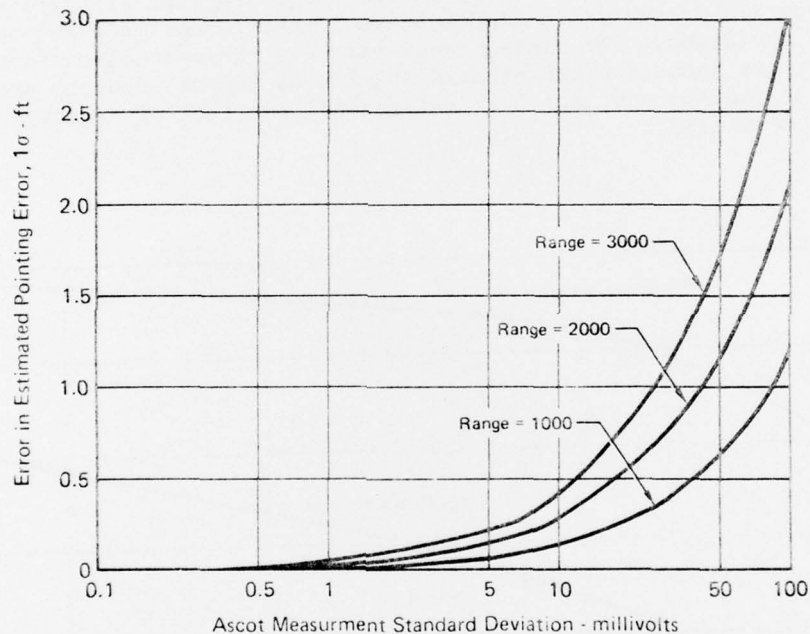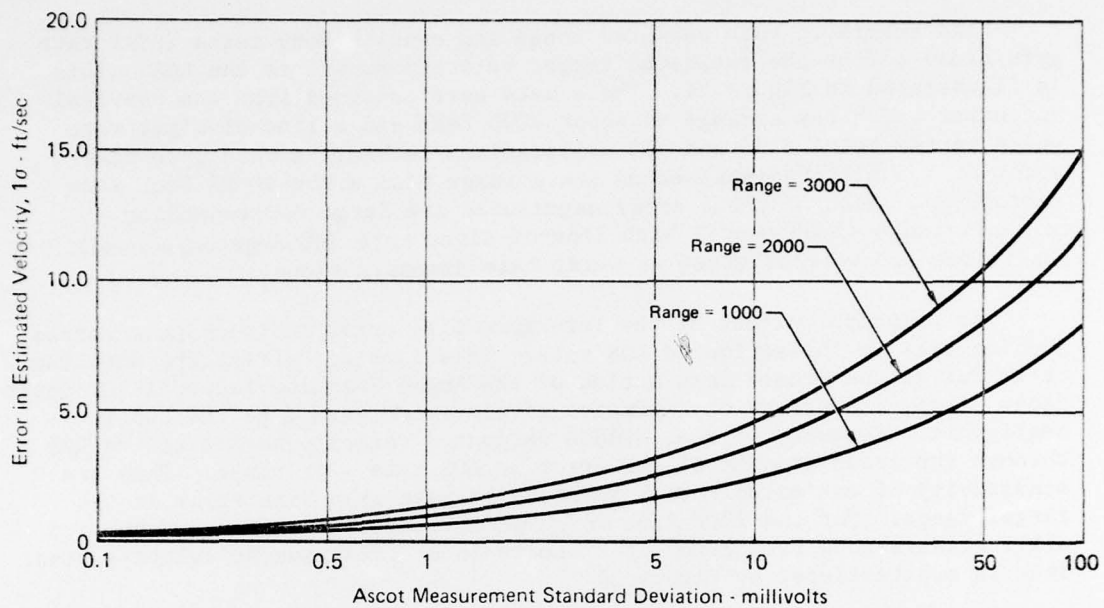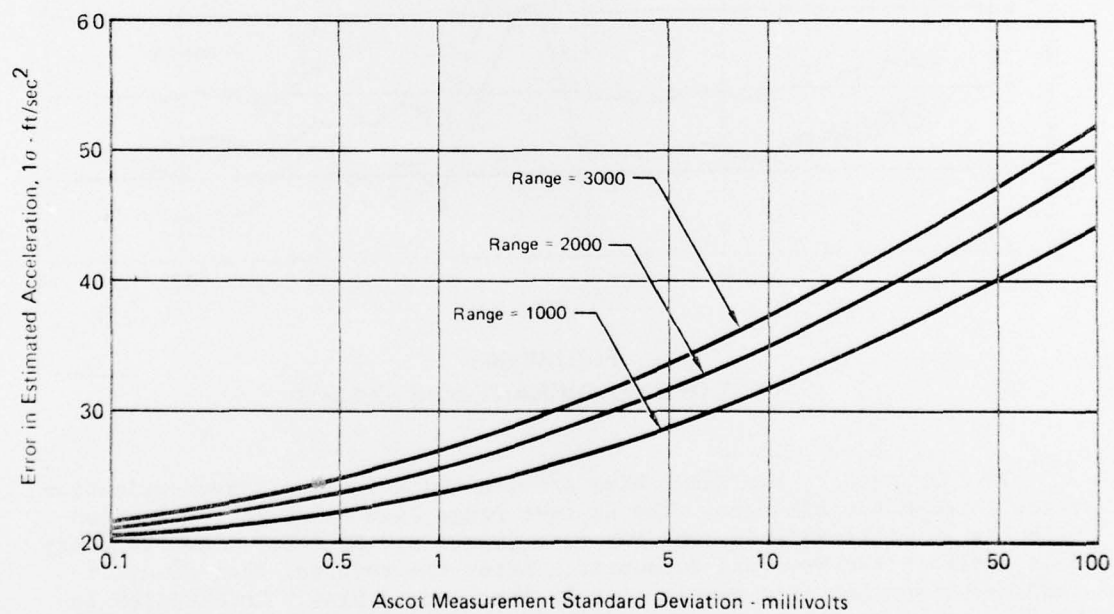 2000 feet and a line-of-sight rate which varies between 30 and -50 milliradians/second. A rate gyro bias error of 1.5 milliradians/second and a range bias error of 22 feet were introduced. Both of these error magnitudes are large corresponding to short-range (1000 feet), high line-of-sight rate (60 degrees/second) conditions and were selected as worst case demonstrations.

The principal effect of the rate gyro bias error is to cause a corresponding bias in the estimated LOS rate. This does not affect the pointing error due to the closed loop action of the Angle Tracking Filter/ASCOT interface. Also, its effect on estimated acceleration normal to the LOS is negligible. However, it does affect estimated velocity normal to the LOS through the cross-product of the error in LOS rate with range. Thus the sensitivity of estimated normal velocity to rate gyro bias error is the target range. For the 2000 feet range of the reversal encounter, the 1.5 milliradian/second rate gyro bias results in a 3 feet/second velocity bias. This is substantiated by Figure 54.
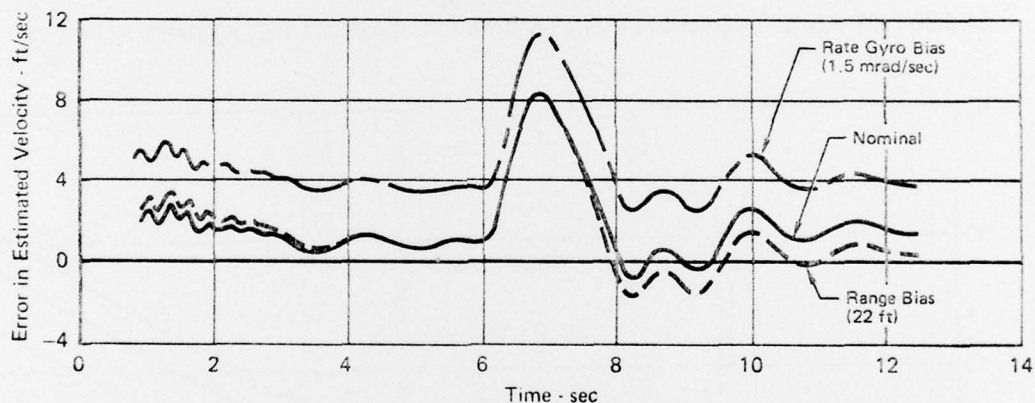
FIGURE 54

EFFECT OF PREDOMINANT BIAS ERRORS

GP74-0122-119

In like manner, the range bias affects the normal velocity estimation error through the LOS rate. The 22 feet range bias error in combination with the 30 milliradian/second LOS rate causes a 0.66 feet/second velocity bias early in the Reversal encounter. After the reversal the -60 milliradians/second LOS rate causes a -1.32 feet/second bias. In addition to biasing the normal velocity the range bias reflects directly into a constant error in estimated range but does not affect range-rate or range-acceleration estimates.

Based upon these considerations and the state-of-the-art in ASCOT and SSR-1 development the ATS error budget is selected as follows:

o SSR-1 Error Budget – The SSR-1 error budget will correspond to the anticipated SSR-1 performance as defined by Table 10. That is compensated bias errors of less than 40 feet and short-range (less than 3000 feet) random errors of less than 15 feet, 1σ.

o ASCOT Error Budget – The ASCOT error budget is selected as the equivalent of 50 millivolts (2.5 milliradians), 1σ, at maximum firing range (3000 ft). This figure includes both random and bias errors over the entire ASCOT FOV.

o SGAP Error Budget – The ATS SGAP should meet the medium-quality specifications for rate gyros and accelerometers presented in Tables 11 and 12 with converter accuracies as specified by Table 13.

Figures 55 through 58 present the effect of the increase in the ASCOT error budget over the nominal ASCOT noise used in generating the reference ATS performance (Figures 46 through 49). These results confirm the utility of the sensitivity analysis in determining the effect of degraded measurement accuracy, and illustrate the ability of the ATS tracking filter design to perform within the AGFCS requirements established in Phase I with the budgeted sensor errors.
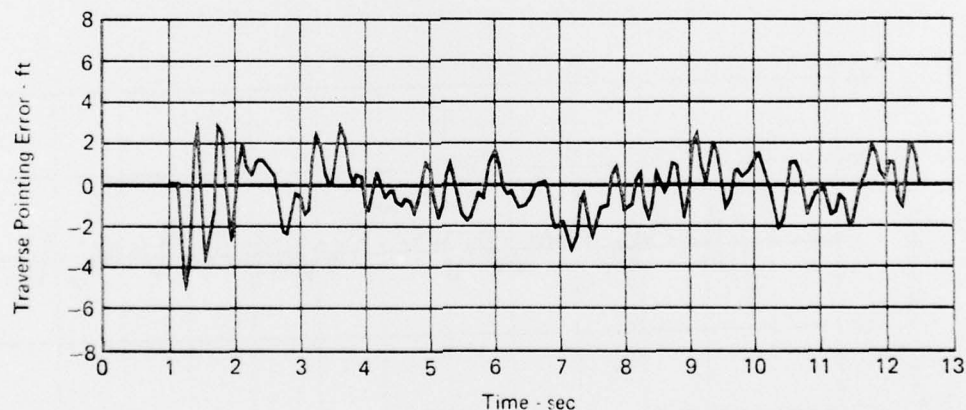

FIGURE 55
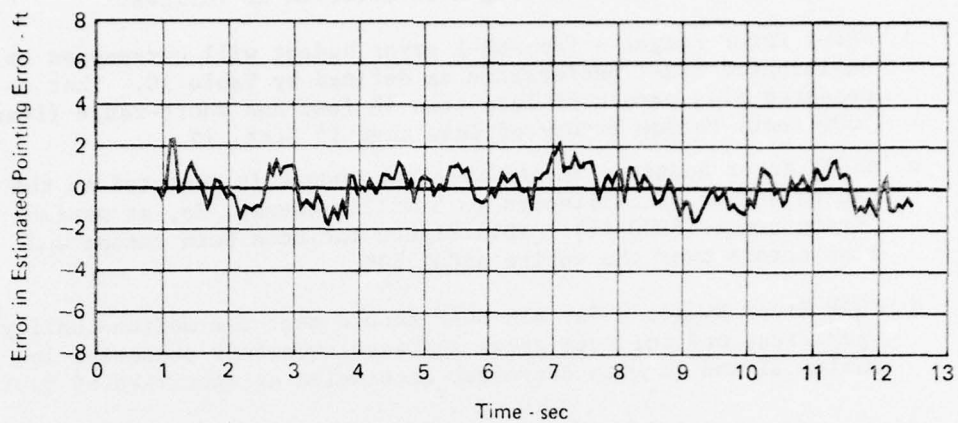ANGLE SENSOR POINTING ERROR - BUDGETED ANGLE SENSOR ERRORS

GP74-0122-143

109

FIGURE 56
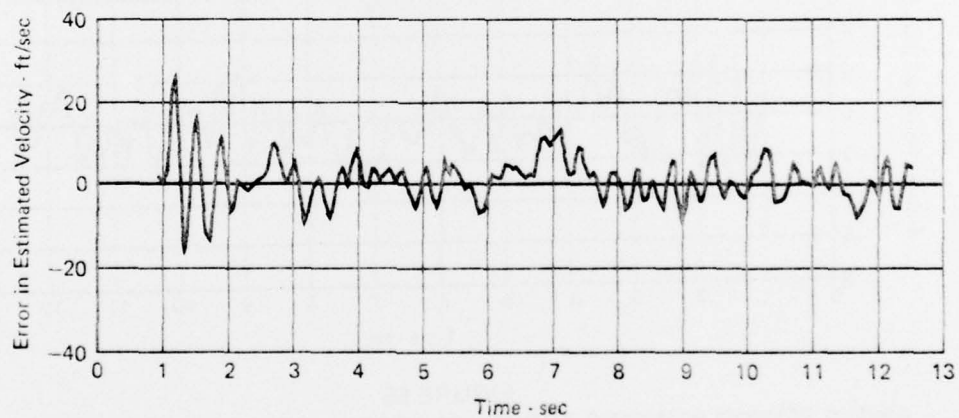ERROR IN ESTIMATED POINTING ERROR - BUDGETED ANGLE SENSOR ERRORS

GP74-0122-142

FIGURE 57
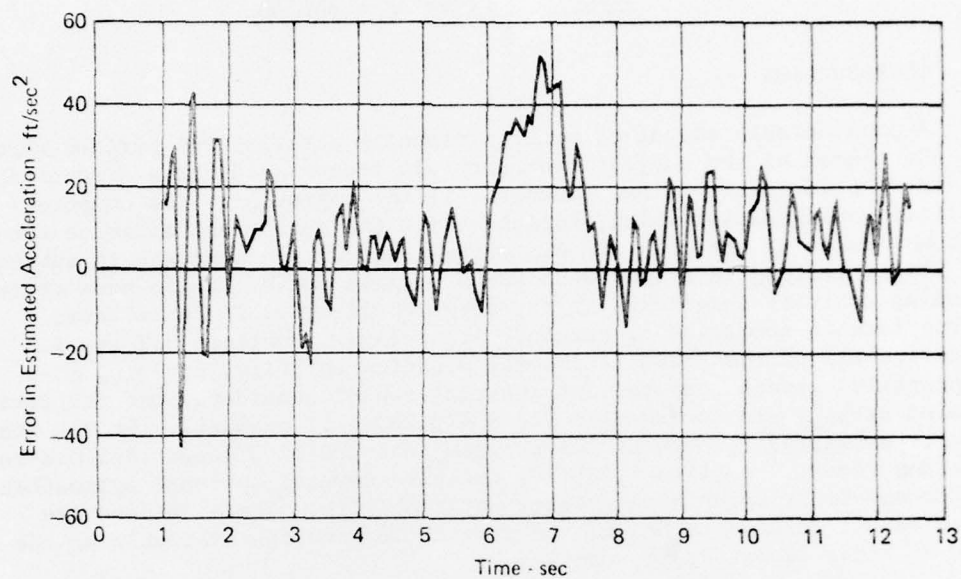ERROR IN ESTIMATED VELOCITY - BUDGETED ANGLE SENSOR ERRORS

GP74-0122-141

110

FIGURE 58
ERROR IN ESTIMATED ACCELERATION - BUDGETED ANGLE SENSOR ERRORS

GP74-0122-140

111

SECTION 5   PROGRAM PLANNING

5.1   INTRODUCTION

A considerable amount of program planning activity was pursued through-
out the course of the subject contract. It took many diverse directions,
depending principally on two factors: 1) the approach to the computer/
platform configuration which, together with the sensor and software sub-
systems, makes up the complete ATS system; and 2) the approach to subsequent
ATS flight testing in a follow-up AGFCS program phase. While much of the
planning activity undertaken is no longer applicable, it is believed
appropriate to summarize it herein. Accordingly, Sections 5.2 and 5.3
summarize all of the Phase II program planning activity, dividing it
principally between computer and inertial sensor considerations respectively.
Related details are included in the MCAIR Phase II proposal, the R&D Status
Reports submitted throughout the program, and the 17 October 1973 mid-term
briefing report. Section 5.4 below includes several optional approaches to
follow-on effort which have greater applicability. These options are
based on all related technical and program information available at the
time of final report draft submittal.

5.2   COMPUTER CONSIDERATIONS

The computer and associated software development considerations have
had a significant effect on the program planning activity throughout the
Phase II effort. This activity relates principally to the three computers
which, at various times, have been identified as potential ATS candidates:
IBM TC-2, Singer-Kearfott SKC-2000, and General Electric CP-16. Preliminary
considerations relative to the IBM TC-2 computer identified that, while
the memory was adequate, the computation time might have been a limiting
factor. Off-setting this disadvantage was the similarity of the IBM TC-2
to the IBM AP-1 employed in the F-15. Accordingly, MCAIR software
capability was highly applicable and the related planning activity
included MCAIR's development of the assembly language software. Another
potential advantage was the applicability of the associated interface
hardware already developed by Singer-Kearfott, some of which is employed
in the A-7 aircraft avionics.

Early in the program a change was made from the IBM TC-2 to the
Singer-Kearfott SKC-2000. This change was made for the following reasons:
1) the SKC-2000 is a faster machine and would have no computation time
problems; 2) although not in a full production status, its development was
essentially completed in connection with the B-1 aircraft program; 3) it
was being considered as a standard computer for AFAL development activity;
and 4) its interface with the KT-70 inertial platform (specified as an
AFAL furnished item in the Work Statement) and ATS sensors would also
utilize already-developed Singer-Kearfott interface hardware. Associated
with this computer change, three principal approaches to the related software
development were considered in the program planning activity: 1) MCAIR would

112

provide software development based on establishing the required support software capability by appropriate transfer of software/hardware from AFAL; 2) MCAIR would manage the software development activity with Kearfott-Singer as a support subcontractor; and 3) AFAL would provide the software development with support, as required, from Singer-Kearfott and MCAIR.

The latter approach to SKC-2000 software development became the primary one at the time that the MCAIR ATS development was first associated with the trainable-gun effort of the ASD/YP. Shortly thereafter, however, the concept of an autonomous ATS hardware configuration was pursued by MCAIR. It was based on MCAIR obtaining consigned computers and the associated software development from industry sources. This approach, including the appropriate industry support, was presented in some detail in Status Reports 3 and 4 and in the mid-term briefing report. As of the time of this final report submittal, the concept of an autonomous ATS remains the most viable approach to the computer(s) for a follow-on ATS phase which is directed to the overall system fabrication and test. A possible alternate approach for consideration involves the Westinghouse digital computer which AFAL is currently considering as a standard computer for in-house development activity. Either AFAL software development (with MCAIR support) or MCAIR software development (with AFAL support) would be possible with this computer.

5.3 INERTIAL SENSOR CONSIDERATIONS

The inertial sensor and associated interface considerations, pursued throughout the Phase II effort, have also had a significant effect on related program planning activity. This activity relates principally to the two potential inertial sensor candidate configurations: a gimballed platform system, and a strapdown inertial sensor package. The initial technical coordination and related program planning was pursued in connection with the Singer-Kearfott KT-70 gimballed inertial platform. Its advantage, during the interval that the IBM TC-2 and Singer-Kearfott SKC-2000 computers were being considered, was that Singer-Kearfott was familiar with the required and already-developed interface hardware. Accordingly, at the time of the initial coordination between the ATS and trainable-gun programs, it was planned that Singer-Kearfott would supply all ATS interface hardware to AFAL. This was consistent with AFAL plans at the time which included AFAL development of the SKC-2000 software and AFAL integration of the ATS hot mock-up configuration prior to flight test.

It was because of anticipated technical difficulties associated with the above AFAL approach to ATS integration that MCAIR proposed the autonomous ATS approach identified in Section 5.2. The autonomous approach, from its conception, included the use of strapdown inertial sensors. Even prior to considering an autonomous ATS, the possibility of using the Honeywell H478 inertial reference package (IRP), or equivalent, was considered in accordance with the work statement provisions. It was initially hoped that this IRP and associated computation could provide inputs to both Honeywell and MCAIR ATS configurations on a common flight test bed. When the common-test-bed approach was abandoned (at the time the MCAIR-ATS/

trainable-gun coordination was initiated), MCAIR sought other sources for a consigned IRP and related high-data-rate computer (HDRC). Details of this activity and its outcome are presented in Status Reports 3 and 4 and in the mid-term briefing report.

As of the time of this final report submittal, the strapdown sensor approach presented in the mid-term briefing remains the most viable approach to the ATS inertial requirements for follow-on ATS effort. A possible alternate is the interface of the Bendix ASCOT with a Bendix-furnished IRP and related HDRC. Although the projected schedules considered at the time of the mid-term briefing precluded this possibility, it appears to be a feasible approach at the time of this report submittal. One of the possible advantages of this approach is that the follow-on development of the overall stabilized angle sensor subsystem would then be pursued in conjunction with a single angle sensor subsystem subcontractor.

5.4 OPTIONAL APPROACHES TO FOLLOW-ON ATS DEVELOPMENT

5.4.1 Primary Option

The primary option to a Phase III follow-on ATS development effort is essentially equivalent to that presented at the mid-term briefing except for the elimination of brassboard fabrication and test. Although this elimination results in an increase in the proposed program duration, it is anticipated that it will result in a decreased program cost. The schedules of Figures 59 and 60 summarize this primary option. The companies which previously agreed to a consignment status for the strapdown gyro/accelerometer package (SGAP) and related HDRC, and for the general-purpose computer and related interface hardware are not identified in Figure 59. However, it is believed that these companies, or equivalent sources, would agree to a similar arrangement (i.e. consigned equipment with funded engineering support) at the appropriate future time. Furthermore, it is believed that the schedule from go-ahead would not be affected by a change in these potential subcontractors, if that proved necessary or desirable. The principal ATS sensor subcontractors are identified in Figure 59 and, of course, would be the sole suppliers of the respective ATS sensor designs pursued during Phase II.

5.4.2 Alternate Options

A variety of alternate options are possible for a follow-on AGFCS effort. They involve varying degrees of decreases in program duration and/or cost and are limited to the development of the angle sensor portion of the ATS during Phase III. The range sensor portion, which represents a significantly lower technical risk, could then be included in a Phase IV effort. The first of these options is to simply pursue the angle sensor portion of the primary option. This approach would decrease the Phase III program duration by approximately two-months and would decrease the program cost by approximately 30%. The second alternate option is similar but includes the use of a brassboard ASCOT rather than a flight system ASCOT. It would decrease the program duration by approximately four months and the
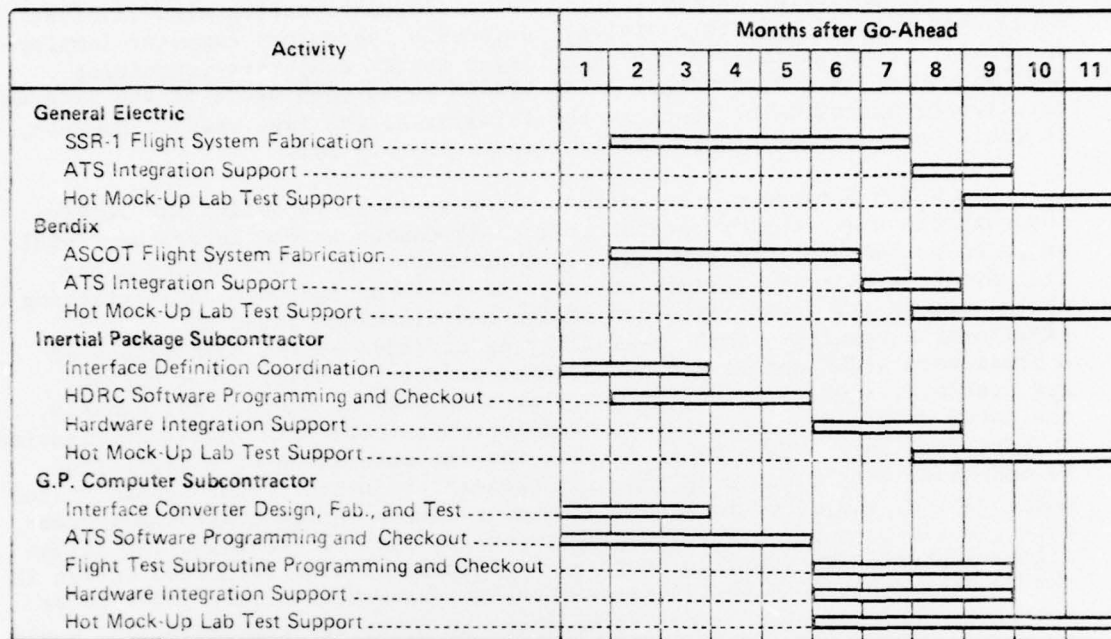
114

Activity	Months after Go-Ahead										
	1	2	3	4	5	6	7	8	9	10	11
General Electric											
SSR-1 Flight System Fabrication											
ATS Integration Support											
Hot Mock-Up Lab Test Support											
Bendix											
ASCOT Flight System Fabrication											
ATS Integration Support											
Hot Mock-Up Lab Test Support											
Inertial Package Subcontractor											
Interface Definition Coordination											
HDRC Software Programming and Checkout											
Hardware Integration Support											
Hot Mock-Up Lab Test Support											
G.P. Computer Subcontractor											
Interface Converter Design, Fab., and Test											
ATS Software Programming and Checkout											
Flight Test Subroutine Programming and Checkout											
Hardware Integration Support											
Hot Mock-Up Lab Test Support											

FIGURE 59
ATS SUBCONTRACTOR SCHEDULE FOR PRIMARY PHASE III OPTION

GP74-0122-145

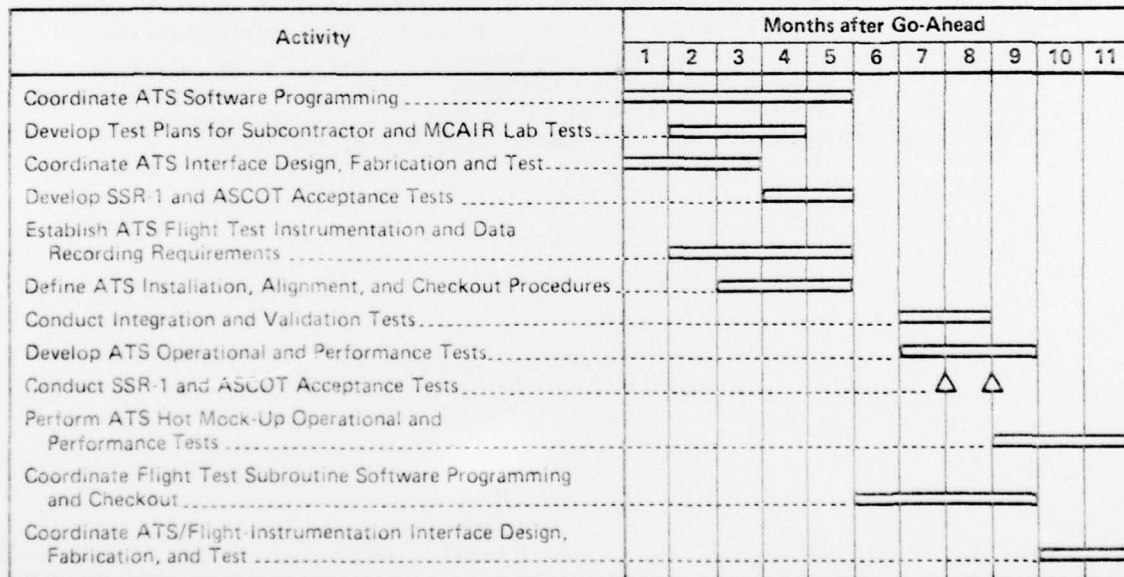| Activity	Months after Go-Ahead										
	1	2	3	4	5	6	7	8	9	10	11
Coordinate ATS Software Programming											
Develop Test Plans for Subcontractor and MCAIR Lab Tests											
Coordinate ATS Interface Design, Fabrication and Test											
Develop SSR-1 and ASCOT Acceptance Tests											
Establish ATS Flight Test Instrumentation and Data Recording Requirements											
Define ATS Installation, Alignment, and Checkout Procedures											
Conduct Integration and Validation Tests											
Develop ATS Operational and Performance Tests											
Conduct SSR-1 and ASCOT Acceptance Tests							△	△			
Perform ATS Hot Mock-Up Operational and Performance Tests											
Coordinate Flight Test Subroutine Software Programming and Checkout											
Coordinate ATS/Flight-Instrumentation Interface Design, Fabrication, and Test											

FIGURE 60
MCAIR SCHEDULE FOR PRIMARY PHASE III OPTION

GP74-0122-144

115

program cost by approximately 40%. A third alternate option also involves a brassboard ASCOT and, in addition, includes a laboratory computer (employing Fortran programming) rather than flight system computers (requiring assembly language programming). This option would also decrease the program duration by approximately four months (similar to the last case). However, it would decrease the program cost by approximately 50%.

The basic purpose of the latter option would be to define and verify the complete angle sensor portion of the ATS design at the laboratory level prior to pursuing a flight-worthy ATS implementation. This approach has the advantage that it could be expected to yield an improved angle tracking design due to its flexibility for design modifications based on experimental results. This flexibility is afforded by the combination of a brassboard ASCOT and Fortran programmed software. Still other options are possible, involving further reductions in program scope. For example, the ASCOT development could be pursued in conjunction with rate-stabilization augmentation only. This would involve the implementation of a simplified second-order loop closure in the high-data-rate computer. The Kalman filter augmentation, and other related features involving the general-purpose computer, would then be pursued in a later phase. Or, alternately, the Kalman filter augmentation could be temporarily eliminated from follow-on effort if the results achieved with rate-stabilization augmentation only prove to be adequate. Another option, not recommended by MCAIR for consideration, would be to pursue further ASCOT development in an unaided strapdown mode. While this is a potentially desirable ASCOT mode for missile seeker applications, it appears to represent an unnecessarily high technical risk for application to a gun fire control system.

Based on the above considerations, it is believed that more specific program planning activity must await AFAL decisions and recommendations regarding which of the many possible alternatives appear to be the most appropriate. Detailed alternate program plans and related costs could then be presented in a response to an AFAL RFP identifying a few specific alternate approaches which are of current interest to the AFAL.

REFERENCES

1. Berg, R. L. and Sears, M. M., <u>Terminal Aerial Gunnery Simulation (TAGS) Program</u>, Report MDC A2236, (April 1973).

2. Bryson, A. E., and Ho, Y. C., <u>Applied Optimal Control</u>, Blaisdell, 1969.